Phase Transitions in Yang-Mills Theories and their Gravity Duals

A thesis presented

by

Joseph Daniel Marsano

to

The Department of Physics

in partial fulfillment of the requirements

for the degree of

Doctor of Philosophy

in the subject of

Physics

Harvard University

Cambridge, Massachusetts

May 2006

Thesis advisor

Shiraz Minwalla

Author

Joseph Daniel Marsano

Phase Transitions in Yang-Mills Theories and their Gravity Duals

Abstract

This thesis is a study of the thermal phase structure of systems that admit dual gauge theory and string theory descriptions. In a pair of examples, we explore the connection between perturbative Yang-Mills and gravitational thermodynamics which arises from the fact that these descriptions probe different corners of a single phase diagram. The structure that emerges from a detailed study of these isolated regions generally suggests a natural conjecture how they may be connected to one another within the full phase diagram. This permits the identification of interesting phenomena in the gauge and gravity regimes under a continuous change in parameters.

We begin by studying the AdS_5/CFT_4 system which, when the supergravity description is valid, exhibits a first order Hawking-Page phase transition as a function of temperature from a thermal gas of gravitons to a large black hole. In the perturbative Yang-Mills regime, we find that the free theory exhibits a weakly first order deconfinement transition whose precise nature at small nonzero coupling depends on the result of a non-trivial perturbative computation. It is conjectured that this deconfinement transition is continuously connected in the full phase diagram to the Hawking-Page transition at strong coupling, with the confined phase identified with the graviton gas and the deconfined phase identified with the black hole.

We then turn to the study of Gregory-Laflamme (GL) black hole/black string transitions in supergravity and their realization in a setup that admits a dual description

via the maximally supersymmetric Yang-Mills theory on T^2. The thermodynamics of Yang-Mills theories on low dimensional tori is studied in detail revealing an intricate structure of which the GL transition at strong coupling is a small piece. We are led to conjecture that GL physics is continuously connected to deconfinement in maximally supersymmetric $0+1$-dimensional gauged matrix quantum mechanics. This identification will then permit us to probe GL transitions from the gauge theory point of view and comment on some puzzles regarding their precise nature.

Contents

Acknowledgments

I would like to begin by thanking my advisor Shiraz Minwalla for his guidance, mentorship, positive energy, and neverending patience throughout my graduate career. I am grateful to him for taking such an active interest in my development as a researcher and for providing consistent encouragement throughout the past several years. I have been extremely fortunate to work with and learn from him and wish him well in his new position at TIFR and, more importantly, in his new role as a father.

I have also had the good fortune to work with a fantastic group of collaborators including Ofer Aharony, Lars Grant, Dan Jafferis, Kyriakos Papadodimas, Mark van Raamsdonk, and Toby Wiseman. I am very grateful to each one of them for a series of educational and fun research experiences from which I learned a great deal.

One of the advantages of studying at Harvard is the existence of an entire community of graduate students studying high energy physics. I would like to express my deep thanks to all of them, including Michelle Cyrier, Morten Ernebjerg, Lars Grant, Monica Guica, Matt Headrick, Jon Heckman, Lisa Huang, Dan Jafferis, Greg Jones, Can Kilic, Josh Lapan, Subhy Lahiri, Alex Maloney, Andy Neitzke, Kyriakos Papadodimas, Suvrat Raju, Kirill Saraikine, Jihye Seo, Aaron Simons, David Thompson, Devin Walker, and Xi Yin, for helping make Harvard such a lively and fun place to study string theory. I am also especially grateful to my office mates, Michelle Cyrier and Can Kilic, for providing Turkish snacks, coffee, and laughs whenever stress levels grew too high.

Throughout my time here, I've learned a great deal from the postdocs and faculty in the group including Nima Arkani-Hamed, Sidney Coleman, Davide Gaiotto, Joe Minahan, Shiraz Minwalla, Lubos Motl, Natalia Saulina, Andy Strominger, and Toby Wiseman. To all of them, I am grateful for taking the time to talk with me and share their knowledge.

Of course, I cannot understate the importance of the constant support that I have received from my family during graduate school and, indeed, throughout my entire life.

To my mother Linda, my father Daniel, my sister Lisa, and my grandmother Jeanne I am grateful for a lifetime of love and encouragement.

Finally, I would like to thank my loving wife Denise, to whom this thesis is dedicated. Because of the late nights and frequent travels, being married to a normal physics graduate student isn't easy. Being married to an abnormal graduate student like me, then, is even harder. I am grateful to Denise for putting up with me and my travels, for nagging me to wear my hat when it's cold, and for putting an umbrella on top of my shoes when it rains so that I don't forget to take it with me. Most of all, though, I am eternally grateful to Denise for her constant support and love without which this thesis could never have been written.

For my wife,

Chapter 1

Introduction

Perhaps the most exciting development in string theory during the past decade is Maldacena's AdS/CFT conjecture relating strings propagating in asymptotically AdS spacetimes to gauge theories defined on their conformal boundaries [1, 2, 3]. Among the various implications of this correspondence is the incorporation of the thermodynamic structure of supergravity (SUGRA) and perturbative gauge theory into a single phase diagram. This is particularly exciting because gravitational thermodynamics is driven primarily by black holes and their higher dimensional cousins while Yang-Mills thermodynamics centers on the physics of confinement. The AdS/CFT correspondence is apparently asserting that these two phenomena, which have been at the heart of theoretical physics research for over thirty years, may be related in a deep manner that is not yet completely understood.

In this thesis, we shall explore these ideas by studying the phase structure of systems that, via AdS/CFT, can be described both by string theory and a dual non-Abelian gauge theory. Because a comprehensive analysis of the full phase diagram will be beyond our reach, the general strategy that we adopt is to use the SUGRA approximation to probe one region and the techniques of perturbative gauge theory to probe another. Though

the regimes that we can directly study in this manner are widely separated in general, we shall find that the structure that emerges in each case is quite similar and, in fact, leads to natural conjectures for how the two regions may be connected in the full phase diagram.

The first part of this thesis is devoted to a study of string theory on (global) $AdS_5 \times S^5$, which admits a dual description in terms of 4-dimensional $\mathcal{N} = 4$ supersymmetric Yang-Mills (SYM) on S^3. In the SUGRA regime, the thermodynamics of this theory is dominated by a gas of gravitons at low temperatures and a black hole at high temperatures with a first order transition separating the two phases [4, 5]. In chapter 2, we review what is known about this structure and how it might naively behave as we continue to the perturbative Yang-Mills regime.

In the next chapter, we study the Yang-Mills description directly following [6, 7]. Perhaps surprisingly, we will find a finite temperature deconfinement transition even at zero coupling that is driven by compactness of the space. The confined and deconfined phases share similar properties, via the AdS/CFT dictionary, with the graviton gas and black hole at strong coupling and are distinguished by the same order parameter. We are thus led to conjecture that, in the full phase diagram, the deconfinement transition that we encounter in the perturbative regime is continuously connected to the Hawking page transition in the SUGRA regime[1]. The particular form of this conjecture is complicated by the fact that a small nonzero coupling can change the qualitative behavior of the deconfinement transition somewhat. We outline the two primary scenarios, which lead to two different conjectures for the full phase diagram, and describe how one might distinguish between the two with a perturbative computation.

The rest of this thesis is devoted to the application of these ideas to study Gregory-Laflamme black hole/black string phase transitions, which arise in higher dimensional the-

[1] This idea was first proposed in [2, 5]

ories of gravity that are compactified on a circle, from a gauge theory point of view. Such transitions occur when black strings that wrap the circle become unstable to "clumping" as the temperature is decreased, eventually giving way to a phase dominated by a localized black hole. The process by which this "clumping" occurs is still not completely understood from the gravity point of view, though a great deal of progress has been made in recent years. In the first part of chapter 4, we briefly review the physics of Gregory-Laflamme transitions in higher dimensional gravity as it is currently understood.

Following this, we search for a realization of Gregory-Laflamme physics in a system that admits a dual Yang-Mills description. There, one might hope to probe the transition line, albeit in a different region of the phase diagram, using the techniques of perturbative gauge theory. In the second part of chapter 4, we find just such a realization using the ideas of AdS/CFT and demonstrate that the dual gauge theory is the maximally supersymmetric Yang-Mills theory on T^2.

Finally, in chapter 5, we study the phase structure of this Yang-Mills theory as a means of probing Gregory-Laflamme physics. Our analysis is complicated by the fact that the system becomes effectively strongly coupled near the phase transition line even far from the SUGRA regime. The physics there can be described in terms of a dimensionally reduced model, though, for which numerical analysis can be done without too much difficulty. In the end, we will associate the Gregory-Laflamme phase transition with deconfinement in this dimensionally reduced theory.

Chapter 2

The Hawking-Page Transition in $AdS_5 \times S^5$

In this first chapter, we review the thermodynamics of string theory on $AdS_5 \times S^5$. After a lightning review of the AdS_5/CFT_4 correspondence, we shall embark on a qualitative discussion of the spectrum and move from there to finite temperature thermodynamics, culminating in a review of the Hawking-Page phase transition from graviton gas to "big" black hole. Some implications of this structure for the dual description via $\mathcal{N} = 4$ supersymmetric Yang-Mills (SYM) theory at strong coupling will then be discussed. While not obvious, much of this structure is retained at weak coupling and will be a main focus of the next chapter.

2.1 Lighting Review of AdS_5/CFT_4

We begin with a quick review of the duality between type IIB strings on $AdS_5 \times S^5$ and the $\mathcal{N} = 4$ supersymmetric Yang-Mills theory [1, 2, 3]. The main purpose of this section is to fix notation and recall the basic dictionary between the two sides and as such it is

far from thorough. The reader interested in a more detailed treatment should consult the classic review paper [8].

At the heart of the correspondence is the physics of a stack of N D3-branes in IIB theory on flat space. Near the branes, one has both open and closed string degrees of freedom, which give rise to gauge field and gravity degrees of freedom in the worldvolume description, respectively. The key insight that drives AdS/CFT is the existence of a limit which decouples the open strings from the closed strings, leaving a worldvolume description in terms of a gauge theory alone. Specifically, we can accomplish this by taking $\alpha' \to 0$ while keeping all energies and dimensionless parameters fixed. The result is that physics near the D3-branes can be described by a gauge theory on their worldvolume, which is fixed by supersymmetry to be $\mathcal{N} = 4$ SU(N) SYM.

For large N and small g_s, the D3-branes admit a description in supergravity (SUGRA) [9], though, given by the charged black 3-brane solution [10]

$$\begin{aligned} ds^2 &= f(r)^{-1/2}\left(-dt^2 + \sum_{i=1}^{3} dx_i^2\right) + f^{1/2}(r)\left(dr^2 + r^2\, d\Omega_5^2\right) \\ f(r) &= 1 + \frac{R^4}{r^4} \end{aligned} \tag{2.1}$$

which also contains a nontrivial RR 5-form flux and R is related to the number of D3-branes, N, by

$$R^4 = 4\pi g_s \alpha'^2 N \tag{2.2}$$

Here, the above decoupling limit takes the form $\alpha' \to 0$ with $U = r/\alpha'$ fixed in order to ensure that energies of modes near the horizon remain fixed as measured by an observer at infinity. The limiting geometry, which provides a SUGRA description of the near-horizon region, is given by

$$ds^2 = \alpha' \left[\frac{U^2}{\sqrt{4\pi g_s N}} \left(-dt^2 + \sum_{i=1}^{3} dx_i^2 \right) + \sqrt{4\pi g_s N} \frac{dU^2}{U^2} + \sqrt{4\pi g_s N}\, d\Omega_5^2 \right] \tag{2.3}$$

This geometry is nothing more than $AdS_5 \times S^5$ with the AdS and S^5 radii both given by R in (2.2). The weak conjecture of AdS/CFT is the equivalence of the two dual descriptions that we have seen of physics near the D3-branes, namely $\mathcal{N} = 4$ $SU(N)$ SYM theory at large N and type IIB SUGRA on $AdS_5 \times S^5$. One might think that this is obviously wrong since these two theories look nothing alike. However, one must pay careful attention to the regimes of validity on which our intuition is based. For the SUGRA approximation to be reliable, one needs not only $g_s \to 0$, but also the AdS radius R to be large in string units

$$\frac{R}{\sqrt{\alpha'}} \gg 1 \tag{2.4}$$

So, in particular, N must be approaching infinity in such a way that the quantity $g_s N$ is fixed and large. Since $g_s = g_{YM}^2$ here, this is nothing other than the 't Hooft coupling of the dual Yang-Mills theory[11]

$$\lambda = g_s N = g_{YM}^2 N \tag{2.5}$$

and consequently the SUGRA approximation is valid in the 't Hooft limit when $\lambda \gg 1$. This corresponds to strong coupling in the gauge theory and is a regime far from the perturbative one where we can trust naive intuition. A stronger form of the AdS_5/CFT_4 conjecture goes beyond this relation of strongly coupled Yang-Mills physics to SUGRA and asserts that the two theories are completely equivalent. It is this statement, for which there is now an overwhelming body of evidence[1], that we shall assume throughout the remainder

[1] See, for instance, the review [8] and references therein.

of this thesis.

The specific version of the correspondence that will interest us, though, is a slight modification of what we have presented so far. As stated above, we have a relation between a field theory in flat space and strings propagating on the so-called Poincare patch (2.3) of $AdS_5 \times S^5$. The region that this metric describes is not geodesically complete and corresponds to only a small part of the maximally extended, global AdS_5 which can be covered by the metric

$$ds^2 = R^2 \left(-\cosh^2 \rho \, dt^2 + d\rho^2 + \sinh^2 \rho \, d\Omega_3^2 \right) \tag{2.6}$$

Global AdS, as this is called, has a well-defined timelike Killing vector which provides a distinguished choice of time variable both here and in the dual Yang-Mills theory. This is related to the time variable of the Poincare patch by an AdS_5 isometry, which is an element of the isometry group $SO(4,2)$ and corresponds to a conformal transformation in the gauge theory. The effect of this transformation on the latter is to map constant time slices from copies of $\mathbb{R}^3 \subset \mathbb{R}^4$ to spheres $S^3 \subset \mathbb{R}^4$ with time evolution proceeding radially. This is analagous to the radial quantization that one encounters in worldsheet string theory by using a conformal transformation to pass from the cylinder to the complex plane. Among other things, this implies that the Yang-Mills theory dual to strings on global $AdS_5 \times S^5$ is defined on $S^3 \times \mathbb{R}$, which is conformally equivalent to $\mathbb{R}^4$ but differs in the important respect that the spatial slices are compact. This is to be expected from the holographic interpretation of AdS/CFT since the boundary of global AdS is $S^3 \times R$. This is also expected from the point of view of the spectrum since that of the Poincare patch is ungapped and hence consistent with a flat space gauge theory, while that of global AdS is gapped and hence consistent with gauge theory on a compact space.

Finally, we close this section with a recap of the basic dictionary for relating gauge

theory and string theory quantities in AdS_5/CFT_4. The primary entry in this dictionary is the relation (2.2) which arises from comparing the RR charge of the black 3-brane solution with that of N D3-branes as computed in string theory. The only other relation that one needs is the standard one relating the 10-dimensional Newton constant with the string coupling and scale

$$G_N \sim \left(g_s \alpha'^2\right)^2 \tag{2.7}$$

which permits one to pass to SUGRA variables as well.

2.2 Spectrum of Strings on $AdS_5 \times S^5$

Though quantizing IIB strings on $AdS_5 \times S^5$ is notoriously difficult, one can still say quite a bit about the qualitative structure of the spectrum provided g_s is small and the AdS radius, R, is much larger than $\sqrt{\alpha'}$ so that the SUGRA approximation is valid. In Yang-Mills variables, this corresponds to the 't Hooft limit, namely small g_{YM} and infinite N, with the 't Hooft coupling $\lambda = g_{YM}^2 N$ fixed and large. We will follow here roughly the treatment of [8, 6], starting with the spectrum at low energies and moving up from there[2]. Note, however, that we shall focus on the spectrum as a function of the energy E meausred by an observer at infinity, and hence an observer in the dual Yang-Mills theory. This differs from the proper energy, $E_{\rm proper}$, of states in the far interior of AdS, which is where our states will be constrained to lie, by a factor of R

$$E = E_{\rm proper} R \tag{2.8}$$

[2]Previous discussions of the thermodynamics that we now describe have also appeared in [12, 13, 14, 15]. See also [16, 17, 18]

2.2.1 Free Graviton Gas

At energies $E_{\text{proper}} < \sqrt{\alpha'} = R/\lambda^{1/4}$, the spectrum consists of gravitons and their superpartners. Energies are quantized in units of $1/R$ and single-particle states are insulated from both quantized string effects and quantum gravity by their BPS nature. Multiparticle states are also essentially uncorrected since the gravitational potential $E^2/(m_P^8 R^7)$ scales with N and consequently is much larger than ${\alpha'}^{-1/2}$.

We thus conclude that for $E \ll \lambda^{1/4}$ the system is well described by a free 1+9-dimensional graviton gas. The entropy of this gas is given by the standard result

$$S(E) \sim E^{9/10} \tag{2.9}$$

2.2.2 Free String Gas

At energies E larger than $\lambda^{1/4}$, excited string modes become accessible. The masses of these modes are quantized roughly in units of ${\alpha'}^{-1/2}$ and, in the usual SUGRA regime $R/\sqrt{\alpha'} \gg 1$, the spectrum is expected to be similar to that of string theory in flat space. In particular, we can imagine expanding the masses in a perturbative expansion in α' of the form

$$m^2 = \frac{1}{\alpha'}\left[n + \mathcal{O}\left(\frac{\alpha'}{R^2}\right)\right] \tag{2.10}$$

The spectrum of free string theory, though, is quite interesting in itself and exhibits a well-known exponential growth in the density of states [19] as we now briefly review.

Hagedorn Growth

To see this quickly, we follow essentially the approach of volume 1 in the book by Green, Schwarz, and Witten [20]. For simplicity, let us consider the density of states in

the subspace generated by just one of the physical bosonic oscillators of the superstring. A generic state in this space is labeled by the number n_m of excitations at level m so that, for instance, the state with $n_1 = 1$ and $n_2 = 1$ corresponds to $\alpha_{-1}\alpha_{-2}|0\rangle$. The proper energy of such a state is given by

$$\alpha' M^2 = N = \sum_m m n_m \tag{2.11}$$

so counting the number of states ρ_N at fixed energy N is a nontrivial combinatorics problem. When faced with such problems in statistical physics, it is often useful to introduce partition function, compute the free energy as a function of temperature, and perform a Legendre transform to obtain the entropy. This situation is no different, so we define z according to

$$z(\beta) = \sum_N \rho_N e^{-\beta N} \tag{2.12}$$

We can think of excitations at different levels as describing distinct noninteracting particles, in which case the partition function factorizes as usual and becomes easier to compute

$$\begin{aligned} z(\beta) &= \prod_n \left[\sum_{\text{states at level } n} e^{-\beta N} \right] \\ &= \prod_n \left(1 - e^{-\beta n}\right)^{-1} \\ &= e^{-\beta/24} \eta\left(\frac{i\beta}{2\pi}\right)^{-1} \end{aligned} \tag{2.13}$$

where in the last line we have written $z(\beta)$ in terms of the Dedekind η function

$$\eta(\tau) = e^{i\pi\tau/12} \prod_{n=1}^{\infty} \left(1 - e^{2\pi i n \tau}\right) \tag{2.14}$$

The appearance of η is of course not surprising given its relation to the exact result for noninteracting closed strings in flat space. The density of states at high energies plays little role in the partition function at large β but is important determining the form of the partition function at small β and consequently it is in this regime that we expect it to be extractible from our general expression for $z(\beta)$. A small β expansion of (2.13) as written is difficult but one can take advantage of the modular property of η

$$\eta\left(-\frac{1}{\tau}\right) = (-i\tau)^{1/2}\,\eta(\tau) \tag{2.15}$$

in order to write $z(\beta)$ in a form more amenable for this analysis. In particular, using (2.15) we can write $z(\beta)$ as

$$\begin{aligned} z(\beta) &= e^{-\beta/24}\sqrt{\frac{\beta}{2\pi}}e^{\pi^2/6\beta}\prod_n\left(1-e^{-4\pi^2 n/\beta}\right)^{-1} \\ &\sim e^{\pi^2/6\beta} \qquad \text{as } \beta \to 0 \end{aligned} \tag{2.16}$$

and hence the leading free energy at high temperatures is given by

$$F(\beta) = -\frac{\pi^2}{6\beta^2} + \ldots \tag{2.17}$$

It is now straightforward to perform a Legendre transform to obtain the entropy as a function of energy. We first find that β as a function of N is given simply

$$\beta = \frac{\pi}{\sqrt{6N}} + \ldots \tag{2.18}$$

which is small in the limit of large N as expected. The entropy is now easily determined from

$$S(N) = \beta(N-F) \approx c\sqrt{N} \tag{2.19}$$

with a coefficient c that here takes the value $2\pi/\sqrt{6}$. Exchanging N for proper energy $E_{\text{proper}} = E/R$, this corresponds to a density of states that exhibits an exponential, or Hagedorn growth at large energies

$$\rho(E) \sim e^{c'\sqrt{\alpha'}E/R} \tag{2.20}$$

and an entropy that is extensive along the string

$$S(E) \sim \frac{E\sqrt{\alpha'}}{R} \tag{2.21}$$

This last result is fairly intuitive and provides a natural explanation for the Hagedorn growth (2.20).

As mentioned above, we expect the same qualitative behavior for strings in $AdS_5 \times S^5$ in the limit that we are considering $R/\sqrt{\alpha'} \gg 1$. Comparing (2.9) and (2.21), we see that this phase has higher entropy than the graviton gas when

$$E > \frac{R^{10}}{{\alpha'}^5} \sim \lambda^{5/2} \tag{2.22}$$

2.2.3 Small Black Hole

As we increase the proper energy beyond m_P, corresponding to taking $E > N^{1/4}$, we expect the gas of strings to collapse and form a small black hole of horizon radius r_0. If we assume that $r_0 \ll R$, the corresponding SUGRA geometry should be well-approximated by the 10-dimensional Schwarzschild solution

$$ds^2 = -f(r)\,dt^2 + f^{-1}(r)\,dr^2 + r^2 d\Omega_8^2 \tag{2.23}$$

where the harmonic function is given by

$$f(r) = 1 - \frac{r_+^7}{r^7} \tag{2.24}$$

The entropy of this solution scales with the horizon area

$$S(r_+) \sim \left(\frac{r_+}{\ell_P}\right)^8 \tag{2.25}$$

and the proper energy is given by the mass

$$E_{\text{proper}} \sim \left(\frac{r_+}{\ell_P}\right)^7 \tag{2.26}$$

where we have inserted factors of the Planck length ℓ_P by dimensional analysis. Combining these, we find that the entropy scales as

$$S(E) \sim \left(\frac{E\ell_P}{R}\right)^{8/7} \tag{2.27}$$

Comparing this with the entropy of the string gas (2.21) we see that small black hole states have higher entropy when

$$E > \frac{R\alpha'^{7/2}}{\ell_P^8} \sim \frac{N^2}{\lambda^{7/4}} \tag{2.28}$$

2.2.4 Big Black Hole

As we move to even higher energies, the Schwarzschild radius of the dominant black hole grows until it eventually becomes of order R, at which point the approximation by 10-dimensional Schwarzschild breaks down completely. Beyond this point, the horizon wraps completely around the S^5 and is strongly affected by the curved geometry in the AdS directions. We will refer to this geometry as the "big" black hole. The corresponding gravity solution given by the AdS-Schwarzschild metric [4, 5]

$$ds^2 = -f(r)\,dt^2 + f^{-1}(r)\,dr^2 + r^2\,d\Omega_3^2 \tag{2.29}$$

with harmonic function

$$f(r) = \frac{r^2}{R^2} + 1 - \frac{\mu}{r^2} \tag{2.30}$$

The ADM mass M of this black hole is proportional to μ and consequently can be related to the Schwarzschild radius by

$$M \sim \frac{r_+^2}{\ell_{P,5}^3}\left(1 + \frac{r_+^2}{R^2}\right) \tag{2.31}$$

where $\ell_{P,5}$ is the effective five-dimensional Planck length which is related to the ten-dimensional one by

$$\ell_{P,5}^3 = \ell_P^8/R^5 \tag{2.32}$$

The entropy is proportional to the horizon area as usual

$$S \sim \left(\frac{r_+}{\ell_{P,5}}\right)^3 \tag{2.33}$$

and consequently the entropy as a function of energy scales as

$$S(E) \sim \left(\frac{R}{\ell_P}\right)^2 E^{3/4} \tag{2.34}$$

This is quite a remarkable result as the scaling of entropy with energy in (2.34) is equivalent to what one finds for a free gas in 1+3-dimensions. We will see in the next chapter that this is for good reason.

As discussed above, the big black hole is expected to overtake the small black hole when its horizon radius becomes of order R. Given (2.31) and (2.32), this corresponds to

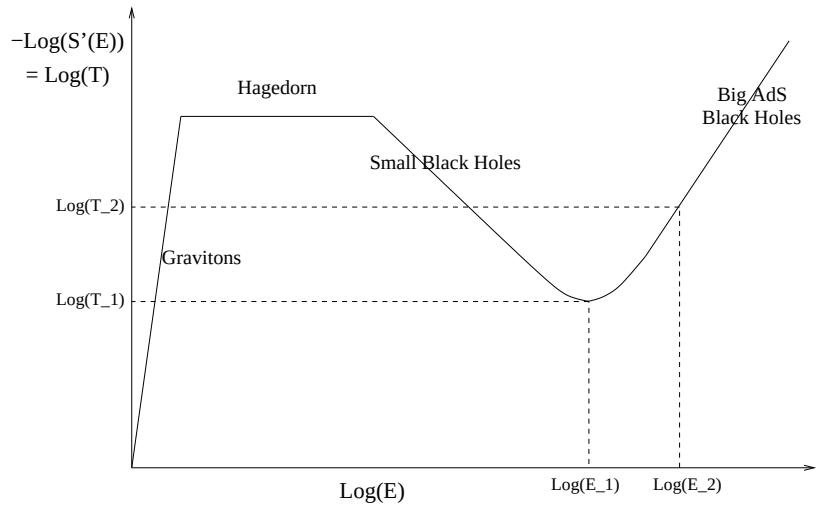

Figure 2.1: $\ln T$ as a function of $\ln E$ for the four phases discussed in section 2.2.

$$E > \frac{R^8}{\ell_P^8} \sim N^2 \tag{2.35}$$

This exhausts our qualitative study. In summary, we have found four phases which dominate the microcanonical ensemble for various ranges of energies.

2.3 Hawking-Page Phase Transition

Now that we have understood the various phases present within the spectrum, we turn next to a study of this system at finite temperature. To get a feel for the qualitative structure of the canonical ensemble, we plot $\ln T$ as a function of $\ln E$ in figure 2.1 for the phases discussed above, using the expressions (2.9), (2.21), (2.27), and (2.34) for their entropies to obtain the corresponding temperatures.

From this plot, we see a few things right away. First, since the sign of the specific heat is equivalent to that of the slope of this curve, the small Schwarzschild black holes are thermodynamically unstable as usual and do not play a role in the canonical ensemble. One

might be surprised, then, that the big AdS black holes are stable. A "physical" reason for this is that their horizon is sufficiently far from the center of AdS that it is sensitive to the curvature, which serves to "reflect" enough Hawking radiation back into the black hole to render it thermodynamically stable.

Since the Hagedorn phase exists only at a fixed temperature, namely the Hagedorn temperature T_H, it doesn't play a role and consequently only the graviton gas and "big" AdS black hole phases are relevant for the finite temperature thermodynamics. At low temperatures, the graviton gas is the only phase and hence dominates by default. At higher temperatures, though, we expect the "big" black hole to become favored and hence we anticipate the existence of a phase transition separating these phases at a finite temperature T_{HP} [4, 5] that should scale as R^{-1} with some constant of order unity. Moreover, the dramatic disparities between the two phases lead us to expect this transition, typically referred to as the Hawking-Page transition, to be of first order[3].

2.3.1 Euclidean Gravity Approach

We now try to be more precise and explicitly demonstrate that this transition occurs and, along the way, determine the value of the critical temperature T_{HP}. How shall we proceed? Let us look to typical quantum field theories for guidance.. The natural framework there for studying finite temperature thermodynamics is the Euclidean path integral with the time direction compactified on a thermal S^1 of length β

$$\int D\phi e^{-S_E} \tag{2.36}$$

In this expression, it is important to note that if the space is noncompact the

[3]Note that the existence of this phase transition prevents us from reaching the divergence associated to the Hagedorn phase at T_H. It has been suggested that a first order transition such as this must occur in flat space string theory as well [21] though it is not clear what the high temperature phase could be in that case.

integral is not taken over all field configurations but instead those with some fixed boundary conditions at infinity. Typically these restrict to configurations that vanish sufficiently fast at infinity, though this need not be the case.

In the classical limit, the integral (2.36) can be evaluated in the saddle point approximation. This corresponds to replacing the integral by a sum over configurations that extremize the action

$$\int D\phi e^{-S_E} \sim \sum_{\text{saddles}} e^{-S_E} \tag{2.37}$$

Hence, we see that the field configurations of the saddles correspond to the various phases that are possible within the system[4] and the Euclidean action indicates their relative weighting in the partition function[5]. The particular phase that dominates the partition function in general depends on the parameters of the system, including the temperature. If the difference between individual terms of (2.37) is parametrically large then the crossovers that occur when the dominant phase changes can be sharpened into phase transitions. In noncompact examples this happens because S_E scales with the volume. In large N gauge theories, on the other hand, it happens because S_E scales with N^2. Note that this latter fact implies that sharp phase transitions are possible in gauge theories even at finite volume provided N is taken to infinity[6].

While we know much less about quantum gravity, the path integral framework exists at least formally and can be used to provide a definition of what one means by the partition function in the classical SUGRA limit [22, 23]. Indeed, one defines the classical limit of the Euclidean path integral at finite temperature in a similar manner

[4]Of course, each such term should be weighted by a 1-loop determinant but this is unimportant in what follows since we assume that the various terms differ exponentially.

[5]This is as we would expect since S_E roughly computes the free energy associated to a given phase.

[6]The reason for this is that by taking N to infinity, we ensure that there are effectively infinitely many degrees of freedom below any fixed energy scale. Of course at finite N, the transitions will be smoothed out.

$$Z_{SUGRA} \approx \sum_{\text{saddles}} e^{-S_E} \tag{2.38}$$

The sum here includes geometries that extremize the Euclidean IIB SUGRA action and satisfy the appropriate boundary conditions. For AdS_5/CFT_4 at finite temperature, the relevant boundary conditions are those of thermal AdS_5. The geometry of thermal AdS_5 itself corresponds to the graviton gas phase and exists for any temperature. The "big" black hole phase, on the other hand, corresponds to the Euclidean version of the metric that we have already written down (2.29). When compactifying Euclidean time on the thermal circle, though, we must be careful because this circle shrinks to zero size in the interior where the horizon was located in the Lorentzian solution. In order to obtain a smooth solution, it is necessary to choose the particular value of β which, for this particular black hole, takes the form

$$\beta = \frac{2\pi R^2 r_+}{2r_+^2 + R^2} \tag{2.39}$$

This is, of course, just the inverse of the Hawking temperature T_H of the "big" black hole. Note that β has a maximum possible value of $\pi R/\sqrt{2}$ and hence we see explicitly that the "big" black hole phase exists, as we knew it must, only for temperatures that are sufficiently large.

To determine which solution dominates, we need to compare the IIB SUGRA action evaluated on the thermal AdS and the "big" black hole solutions. The individual actions actually diverge due to infinite contributions from the boundary but can be suitably regulated to obtain a difference that is finite and can be computed. The result for AdS_5 was first obtained by Witten [5] and takes the simple form

$$S\,(\text{"big" black hole}) - S\,(\text{graviton gas}) = \frac{\pi r_+^3 \left(R^2 - r_+^2\right)}{4G_5 \left(2r_+^2 + R^2\right)} \tag{2.40}$$

The "big" black hole thus becomes dominant precisely when the horizon radius is equivalent to the AdS radius, $r_+ = R$. This corresponds to a critical temperature

$$T_{HP} = \frac{3}{2\pi R} \tag{2.41}$$

that differs from R^{-1} by a constant of order unity, as expected. From (2.40) it is also easy to see that this phase transition of first order.

2.4 Implications for the dual gauge theory

Now that we have a qualitative understanding of the spectrum and phase diagram of the theory in the SUGRA regime, it is natural to ask about the extent to which this structure persists at weak coupling, where the perturbative Yang-Mills description is valid. Provided one doesn't cross a phase transition line while decreasing the coupling, one expects that at least some of the features that we have seen should survive and, in fact, it should be possible to make some rough conjectures as to how this occurs [7].

Let us begin with the spectrum. Since λ is related to the string scale according to $\lambda^{1/4} \sim \alpha'^{-1/2}$, we see that decreasing the coupling has the effect of making the string modes lighter. As a result, we expect the gap between the graviton and string excitations to close, leaving us with one phase whose density of states grows roughly exponentially with energy. This phase shouldn't be a Hagedorn phase with purely exponential growth since we expect that it captures the low temperature thermodynamics. It may eventually give way

[7] Evidence of a phase transition that would invalidate this line of reasoning has been presented in [24]. Because of the consistent picture that emerges here, we believe that this phase transition line, if it exists, does not extend down in the λ/T plane to temperatures of the order that we are considering.

to a Hagedorn phase, though, at some finite energy.

Turning now to the small black holes, their energy is independent of the coupling, scaling as $N^{7/4}$ at large N. However, the range of energies over which they have maximum entropy (2.28) depends on λ and seems to be squeezed out as $\lambda \to 0$. Consequently, we don't expect to see states corresponding to small black holes dominating the spectrum at any energy scale, though they may appear as an unstable phase of the microcanonical ensemble.

Finally, the "big" black holes have energy and range of dominance that are independent of λ and scale with N^2 at large N. We expect this phase to survive at weak coupling and dominate the spectrum at high energies.

Since we expect the phases that dominate the finite temperature thermodynamics to survive at weak coupling in some form, it is natural to expect the Hawking-Page transition line to continue down to this regime as well. There, it will separate phases with free energies of order 1 and N^2 at large N, which is a hallmark of confinement/deconfinement transitions in gauge theories. That the Hawking-Page phase transition connects smoothly to such a transition at weak coupling is an observation that was made by Witten [5], who also noted that there is a natural choice of order parameter in both regimes as well.

2.4.1 Order Parameter at Weak and String Coupling

At strong coupling, the distinguishing characteristic of the black hole phase is the presence of a horizon which, in the Euclidean formulation, corresponds to the fact that the thermal circle is contractible in the bulk. One observable that is sensitive to this fact is the string partition function with the boundary condition that a string worldsheet ends on the thermal circle at infinity. In the SUGRA regime, this quantity will be proportional to e^{-A} where A is area of the minimal worldsheet consistent with the boundary condition. If

the thermal circle is not contractible in the bulk, no finite area worldsheet exists and hence the partition function vanishes [8]. Thus, we see that a nonzero result for this computation signifies contraction of the time circle and hence the existence of a horizon in the bulk [5, 26].

Unfortunately, things are a bit more complicated than this since there is an additional degree of freedom on the worldsheet, the B-field, that we have yet to take into account. As discussed in [5], we must integrate over all values of the B field with $H = dB = 0$. These contribute a phase $i \int B$ to the action so that this integral leads to a vanishing of the string partition function in question[9]. Of course this vanishing is of a different nature than that which occurs when the time circle is not contractible in the bulk. We will encounter a similar phenomenon in the next chapter as well. For now, we simply note that one can distinguish between these two situations and hence render this object a suitable order parameter by deforming the theory in a suitable way.

As argued in [25, 27], the string computation described above corresponds, in the Yang-Mills description, to expectation values of Wilson loop operators[10]

$$W(C) = P \exp\left(i \oint_C A\right) \tag{2.42}$$

The motivation for this correspondence is roughly as follows. The insertion of $W(C)$ into the path integral essentially mimics the placement of heavy classical sources of the non-Abelian gauge field along the loop. To see what this looks like from the point of

[8] Actually, all worldsheets are technically infinite in area due to divergent contributions from the region near the boundary. This divergence can be regulated in a sensible manner, though, so that we can associate a finite area to worldsheets capable of capping off in the bulk [25]

[9] As pointed out by Witten, this is necessary to avoid an obvious contradiction since a nonzero result would have led to spontaneous breaking of the gauge group center in finite volume [5].

[10] Actually, the object to which the string computation corresponds is a bit more complicated, involving couplings to scalar fields as well. This complication does not change the qualitative features of our order parameter, though, so we do not worry about it. Computations of "generalized Polyakov loops" such as this first appeared in [5, 28, 29, 30].

view of the N $D3$-branes on whose world volume the gauge theory propagates, consider instead starting with a stack of $N+1$ branes which is Higgs'ed down to an $SU(N)$ theory by separating one of the branes from the rest. The Higgs multiplets arise from strings stretched between the separated brane and the stack and hence have mass proportional to the distance between them. Taking the separated brane to infinity gives us infinitely massive Higgs multiplets which then behave like classical sources from the point of view of the remaining stack. Consequently, we see that the insertion of classical sources in the Yang-Mills theory corresponds to the imposition of boundary conditions in the string description in which a string extends out toward infinity. A Wilson loop $W(C)$, then, is associated to boundary conditions in which the string worldsheet ends at infinity along the curve C.

As discussed above, the particular Wilson loop that we shall be interested in is that which winds around the Euclidean time circle since it is this object that, at strong coupling, indicates the presence of absence of a horizon. In perturbative gauge theory this object, often referred to as the Polyakov loop [31, 32], computes the exponential of the free energy cost $F_q(T)$ associated to the placement of a classical quark at a fixed point in space

$$W(S^1_\beta) \sim e^{-F_q(T)} \tag{2.43}$$

If the Polyakov loop expectation value vanishes, the free energy cost for adding a classical charge is apparently infinite. This is a characteristic of a confined phase in which the independent degrees of freedom correspond to gauge singlets, leading to difficulty in charge screening and a free energy that scales as N^0 at large N. On the other hand, if the Polyakov loop expectation value is nonvanishing, the free energy cost is finite. This is a characteristic of a deconfined phase in which gluons effectively behave as N^2 independent degrees of freedom, leading to ease of charge screening and a free energy that scales as N^2 at large N.

We thus see that the Yang-Mills situation closely resembles the stringy one in that two phases with free energies of order N^0 at N^2 at large N are distinguished by the Polyakov loop expectation value. We thus expect that the gauge theory counterpart to the Hawking-Page phase transition is simply a confinement/deconfinement transition that occurs at a temperature of order R^{-1} [5]. At strong coupling, AdS/CFT directly implies that such a transition is present. That it continues to weak coupling is not immediately obvious and will be the focus of the next chapter.

Chapter 3

Deconfinement Transition in Yang-Mills Theories on S^3

In this chapter, we seek to probe the phase structure of the AdS_5/CFT_4 system in the weak coupling regime, where the description in terms of perturbative gauge theory is valid. We shall find, perhaps surprisingly, that the qualitative structure of the spectrum and phase diagram is quite similar to what we anticipated in section 2.4 even in the free theory. In particular, we shall find a Hagedorn growth in the density of states up to a limiting temperature equivalent to the Hagedorn temperature, T_H. At this point, the system undergoes a confinement/deconfinement transition that we conjecture is continuously connected to the Hawking-Page transition present at strong coupling.

Perhaps more surprisingly, this structure turns out to be quite generic, at least for asymptotically free Yang-Mills theories on S^3 coupled to adjoint matter. Because of this, we shall be quite general in our analysis throughout most of this chapter, specializing to the $\mathcal{N} = 4$ theory only when absolutely necessary. Of course, one might worry about the validity of perturbation theory in the asymptotically free theories since one cannot simply

set the coupling to be small as in the $\mathcal{N} = 4$ theory. Because we are studying the theories on a compact manifold, though, the size provides us with a dimensionful scale that can be adjusted independently of Λ_{QCD}. In particular, perturbation theory is reliable when the radius R of the S^3 is sufficiently small that $R\Lambda_{QCD} \ll 1$. Moreover, it is natural to conjecture that the transition we shall find in this regime continues, upon varying $R\Lambda_{QCD}$, to the usual flat space confinement/deconfinement transition at $R\Lambda_{QCD} \gg 1$[1].

Most of this chapter will thus be devoted to a systematic study of free Yang-Mills theories on S^3 coupled to adjoint matter following [6]. For simplicity we shall focus primarily on $U(N)$ theories, though the generalization to the $SU(N)$ theories is not difficult and should be clear from our analysis. We shall begin with a toy example that illustrates the main ideas and then proceed to demonstrate that it is dominated at low temperatures by a confined phase with a Hagedorn growth in the density of states. This analysis will depend crucially on the assumption of infinite N and consequently will not be suitable for a study of the deconfined phase. To go further, we will then demonstrate, using two different approaches, that the thermal partition function of free Yang-Mills theories on S^3 is effectively computed by a unitary matrix model. This will permit a more detailed analysis of the transition point and provide a framework for studying the effects of a small nonzero coupling.

We finally note that much of the material in this chapter appeared before the publication of [6] in a beautiful paper written by B Sundborg [34] of which we became aware only after [6] was completed. A phase transition of the sort that we shall discuss was also studied in a specific example in [35].

[1] See [33] for a review of this system.

3.1 Confinement in a Free Theory?

To begin our study, we first address the important issue of how confinement can possibly occur in a free gauge theory. After all, one normally associates confinement with strong coupling dynamics which are obviously absent in theories without interactions. In the case of Yang-Mills theories on compact spaces such as S^3, though, there is a sense in which confinement comes for free. What drives this is the Gauss law constraint, which restricts the space of physical states to those which are gauge invariant[2]. Roughly speaking, this is required by the fact that field lines for a single gluon, for instance, have nowhere to end on the S^3. From the path integral point of view, one can see this more directly, as we will later on, by noting that the restriction to gauge singlets is imposed by integrating over the constant mode of the component of the gauge field along the Euclidean time circle, ${A_0}^3$.

In some sense, then, the theory is always confined since nonsinglet states can never appear. As a result, we expect the free energy cost of adding a classical charge to be infinite, leading to vanishing of the Polyakov loop at all temperatures. Nonetheless, we shall see deconfinement in two ways. First, above the critical temperature the free energy will scale as N^2 at large N, indicating that the system indeed behaves as though there are roughly $\mathcal{O}(N^2)$ degrees of freedom. Second, we will find that there is a sense in which the Polyakov loop is nonzero at high temperatures.

[2]Note that the situation differs from that of flat space because here one cannot define asymptotic gauge invariant single gluon states by adiabatically turning off the coupling. Consequently, one is restricted to singlet combinations even at infinitesimal coupling. Of course, if one starts with a free theory then there is a choice as to whether or not to impose this condition. The two possibilities correspond to the $g_{YM} \to 0$ limit of the $U(N)$ and $U(1)^{N^2}$ theories. We wish to focus on the former and consequently impose the constraint.

[3]Note that this mode is nonnormalizeable in theories on noncompact spaces so in such cases it is not integrated over.

3.1.1 A toy model of two matrices

To demonstrate how application of the Gauss law impacts the thermodynamics, we turn now to a simple toy system, namely free quantum mechanics of two $U(N)$ adjoint-valued fields A and B of unit mass. We can think of these fields as corresponding to the constant modes of two scalars of the $\mathcal{N} = 4$ theory on S^3 with mass arising from the usual coupling $\mathcal{R}\phi^2$ of scalars to the background curvature that is required for conformal invariance. With this in mind, we impose the constraint that physical states in our model must be singlets under the $U(N)$ gauge group.

Because this system is simply a pair of matrix-valued harmonic oscillators, the states are enumerated by the Fock space associated to two $N \times N$ matrices of creation operators, $A^\dagger$ and $B^\dagger$. Physical states then correspond to those that are created by gauge-invariant combinations of $A^\dagger$ and $B^\dagger$. There is another way to think about the state space that provides a more useful language in our study of of gauge theories, though. In particular, note that the various combinations of creation operators are trivially in one-to-one correspondence with local operators formed from the fields A and B. That this is true is hardly surprising since our toy model, by virtue of being a theory of noninteracting scalar fields with the appropriate $\mathcal{R}\phi^2$ couplings, is itself conformal. As a result, this correspondence is nothing more than the usual state-operator map.

State-Operator Map

Because we shall make extensive use of it later, we pause now to say a few brief words about the state-operator correspondence in conformal field theories and, specifically, in the systems of interest to us. The basic idea is that, in the path integral, the effect of boundary conditions associated to a particular state on an initial value surface are completely captured by the insertion of a local operator in a conformally equivalent formulation.

The example most familiar in string theory is that of two-dimensional conformal field theory on a cylinder $S^1 \times \mathbb{R}$ with the $\mathbb{R}$ direction identified with time. There, one associates states of the CFT with boundary conditions on the circles in the far past and far future. This system can be conformally mapped to the complex plane in such a manner that constant spatial slices are mapped to circles of increasing radius centered at the origin. In particular, the circle in the infinite past gets mapped to the origin itself so that, roughly speaking, all information regarding the boundary conditions there determine a local operator insertion. Moreover, because the time coordinate on the cylinder is mapped to the radial direction on the complex plane, energies of states correspond to scaling dimensions of operators. The situation for the four-dimensional conformal theories that we shall study is completely analagous, with quantization along the "cylindrical" $S^3 \times \mathbb{R}$ being conformally mapped to radial quantization on $\mathbb{R}^4$. A state on the S^3 in the infinite past with energy E is mapped to the origin in $\mathbb{R}^4$ where it is identified with a local operator of scaling dimension E.

Hagedorn Growth and Confinement in the Strict $N = \infty$ Limit

We now return to our toy model and describe some basic features of the thermodynamics at large N, postponing a precise treatment to the next section. In the strict $N = \infty$ limit, this system is particularly easy to study since all gauge invariant operators can be written uniquely as polynomials of single trace operators. Because of this, we can think of single (multi) trace operators as single (multi) particle states in a Bose gas. The full partition function can then be constructed from that of single trace operators using simple Bose statistics.

A single trace operator of energy E is specified by a string of E fields, each of which can be either an A or a B. Because of the cyclicity property of the trace, though, we must impose a series of relations on these strings that cut down the number which correspond to

distinct operators. In particular, a given string of E operators will be identified with up to $E-1$ others. From these considerations, we obtain the following upper and lower bounds on the number $n(E)$ of single trace operators at energy E

$$\frac{2^E}{E} < n(E) < 2^E \tag{3.1}$$

With this result alone, we can already say quite a lot about the thermodynamics. In particular, we note that the spectrum of single trace states exhibits the Hagedorn growth that we anticipated in section 2.4[4]

$$\rho(E) \sim E^\alpha e^{\beta_H E} \tag{3.2}$$

where $\beta_H = \ln 2$ and α is a constant that we have not determined. The finite temperature partition function for single trace states can be computed directly from this and is perfectly well-behaved for sufficiently small temperatures. Due to the exponential growth in the density of states, though, this partition function, and hence the full multi-trace partition function as well, diverges for temperatures larger than β_H^{-1}.

How are we to interpret this structure? Because we have implicitly assumed strictly infinite N throughout this discussion, the free energy at low temperatures, which is finite in this limit, must scale as N^0 at large N. Consequently, we see that the gauge invariance constraint has led to the expected confining behavior at least at low temperatures. More interestingly, though, the divergence of the partition function caused by the Hagedorn growth should be associated with diverging N-dependence and hence suggests that the free energy scales as a positive power of N at high temperatures.

We can understand this roughly as follows. The importance of the infinite N limit was our ability to write gauge invariant operators as polynomials of single traces of

[4]Hagedorn-like behavior in free large N systems has also been observed in [36].

arbitrary length. At finite N, however, the number of gauge-invariant degrees of freedom of the two fields is of order N^2 [5] and consequently there are a finite number of independent operators that one can write down. In the language of traces, this cut down in the number of operators arises from nontrivial relations between polynomials of traces of varying degree. For instance, single traces with more than N^2 fields can be written as polynomials of traces of fewer fields. The effect of this is to render our polynomial basis of single trace operators vastly overcomplete. Our method thus leads to significant overcounting that drives the divergence at β_H^{-1}. Unfortunately, there is no clear choice of complete polynomial basis at finite N which permits us to construct the full partition function from a simpler one over a reduced sector of "single-particle" states. Consequently, we will have to be a bit more clever in order to see the deconfined phase explicitly. We will demonstrate how to do this in the next section.

3.2 Partition Function of the Free Theory I – Counting

We now move on to study free theories with more general adjoint matter content. Provided the scalars are conformally coupled, we can use the state-operator correspondence as in the previous section to formulate the computation of the thermal partition function as a constrained counting problem. The basic "letters" which form the building blocks of operators and play the role of A and B in our toy model consist of the fields themselves, ϕ, as well as derivatives of fields, $\partial^k\phi$, modulo combinations that vanish by the equations of motion. A convenient way of packaging the information related to matter content is with the "letter" partition functions

[5] One might think that since there are N eigenvalues the number of gauge invariant degrees of freedom scales like N. Note, however, that we do not assume the two fields to be commuting so it is impossible to simultaneously diagonalize them both.

$$z(x) = \sum_{\text{letters}} x^{\Delta} \tag{3.3}$$

where $x = e^{-\beta}$ and Δ is the scaling dimension of each letter. For instance, in the $\mathcal{N} = 4$ SYM theory, the full letter partition function $z(x)$ receives contributions from scalar, fermion, and gauge field letters. The partition functions $z_S(x)$, $z_F(x)$, and $z_V(x)$ corresponding to these three contributions are easy to compute. This is done in appendix A with the result

$$z_S = \frac{x(1+x)}{(1-x)^3} \qquad z_F(x) = \frac{4x^{3/2}}{(1-x)^3} \qquad z_V(x) = \frac{x^2(6-2x)}{(1-x)^3} \tag{3.4}$$

As we shall now demonstrate, the full partition function can be expressed, both in the strict infinite N limit as well as the more general case of finite N in terms of the total letter partition function, $z(x)$. In particular, it is only through $z(x)$ that model-specific information enters into the problem. Interestingly, the qualitative structure will depend only on generic properties of $z(x)$ so we will not find it necessary to restrict to the $\mathcal{N} = 4$ theory at any point in this analysis.

3.2.1 Partition Function at $N = \infty$

We begin by reconsidering the strict infinite N limit, this time in a bit more detail. For simplicity, we also restrict ourselves to bosonic fields for now. As in the previous section, we expect in this limit to compute the full partition function from that of the single-trace sector through the application of Bose statistics. The partition function Z_k of single-trace states built from k letters is naively given by the kth power of the letter partition function. However, as we have seen before, one must also impose relations arising from cyclicity of the trace. This implies that Z_k takes the form

$$Z_k = \frac{z(x)^k}{k} + \dots \tag{3.5}$$

where the contributions that we have neglected are positive. For now, let us be a bit naive and simply drop these additional terms entirely. In this case, the single trace partition function can be written as

$$Z_{ST} = \sum_{k=1}^{\infty} Z_k = -\ln\left(1 - z(x)\right) \tag{3.6}$$

and consequently the full partition function takes the form

$$\begin{aligned} Z(x) &= \exp\left\{\sum_{n=1}^{\infty} \frac{1}{n} Z_{ST}(x^n)\right\} \\ &= \exp\left\{\sum_{n=1}^{\infty} \frac{1}{n} \ln\left(1 - z(x^n)\right)\right\} \end{aligned} \tag{3.7}$$

To study the behavior of $Z(x)$, we note that the letter partition function $z(x)$ increases monotonically with x starting from $z(0) = 0$. This implies that for sufficiently small x, corresponding to sufficiently small temperatures, the partition function $Z(x)$ is well-behaved, even at infinite N. This is the confined phase.

At the critical value x_H satisfying $z(x_H) = 1$, though, we see that the partition function diverges at infinite N, signaling the likely onset of deconfinement as discussed in the previous section. The divergence of the single-trace partition function is proportional to $-\ln(\beta - \beta_H)$ which is a hallmark of exponential growth in the density of states

$$\rho_{ST}(E) \sim e^{\beta_H E} \tag{3.8}$$

Note that, for the two matrix example of the previous section, $z(x) = 2x$ so that $x_H = 1/2$. This corresponds to $\beta_H = \ln 2$ as we saw there.

Of course, we have neglected the impact of the cyclic property of the trace in the analysis above. To include this, we need to do a more careful counting of single-trace states. This can be accomplished using Polya theory, as demonstrated in the appendix A. Here, we simply quote the result that the actual single-trace partition function takes the form

$$Z_{ST} = -\sum_{q=1}^{\infty} \frac{\varphi(q)}{q} \ln\left(1 - z(x^q)\right) \tag{3.9}$$

with $\varphi(q)$ the Euler totient function yielding the number of positive integers which are relatively prime to and not larger than q. Using this result, it is straightforward to obtain the exact expression for the full partition function

$$Z = \exp\left\{-\sum_{n=1}^{\infty} \ln\left(1 - z(x^n)\right)\right\} \tag{3.10}$$

which differs from the naive result (3.7) only in the disappearance of a factor of n^{-1} in the summand. Taking care to impose trace cyclicity thus has very little effect on the qualitative structure of this partition function below the critical temperature at which it diverges. Indeed, the Hagedorn temperature itself even continues to be determined by the equation $z(x_H) = 1$.

Before concluding this subsection, we note that it is straightforward to include fermi fields into the analysis above. The result of doing this is simply the replacement [6]

$$z(x^k) \to z_B(x^k) + (-1)^{k+1} z_F(x^k) \tag{3.11}$$

in equation (3.10) where z_B (z_F) is the bosonic (fermionic) letter partition function.

3.2.2 Exact Partition Function

As discussed at the end of section 3.1.1, we will need more sophisticated analysis in order to directly probe the deconfined phase where the leading free energy scales with

N^2. For this reason, we drop our attempts to reformulate the counting problem as one of Bose statistics and instead attack the counting of gauge invariant states as a group theory problem. In particular, we wish to sum over all series of letters weighted by the number of ways in which a given series can be combined to form a gauge singlet. Schematically, this can be written as

$$Z(x) = \sum_{n_1=0}^{\infty} x^{n_1 E_1} \sum_{n_2=0}^{\infty} x^{n_2 E_2} \ldots \{\#\text{of singlets in } \mathrm{sym}^{n_1}(R_1) \otimes \mathrm{sym}^{n_2}(R_2) \otimes \ldots\} \quad (3.12)$$

where R_i is the representation in which the ith letter transforms and $\mathrm{sym}^{n_i}(R_i)$ denotes the n_i-fold symmetric tensor product of the representation R_i. Determining the number of singlets that appear in a given tensor product is a purely group theoretical question so one might hope that a general answer is simple to obtain. Indeed, this is easily done using group characters, which we now briefly review.

Group Characters

Given a group G and a representation R, the character $\chi_R(U)$ evaluated on the element U of G is simply the trace of U in the representation R. Among the various properties of $\chi_R(U)$ are the useful relations

$$\chi_{R_1 \oplus R_2} = \chi_{R_1} + \chi_{R_2} \qquad \chi_{R_1 \otimes R_2} = \chi_{R_1} \cdot \chi_{R_2} \quad (3.13)$$

as well as the orthogonality property

$$\int dU \, \chi^*_{R_1}(U) \chi_{R_2}(U) = \delta_{R_1 R_2} \quad (3.14)$$

where R_1 and R_2 are irreducible representations and dU denotes the Haar measure normalized so that the group volume is unity. Consider now the tensor product rep-

resentation $R_1 \otimes R_2 \otimes \ldots$ which decomposes into irreducible representations according to $R_1' \oplus R_2' \oplus \ldots$. Using (3.13), (3.14), the the fact that the character $\chi_{\mathbf{1}}(U)$ of the singlet representation is 1 for all U, we see that integrating the character of the tensor product over the group manifold yields the result

$$\begin{aligned}\int dU\, \chi_{R_1 \otimes R_2 \otimes \ldots}(U) &= \int dU\, \chi_{R_1' \oplus R_2' \oplus \ldots}(U) \\ &= \int dU\, \chi_{\mathbf{1}}^*(U) \left(\chi_{R_1'}(U) + \chi_{R_2'}(U) + \ldots\right) \\ &= \sum_i \delta_{\mathbf{1},R_i'}\end{aligned} \tag{3.15}$$

This is nothing more than the number of singlets that appear in the tensor product. We thus see that the group theoretic factor we seek is nothing more than a character integral. For this result to be useful, though, we wish to find a simple expression for the character of the n-fold symmetric tensor product of a given representation R. Letting U_R denote the matrix representation of the element U in the representation R, this character can be written as

$$\chi_{\mathrm{sym}^n(R)}(U) = (U_R)^{a_1}_{\{a_1} \ldots (U_R)^{a_n}_{a_n\}} \tag{3.16}$$

where the curly braces $\{\,\}$ denote symmetrization of indices with unit weight. Fortunately, the object that will arise in our analysis is actually a generating function of such characters, for which a simple formulae is easy to obtain. Indeed, if we define

$$G_+(U,t) = \frac{1}{\pi}^{\dim(R)} \int d\phi\, \exp\left\{-\bar{\phi}\phi + t\bar{\phi}U_R\phi\right\} \tag{3.17}$$

for ϕ a complex bosonic variable in the representation R, then it is easy to verify the following by expanding the integrand in powers of t

$$G_+(U,t) = \sum_{n=0}^{\infty} t^n \chi_{\mathrm{sym}^n(R)}(U) \tag{3.18}$$

The integral in $G_+(U,t)$ is Gaussian, though, so can be evaluated directly

$$\begin{aligned} G_\pm(U,t) &= \left(\det(1 \mp tU_R)\right)^{-1} \\ &= \exp\left\{-\mathrm{tr}\, \ln\left(1 - tU_R\right)\right\} \end{aligned} \tag{3.19}$$

Expanding in t we thus finally arrive at the result

$$\sum_{n=0}^{\infty} t^n \chi_{\mathrm{sym}^n(R)}(U) = \exp\left\{\sum_{\ell=1}^{\infty} \frac{t^\ell}{\ell} \chi_R(U^\ell)\right\} \tag{3.20}$$

It is a simple manner to repeat this procedure for antisymmetric tensor products to obtain the analagous result [6]

$$\sum_{n=0}^{\infty} t^n \chi_{\mathrm{anti}^n(R)}(U) = \exp\left\{\sum_{\ell=1}^{\infty} \frac{(-1)^{\ell+1} t^\ell}{\ell} \chi_R(U^\ell)\right\} \tag{3.21}$$

Exact Result as a Unitary Matrix Model

Let us return now to the expression (3.12), which we rewrite using group characters as

$$Z(x) = \int dU \left[\prod_i \left(\sum_{n_i} x^{n_i E_i} \chi_{\mathrm{sym}^{n_i}(R_i)}(U)\right)\right] \tag{3.22}$$

where as usual we include only bosonic fields for simplicity. Using the result (3.20) we can rewrite this as

$$Z(x) = \int dU \, \exp\left\{\sum_i \sum_{\ell=1}^{\infty} \frac{x^{\ell E_i}}{\ell} \chi_R(U^\ell)\right\} \tag{3.23}$$

We now specialize to the case of adjoint matter so that the character $\chi_R(U)$ can be written in terms of traces in the fundamental as

$$\chi_{R=\text{Adj}}(U) = \text{tr}\,(U)\text{tr}\,(U^\dagger) \tag{3.24}$$

Using this and the definition (3.3) of the letter partition functions we can finally write (3.23)

$$Z(x) = \int dU\, \exp\left\{\sum_{\ell=1}^{\infty} \frac{z(x^\ell)}{\ell}\text{tr}\,(U^\ell)\text{tr}\,(U^{-\ell})\right\} \tag{3.25}$$

As usual, it is not difficult to generalize this to include the possibility of fermionic letters. The resulting expression is identical to (3.25) with the replacement (3.11).

We have thus demonstrated that the exact partition function of a free conformally invariant Yang-Mills theory with generic adjoint matter content is equivalent to a unitary matrix model. A direct analysis of (3.25) should be able to reproduce the Hagedorn growth at low temperatures as well as permit a direct study of the deconfined phase at high temperatures. The meaning of the matrix U here, though, is quite unclear as it was introduced as an auxiliary object to faciliate the computation of group theoretical factors. Before proceeding to analyze this matrix model in detail, we digress for a moment to derive it directly from the path integral point of view. This will make clear the physical interpretation of U as well as provide a framework with which we can extend our analysis to theories with small nonzero coupling.

3.3 Partition Function of the Free Theory II – Path Integral

We now seek to study the thermal partition function of free $U(N)$ Yang-Mills theories coupled to adjoint matter from the path integral point of view. This is accomplished

by considering the Euclidean path integral on $S^3 \times S^1_\beta$ where the radius of the S^3 is denoted by R and the circumference of the thermal circle is the inverse temperature. We shall find it convenient to instead rescale the entire system so that the S^3 has unit radius and the thermal circle has circumference given by the dimensionless inverse temperature $\beta = 1/RT$.

3.3.1 Partition Function as an Integral over a Single Matrix?

Our goal is to reproduce the unitary matrix model (3.25) from this approach. While the equivalence of the partition function of a four-dimensional field theory to an integral over a single unitary matrix may seem surprising at first glance, it is actually quite easy to see how it occurs from a quick perusal of the mode spectrum. Because the theory is free, the action contains a collection of noninteracting modes corresponding to various eigenfunctions of the Laplace operator. The scalar fields, for instance, admit a decomposition into S^3 scalar spherical harmonics. As mentioned in appendix A, these transform in representations $(k/2, k/2)$ of the isometry group $SU(2) \times SU(2) = SO(4)$ and have eigenvalue $k(k+2)$. Combined with the unit mass that arises from the conformal coupling $\mathcal{R}\phi^2$ of scalars to the sphere's curvature, the energies of these modes are given by $(k+1)^2$ for integer $k \geq 0$. The key point here is that all of the scalar modes are massive.

Similar arguments apply for the fermions, which can be expanded in spinor spherical harmonics, and gauge fields, whose components can be expanded in combinations of vector and scalar spherical harmonics. Studying the spectrum in each case, we find that all modes in the problem are massive except for exactly one, namely the constant mode α of A_0

$$\alpha = \frac{1}{\mathrm{Vol}(S^3 \times S^1)} \oint_{S^3} \oint_{S^1} A_0 \tag{3.26}$$

We actually knew that something like this had to be the case from the state-

operator map since a massless mode would have corresponded to an operator of scaling dimension zero. There are no such operators other than the identity operator, which is identified with the vacuum, so all modes should be massive.

This presents us with a slightly different puzzle, then. Since the state-operator map suggests that all states are massive how do we interpret the massless mode α? As we have hinted at before, α plays a rather special role from the path integral point of view in that performing the integral over this mode precisely enforces the Gauss law constraint that drives all of the interesting physics. Let us see this in a bit of detail.

The Gauss Law Constraint

Consider pulling the integral over α outside of the others in the path integral. We would naively like to perform a gauge transformation within the remaining integral to remove this mode so that the integral over α can be performed trivially. This can be accomplished with a gauge transformation generated by

$$U_\alpha(t) = e^{i\alpha t} \tag{3.27}$$

since

$$\alpha \to U_\alpha(t)\alpha U_\alpha^\dagger(t) - i\left[\partial_t U_\alpha(t)\right] U_\alpha^\dagger(t) = 0 \tag{3.28}$$

In addition to removing the zero mode from A_0, though, this gauge transformation shifts the boundary conditions in the path integral from periodic along β to

$$A_\mu(t=0) = A_\mu^\alpha(t=\beta) \tag{3.29}$$

where A_μ^α denotes the image of A_μ under the constant unitary rotation generated by

$$U_{\alpha,\beta} = e^{i\beta\alpha} \tag{3.30}$$

Integrating over α now corresponds to integrating over boundary conditions for the gauge fields twisted by gauge transformations of this type. This amounts to a projection onto invariant states and hence is responsible for imposing the constraint that only configurations that are invariant under global $U(N)$-transformations contribute to the path integral[6]. It is now clear why there is no operator corresponding to α in the counting arguments of the previous section. When we impose this constraint on physical states, we have already implicitly integrated over α.

Form of the Matrix Integral

Since we have seen that the spectrum of the free theory on S^3 is gapped, it is sensible to integrate all of the massive modes in order to obtain an effective action $S_{\text{eff}}(\alpha)$ for the massless one. Before actually computing this action, wow much can we say about its from simply from the constraints of gauge invariance?

We first note that $S_{\text{eff}}(\alpha)$ should be invariant under constant $U(N)$ rotations. This implies that the action should depend only on the eigenvalues of α, which we can now take to be diagonal. In addition, because they don't mix α with other modes of the gauge field, the effective action should also be invariant under gauge transformations of the form

$$V(t) = e^{itD} \tag{3.31}$$

for D a diagonal matrix with eigenvalues that must be integer multiples of $2\pi/\beta$ to guarantee single-valuedness on the thermal circle. This individually shifts the eigenvalues

[6]Note that this is enough to completely account for the Gauss law constraint that we imposed on local operators at zero coupling.

of α and consequently implies that α appears in $S_{\text{eff}}(\alpha)$ only through the quantity

$$U = e^{i\beta\alpha} \tag{3.32}$$

Finally, the action should also be invariant under gauge transformations of the form

$$V'(t) = e^{i\theta t/\beta} \tag{3.33}$$

which are single-valued by virtue of the fact that $e^{i\theta}$ belongs to the center of $U(N)$. Since the effect of this is an arbitrary constant shift of all eigenvalues of α, Invariance under $V'(t)$ implies that U may only appear in combinations for which the total power of U is equivalent to the total power of $U^\dagger$ as in

$$\text{tr}\,(U^{n_1})\ldots\text{tr}\,(U^{n_k})\text{tr}\,(U^{-n_1-\ldots-n_k}) \tag{3.34}$$

Of course, all of the arguments that we made above apply to the full path integral so we expect that the integration measure of the model obtained after integrating out the massive modes is simply the Haar measure of $U(N)$. We have thus found that the effective theory for the dynamics of α must take the form of a unitary matrix model whose form is somewhat constrained. Not surprisingly, the resulting model in the free theory will turn out to be (3.25) with the matrix U identified with α as in (3.32).

3.3.2 Deriving the Matrix Model

We now proceed to integrate out the massive modes of the free theory to directly obtain an effective action for α (3.26). This corresponds to a 1-loop computation in the weakly coupled theory that can be supplemented by higher loop contributions later if we

wish to consider the effects of interactions. For simplicity, we shall specialize to pure $U(N)$ Yang-Mills theory with no matter fields. The generalization to theories with adjoint matter will then be straightforward.

Gauge Fixing and the Measure

Our first task is to choose a suitable gauge in which to perform the computation. Because of the natural splitting of space, S^3, and time, S^1, a convenient choice is provided by Coulomb gauge

$$\partial_i A^i = 0 \tag{3.35}$$

where i runs over the three S^3 directions. This choice fixed the gauge freedom only partially, though, as it leaves unfixed gauge transformations that are spatially independent but time dependent. We fix this residual gauge-invariance with the further condition

$$\partial_t \oint_{S^3} A_0 = 0 \tag{3.36}$$

This has the effect of eliminating all spatially constant modes of A_0 except for the zero mode α.

As usual, when we impose the gauge fixing conditions (3.35) and (3.36), we pick up Fadeev-Popov determinant factors. That associated to (3.35) is given by

$$\Delta_1 = \det{}' \left(\partial^i D_i\right) \tag{3.37}$$

where D_i denotes a gauge covariant derivative along one of the spatial S^3 directions and the prime on the determinant indicates that zero modes are omitted. In the free theory, D_i is simply ∂_i so this is nothing more than

$$\Delta_1 = \det{}' \left(\partial_i \partial^i\right) \tag{3.38}$$

When we turn on interactions, the full covariant derivative will become important and it will be necessary to introduce Fadeev-Popov ghosts to facilitate the computation of Δ_1.

The determinant associated to the second condition, (3.36), will turn out to be a bit more interesting. It takes the form

$$\Delta_2 = \det{}' \left(\partial_0 - i[\alpha, *]\right) \tag{3.39}$$

where the prime on the determinant again indicates that zero modes are omitted. Letting λ_i denote the eigenvalues of α, we can evaluate this determinant explicitly as follows

$$\begin{aligned} \Delta_2 &= \prod_{n\neq 0} \prod_{i,j} \left[\frac{2\pi i n}{\beta} - i\left(\lambda_i - \lambda_j\right)\right] \\ &= \left(\prod_{m\neq 0} \frac{2\pi i m}{\beta}\right) \left[\prod_{i,j} \frac{2}{\beta(\lambda_i - \lambda_j)} \sin\left(\frac{\beta\left(\lambda_i - \lambda_j\right)}{2}\right)\right] \end{aligned} \tag{3.40}$$

To see the importance of this, recall that the measure for integrating over the eigenvalues of a Hermitian matrix is

$$d\alpha = \prod_k d\lambda_k \prod_{i<j} \left(\lambda_i - \lambda_j\right)^2 \tag{3.41}$$

while the measure for integrating over the eigenvalues $e^{i\beta\lambda_i}$ of the unitary matrix U (3.32) is

$$dU = \prod_k d\lambda_k \prod_{i<j} \sin^2\left(\frac{\beta(\lambda_i - \lambda_j)}{2}\right) \tag{3.42}$$

Consequently, up to an overrall constant the Fadeev-Popov determinant (3.40) has the effect of converting the Hermitian integration over α (3.26) to unitary integration over U (3.32)

$$d\alpha\, \Delta_2 = dU \tag{3.43}$$

This natural emergence of unitary measure is quite encouraging.

The Effective Action $S_{\text{eff}}(U)$

Now that we have gauge-fixed the path integral, let us turn to its evaluation. In Coulomb gauge, the path integral of the free Yang-Mills theory takes a particularly simple form

$$Z = \int dU\, DA_i\, DA_0\, \delta\left(\partial_i A^i\right)\, \Delta_1\, \exp\left\{-\int \text{tr}\, \left(\frac{1}{2}A_i\left(\tilde{D}_0^2 + \partial^2\right) A^i + \frac{1}{2}A_0 \partial^2 A_0\right)\right\} \tag{3.44}$$

where

$$\tilde{D}_0 = \partial_0 - i[\alpha, *] \tag{3.45}$$

To proceed further, we note that any vector field on the sphere may be decomposed as

$$A_i = \partial_i \phi + B_i \tag{3.46}$$

where $\partial_i B^i = 0$. Integration over the scalar piece, ϕ, can be done using the δ-function. In the process, we pick up a determinant factor

$$\det{}'\left(\partial_i \partial^i\right)^{-1/2} \tag{3.47}$$

Performing the integral over A_0 yields an equivalent factor so that these two combine to cancel the determinant from Δ_1. In the end, we are thus left with

$$\begin{aligned} Z &= \int dU\, dB_i\, \exp\left\{-\frac{1}{2}\int \text{tr}\, \left(B_i \left(\tilde{D}_0^2 + \partial^2\right) B^i\right)\right\} \\ &= \int dU\, \exp\left\{-S_{\text{eff}}(U)\right\} \end{aligned} \tag{3.48}$$

where $S_{\text{eff}}(U)$ is computed by performing the Gaussian integration over B_i. The result of this is

$$\begin{aligned} S_{\text{eff}}(U) &= \frac{1}{2} \ln \det \left(-\tilde{D}_0^2 - \partial^2\right) \\ &= \frac{1}{2} \sum_{\Delta} n(\Delta) \ln \det \left(-\tilde{D}_0^2 + \Delta^2\right) \end{aligned} \tag{3.49}$$

where Δ^2 are the eigenvalues of the Laplace operator acting on vector spherical harmonics and $n(\Delta)$ is the corresponding degeneracy. The above functional determinant is straightforward to compute by passing to momentum space

$$S_{\text{eff}}(U) = \det_{U(N)} \left[\prod_{n=-\infty}^{\infty} \left(\frac{4\pi^2 n^2}{\beta^2} + \frac{4\pi n}{\beta}\alpha + \alpha^2 + \Delta^2\right)\right] \tag{3.50}$$

The above product is similar to those that appear when studying harmonic oscillators and is hence straightforward to evaluate [6]. The result is given by

$$\prod_{n=-\infty}^{\infty} \left(\frac{4\pi^2 n^2}{\beta^2} + \frac{4\pi n}{\beta}\alpha + \alpha^2 + \Delta^2\right) = \mathcal{N} e^{\beta\Delta} \left(1 - e^{-\beta\Delta} U\right) \left(1 - e^{-\beta\Delta} U^{-1}\right) \tag{3.51}$$

where $\mathcal{N}$ is a divergent β-dependent constant that we set to unity in order to correctly reproduce the free energy of the harmonic oscillator at $\alpha = 0$. Using this result, we can write $S_{\text{eff}}(U)$ as

$$S_{\text{eff}}(U) = \frac{1}{2}\sum_{\Delta} n(\Delta)\text{tr}\,\left(\beta\Delta + \ln\left(1 - e^{-\beta\Delta}U\right)\left(1 - e^{-\beta\Delta}U^{-1}\right)\right) \tag{3.52}$$

We now drop the U-independent $\beta\Delta$ term, which contributes a Casimir energy that we shall neglect, and expand the logarithms. Passing from the adjoint representation to the fundamental via (3.24) and using the definition (3.3) we finally obtain the result

$$S_{\text{eff}}(U) = -\sum_{n=1}^{\infty}\frac{z_V(x^n)}{n}\text{tr}\,(U^n)\text{tr}\,(U^{-n}) \tag{3.53}$$

which is precisely the matrix model (3.25) that we derived before by completely different means. It is now straightforward to include adjoint matter fields and demonstrate that in these cases the matrix models agree as well.

3.4 The Unitary Matrix Model – A Heuristic Analysis

Now that we have demonstrated the equivalence of the thermal partition function of our free Yang-Mills theory with the unitary matrix model (3.25) in two different ways, we turn to a direct study of the model with particular attention to its phase structure. The analysis of this section will be somewhat heuristic as we seek to demonstrate the existence of a large N phase transition and study its general behavior. Some technical details that are not immediately necessary for what we want to say are relegated to appendix B.

To study the matrix model (3.25) at large N, we first write it as an integral over eigenvalues α_i which take values on a circle of unit radius

$$Z = \int\prod_k d\alpha_k \prod_{i<j}\sin^2\left(\frac{\alpha_i - \alpha_j}{2}\right)\exp\left\{\sum_n\sum_{i,j}\frac{1}{n}z(x^n)\left(e^{in(\alpha_i-\alpha_j)}\right)\right\} \tag{3.54}$$

At large N, there are enough eigenvalues that we can describe any given configuration by a density function $\rho(\alpha)$ on the circle. Choosing this function to have unit norm

$$\int d\alpha\, \rho(\alpha) = 1 \tag{3.55}$$

we see that its Fourier moments correspond precisely to the normalized traces

$$\rho_n = \int \rho(\alpha) e^{in\alpha} = \frac{1}{N}\mathrm{tr}\,(U) \tag{3.56}$$

To approximate the matrix integral (3.25) at large N, we now replace sums over eigenvalues with integrals weighted by the density function ρ. Because the action contains N^2 terms at large N, we can effectively treat the model as a functional integral over ρ of the form [6][7]

$$Z = \int D\rho\, \exp\left\{ -N^2 \sum_{n=1}^{\infty} \frac{1}{n} \left(1 - z(x^n)\right) |\rho_n|^2 \right\} \tag{3.57}$$

where the "1" in the sum arises from exponentiating the unitary measure and expanding the logarithm. Roughly speaking, what we have now is a model with infinitely many modes ρ_n of with mass $m_n^2 = 1 - z(x^n)$. Recalling the general fact that $z(x)$ increases monotonically from 0 at $x = 0$, we see that for x less than the critical point x_H defined by $z(x_H) = 1$ all modes are massive and hence the dominant configuration is given by a density with all nonzero ρ_n vanishing. This is simply a uniform distribution of eigenvalues on the circle. Since the action evaluates to zero on this configuration, the leading contribution to the free energy arises from the 1-loop determinant associated to integrating out the ρ_n and scales as N^0 at large N

[7] The Jacobian associated with changing variables from the eigenvalues α_i to the moments ρ_n of ρ appears to be irrelevant at all orders in the $1/N$ expansion [37].

$$\ln Z \sim \sum_n -\ln\left[1 - z(x^n)\right] \tag{3.58}$$

This is precisely the low temperature result that we obtained from operator counting (3.10).

For x larger than x_H, the mode ρ_1 becomes tachyonic and is driven away from zero. One might think that it is actually driven all the way to infinity but this isn't quite right because the allowed configuration space for the ρ_n is complicated by the normalization constraint (3.55) and the requirement that $\rho(\alpha)$, as a density, must be positive definite. These conditions impose complicated relations among the various ρ_n's as well as limit how large any individual moment can become. Since ρ_1 is the only tachyonic mode near x_H, it is reasonable to expect that it rolls to the boundary of the allowed configuration space. However, the particular point on the boundary to which it rolls depends on these relations and in general will have nonzero expectation values for the higher moments as well. Indeed, as described in appendix B one can actually obtain an explicit expression for the saddle point density very near the critical point $x - x_H \ll 1$ and see explicitly that it is clumped in the sense that it vanishes over a finite region on the S^1. It follows that the density here must receive contributions from infinitely many modes.

All of these complications aside, we see that ρ_1 is driven to a nonzero value for $x > x_H$ and hence the action evaluated on the saddle point no longer vanishes. The leading contribution to the free energy thus scales as N^2 at large N, indicating that there are effectively N^2 degrees of freedom, and the theory is said to be deconfined. Moreover, we see that ρ_1 is a natural order parameter for the transition from confined to deconfined phase as it seems to vanish at low temperatures and become nonzero above the critical point $x = x_H$. Thanks to our path integral derivation of the matrix model, we can in fact identify this order parameter with the usual one for deconfinement, namely the normalized Polyakov

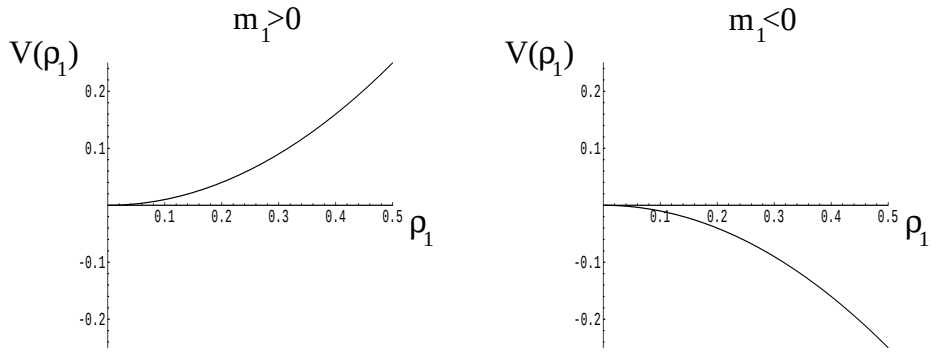

Figure 3.1: LG Effective Potential $V(\rho_1)$ in the Free Theory

loop.

The qualitative structure of the phase transition should be captured by a Landau-Ginzburg effective potential for the order parameter ρ_1. This is easily obtained from the matrix model by replacing the heavy modes with a simple upper limit on the magnitude of ρ_1. The resulting potential is purely quadratic

$$V_{LG}(\rho_1) = m^2|\rho_1|^2 \qquad\qquad m^2 = 1 - z(x) \tag{3.59}$$

and is depicted in figure 3.1. While this is indicative of a first order phase transition, the potential (3.59) is completely flat at the critical point so an infinitesimal correction can potentially raise the order. In this sense, the transition in the free theory is "weakly" first order and may lift to higher order when the coupling is turned on. We will discuss this more in the next section.

Before concluding our present analysis, though, we pause to discuss a subtle issue regarding the order parameter, ρ_1. While it is true that its magnitude has a nonzero expectation value in the deconfined phase, ρ_1 itself actually vanishes due to the fact that we must average over its phase, which is completely unconstrained by the effective action

due to a global $U(1)$ symmetry. This is analagous to the vanishing that we saw at strong coupling in section 2.4.1 and reflects the fact that the theory is always confined in some sense due to compactness of the space.

The problem here is similar to one which arises in the study of ferromagnets in the absence of an external field. In this case, if one measures the expectation value of the spin, the result vanishes because the average must include both the configuration with all spins up and that with all spins down. To define an order parameter sharply in this case, we can consider measuring the spin in the presence of a small field, which selects a preferred direction, that we slowly turn off. This avoids a trivial cancellation and renders the spin expectation value sensitive to order within the system.

We can do something analagous here, namely introduce a small deformation that breaks the $U(1)$ symmetry and take the limit in which it goes to zero. An extra term in the action of the form $\mathrm{tr}\,(U) + \mathrm{tr}\,(U^{-1})$, for instance, will do the trick by selecting a preferred location on the circle for the eigenvalues to clump. It is this sense in which the Polyakov loop becomes a good order parameter for the confinement/deconfinement transition in this theory.

3.5 The Phase Transition at Weak Coupling

We saw above that the degenerate nature of the effective potential near the critical point implies that perturbative effects can potentially lift the order. This can have a dramatic impact on the phase diagram and consequently it is important to extend our analysis to weakly coupled theories. The most natural framework for doing this is the path interal approach of section 3.3. To determine the impact of a small nonzero coupling on the effective action $S_{\text{eff}}(U)$, we need only include higher loop contributions that arise when

integrating out the massive modes.

3.5.1 Corrections to V_{LG}

The form of the effective action obtained in this manner is not only constrained by the considerations of section 3.3.1 but also by the structure of perturbation theory itself. In particular, diagrams that occur at order λ^{k-1} have at most $k+1$ index loops and consequently terms with at most $k+1$ independent traces can be generated. To order λ^2, then, the most general form of the effective action is given by

$$\begin{aligned} S_{\text{eff}}(\rho_n) = N^2 \Bigg[& \sum_n m_n^2(x)|\rho_n|^2 + \lambda \sum_{m,n} F_{m,n}(x) \left(\rho_m \rho_n \rho_{-n-m} + \text{cc}\right) \\ & + \lambda^2 \sum_{m,n,p} F_{m,n,p}(x) \left(\rho_m \rho_n \rho_p \rho_{-m-n-p} + \text{cc}\right) + \ldots \Bigg] \end{aligned} \tag{3.60}$$

where m_n and $F_{m,n}$ may acquire a dependence on λ. From this it is straightforward to obtain the corrected LG effective potential relevant for describing physics near the critical point by integrating out the modes $\rho_{n>1}$ that are heavy there. To order λ, the resulting potential continues to be quadratic but at order λ^2 a quartic term may be generated. To see this explicitly, note that the terms of (3.60) that contribute to V_{LG} to order λ^2 are simply

$$S_{\text{eff}}(\rho_n) = m_1^2|\rho_1|^2 + m_2^2|\rho_2|^2 + \lambda I \left(\rho_{-2}\rho_1^2 + \rho_2 \rho_{-1}^2\right) + \lambda^2 A|\rho_1|^4 + \ldots \tag{3.61}$$

Integrating out ρ_2 from the above we obtain the corrected LG effective potential

$$V_{LG}(\rho_1) = m_1^2|\rho_1|^2 + b|\rho_1|^4 \tag{3.62}$$

where

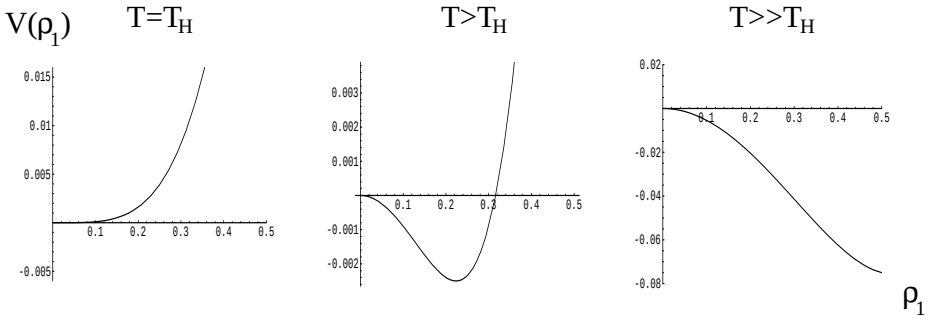

Figure 3.2: Effective Potential if $b > 0$ at various values of T.

$$b = \lambda^2 \left(A - \frac{I^2}{m_2^2} \right) \tag{3.63}$$

3.5.2 Implications for the Phase Structure

The phase structure described by the LG effective potential (3.62) is highly dependent on the sign of b at the critical temperature $T_H = -\ln x_H$ where ρ_1 becomes massless. Before addressing the computation of this sign, we first describe the qualitative features of both possible scenarios.

Case 1 $- b > 0$

In this scenario, the system undergoes a second order phase transition at T_H to a new phase that, as T is increased further, moves toward the boundary of the ρ_1 configuration space. Upon reaching the boundary, we expect another phase transition that, as demonstrated explicitly in appendix B, is of third order[8]. A depiction of the effective potential in this case is presented in figure 3.2.

If this scenario is realized in the $\mathcal{N} = 4$ theory, it would have striking implications

[8]Polyakov loops associated to larger representations of $U(N)$ can be useful for distinguishing the two phases of this transition [38]

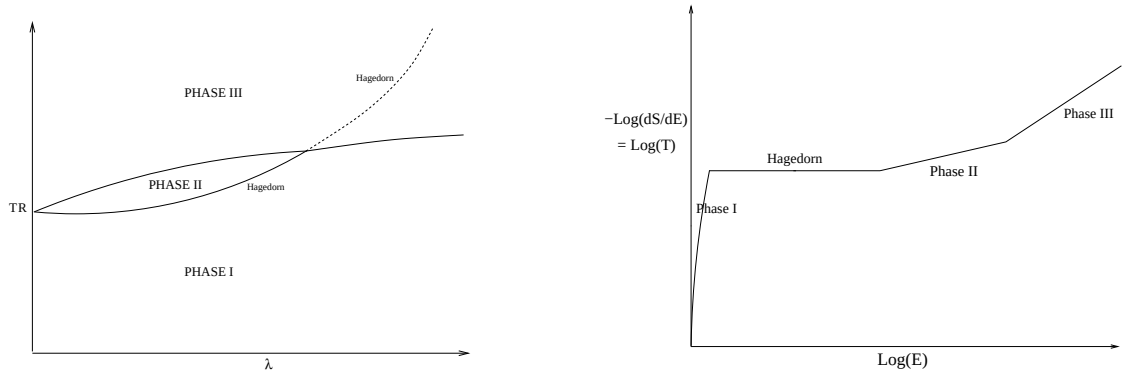

Figure 3.3: Conjectured phase diagram for the $\mathcal{N} = 4$ theory if $b > 0$. Phase I is the confined phase at $T < T_H$, phase II the new phase which emerges for T just beyond T_H, and phase III the phase in which ρ_1 sits at the boundary of its configuration space. The continuation to strong coupling connects phase I with the graviton gas and phase III with the "big" black hole.

for the phase structure of the full theory. Among other things, it predicts the existence of a third phase intermediate between the confined and deconfined phases that we are inclined to associate with the graviton gas and "big" black hole at strong coupling. A conjectured phase diagram that represents the simplest possible connection of the weak and strong coupling regimes in this scenario is depicted in figure 3.3. Notice that we are forced to include a tricritical point at a finite value of the 't Hooft coupling, λ, beyond which the intermediate phase ceases to exist. For comparison with figure 2.1, we also include in figure 3.3 a conjectured plot of $\ln T$ as a function of $\ln E$ at weak coupling.

Case 2 – $b < 0$

In this scenario, the system undergoes a first order phase transition at a temperature T_c less than T_H. Intermediate between the minima at the origin and the boundary of the ρ_1 configuration space is a maximum corresponding to a thermodynamically unstable phase. A depiction of the effective potential in this case is presented in figure 3.4.

The qualitative structure of this scenario is quite similar to what we saw in the

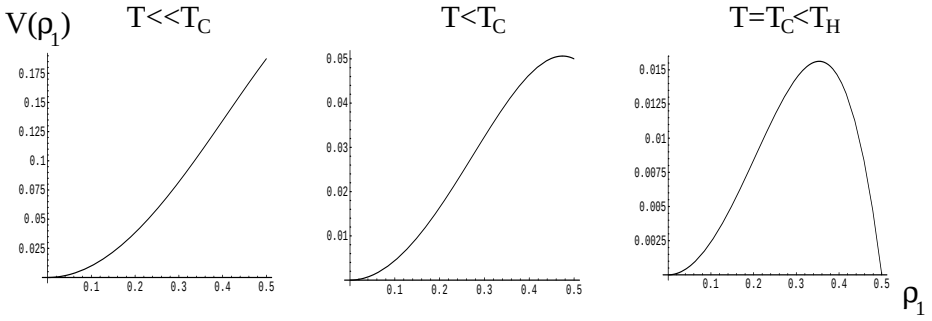

Figure 3.4: Effective Potential if $b < 0$ at various values of T

$\mathcal{N} = 4$ theory at strong coupling. It thus seems most likely that this is the situation realized by $\mathcal{N} = 4$ SYM at weak coupling. The simplest possible connection of the weak and strong coupling regimes in this scenario is obtained by simply continuing the Hawking-Page transition line down to $\lambda = 0$, where it is directly identified with the confinement/deconfinement transition studied in this chapter. A phase diagram depicted this behavior is presented in figure 3.5. In that figure we also plot $\ln T$ as a function of $\ln E$ for this scenario. Comparing this to figure 2.1, it is natural to conjecture that the unstable phase in this scenario is smoothly connected to the small black hole phase at strong coupling.

3.5.3 Determining the sign of b

Since we are unaware of any physical principle which selects one scenario over the other, it is necessary to embark on a perturbation computation of the parameter b in order to determine which is realized in a given theory. Unfortunately, we see from equations (3.61) and (3.63) that a three-loop calculation is required so our task is far from easy. Things are complicated even further by the fact that placing the theory on an S^3 adds a host of new technical challenges.

In pure Yang-Mills theory without matter, this computation has been performed

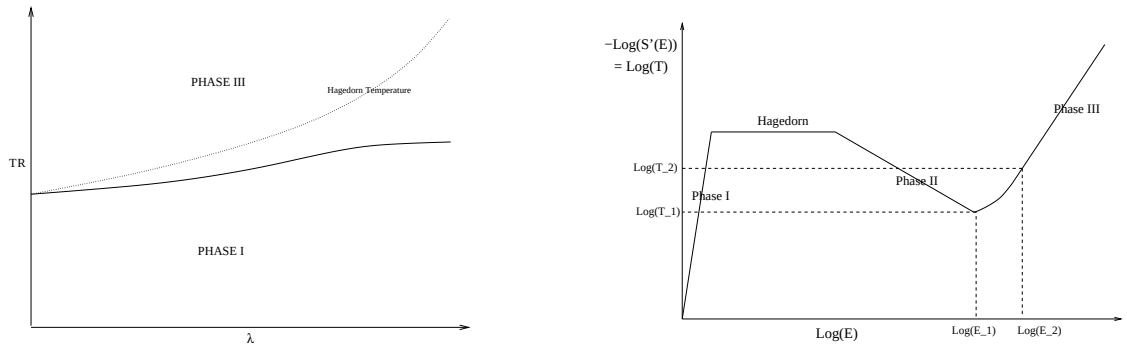

Figure 3.5: Conjectured phase diagram for the $\mathcal{N} = 4$ theory if $b < 0$. Phase I is the confined phase at $T < T_c$, phase II the unstable phase associated to the maximum in the effective potential in figure 3.4, and phase III the deconfined phase in which ρ_1 sits at the boundary of its configuration space. The continuation to strong coupling connects phase I with the graviton gas, phase II with the "small" black hole, and phase III with the "big" black hole.

in [7] with the result that, at the critical point of the free theory

$$b = -5.7 \times 10^{-4} \tag{3.64}$$

As a result, we see that the phase transition in this model remains of first order at small nonzero coupling. Unfortunately, extending the calculation to the $\mathcal{N} = 4$ SYM theory is a difficult task that has not yet been addressed. Thus, the nature of the phase structure of this theory at weak coupling remains unknown, though we repeat again that a first order transition there seems most likely.

3.6 Summary

In this chapter, we have seen that the thermodynamics of free large N Yang-Mills theories on S^3 exhibit all of the qualitative features that we anticipated in section 2.4. Due to the Gauss law constraint, these theories are confined at low temperatures with a free energy of order 1 and vanishing Polyakov loop. The spectrum exhibits a Hagedorn growth

in the density of states which culminates in a phase transition at the Hagedorn temperature T_H. The high temperature phase is deconfined with free energy of order $\mathcal{N}^2$ and Polyakov loop nonvanishing in an appropriate sense. The phase transition is of first order and is most naturally identified, in the context of the $\mathcal{N} = 4$ theory, directly with the Hawking-Page transition at strong coupling.

As one moves from zero to small coupling, though, the degenerate nature of the phase transition in the free theory is such that perturbative effects can lift the order. We have presented two scenarios for the structure that may emerge in the weak coupling regime though others, in which the quartic term in (3.62) vanishes, are possible. To distinguish among the possibilities, a perturbative computation is required. For pure Yang-Mills theory in the absence of additional matter fields, this calculation has been done [7] with the result that the phase transition there continues to be of first order as one turns on the coupling. It is natural to conjecture that this is true in the $\mathcal{N} = 4$ theory as well but one cannot be sure until the analagous calculation is done for this case.

We finally complete our study of this first system by noting that it is quite remarkable that a free gauge theory realizes such a nontrivial phase structure.

Chapter 4

Black Hole/Black String Phase Transitions

We now move on to the second topic of this thesis, namely Gregory-Laflamme (GL) black hole-black string transitions and their gauge theory duals. In this chapter, we will give a brief introduction to the GL transition, which has been a subject of intensive study in the GR community for a number of years, and review some of the recent results. As our primary interest lies elsewhere, this discussion will not be extensive and the interested reader is referred to B Kol's excellent review [39]. We will then discuss a setup in which GL transitions arise in type II SUGRA, where a gauge theory dual can be realized. The implications of GL physics on the gauge theory are briefly discussed with details postponed to the following chapter.

4.1 Black Holes, Black Strings, and the GL Instability

4.1.1 Gravity in $d > 4$ – Some new players

One of the reasons for the significant interest in higher dimensional gravity is the existence of an increasingly large variety of "black" objects of different types. Indeed, the restrictive uniqueness theorems [40, 41, 42, 43, 44] that exist in four dimensions break down for $d > 4$, where exotic objects such as black rings [45] and black branes [10] can be found. The existence of this multitude of objects implies the possibility of a rich phase structure that we wish to probe both from the point of view of gravity as well as that of the dual gauge theory where one exists.

In the present context, we shall focus our attention on what is arguably the simplest setup with exotic "black" objects, namely five-dimensional gravity with one direction compactified on a circle of radius R. What sort of interesting solutions might we find here? To start, let us look for solutions with radius R much smaller than the inverse ADM mass, M^{-1}. In this regime, our setup is not so different from 4-dimensional gravity in flat space where the well-known uniqueness theorem permits only one solution, the Schwarzschild black hole [40, 41]:

$$ds^2_{Sch} = -f(r)\,dt^2 + f^{-1}(r)\,dr^2 + r^2 d\Omega_3^2 \tag{4.1}$$

where

$$f(r) = 1 - \left(\frac{r_0}{r}\right) \tag{4.2}$$

and the Schwarzshild radius, r_0, is related to the mass, M, by

$$r_0 = 2G^{(4)}M \tag{4.3}$$

As a result, we expect our five-dimensional solution to approach (4.1) in the large 4-dimensions as $R \to 0$. Moreover, when $R \ll r_0$, we expect the horizon, which has characteristic size r_0, to wrap completely around the circle. Such solutions, which have horizon topology $S^1 \times S^2$, are generally termed black strings. In this case, the black string's nontrivial horizon topology is supported by the existence of a compact cycle in the geometry that it can wrap. Such an object should not be confused with the recently discovered five-dimensional black ring solutions, which have nontrivial horizon topology supported instead by a pair of angular momenta [45].

It is easy to write down a solution describing a black string wrapping the S^1 as the product of (4.1) with S^1 does the trick

$$ds^2_{UBS} = ds^2_{Sch} + R^2\, d\theta^2 \tag{4.4}$$

This solution exists for all radii, R, and is referred to as a uniform black string due to its preservation of translational symmetry along the S^1. In addition to this, one might also hope to find analagous nonuniform black string solutions which break translation symmetry along the S^1. While this seems unlikely at small radius due to four-dimensional uniqueness theorems, it is quite plausible that such solutions emerge at larger radii. Writing analytic expressions for a nonuniform black string is a very difficult enterprise, but numerical techniques have been developed to study them. See for instance [46, 47, 48].

While black strings are the only solutions that we expect at small radius, what new solutions might emerge as we increase the radius? If we instead take R much larger than the inverse ADM mass, our setup now looks similar to 5-dimensional gravity in flat space, where we expect to find the 5-dimensional analog of the Schwarzschild black hole (4.2). In flat space, this solution is easy to write down

$$ds^2_{Sch} = -f(\rho)\,dt^2 + f^{-1}(\rho)\,d\rho^2 + \rho^2 d\Omega_3^2 \tag{4.5}$$

where

$$f(\rho) = 1 - \left(\frac{\rho_0}{\rho}\right)^2 \tag{4.6}$$

and the five-dimensional Schwarzschild radius, ρ_0, is related to the mass, M, by

$$\rho_0 = \sqrt{\frac{8G^{(5)}M}{3\pi}} \tag{4.7}$$

While (4.5) is not compatible with periodic boundary conditions along one of the spatial directions, it is natural to expect that for $R \gg r_0$ a suitable deformation of (4.5) can be found that yields a solution with horizon localized around a point on the S^1. We will follow B Kol and refer to solutions such as this as "caged" black holes. While it has proven very difficult to obtain analytic expressions for caged black hole metrics, there has been a great deal of progress in both analytical [49, 50, 51, 52] and numerical techniques to study them [53, 54, 55, 56].

In five dimensions, this exhausts the set of solutions without charge or angular momentum that have been found or conjectured to date and it is unlikely that others exist. Black hole uniqueness theorems in four dimensions suggest that any new solutions in five-dimensional gravity on a circle will be rather mundane and Schwarzschild-like in the four large dimensions with only variations of behavior along the S^1 distinguishing the various possibilities. Here, the possibilities are that the horizon is localized or wrapped on the circle, corresponding to "caged" black holes and black strings as we have seen.

4.1.2 A Transition in the Microcanonical Ensemble

With the increased number of nontrivial solutions, the possibility exists for an interesting and nontrivial phase structure in 5-dimensional gravity on a circle. Indeed, at small radii the uniform black string is entropoically favored by virtue of being the only solution. On the other hand, it seems reasonable to expect that the caged black hole becomes favored at larger radii due to the tendency of matter to "clump" up in gravitational systems. We can see this somewhat more explicitly by comparing their entropies. Defining the dimensionless parameter μ by

$$\mu = \frac{G^{(5)}M}{R^2} \tag{4.8}$$

and using the fact that $G^{(4)} \sim G^{(5)}/R$, we can write the uniform black string entropy as

$$S_{UBS} \sim \mu^2 \tag{4.9}$$

On the other hand, if we use the horizon of five-dimensional Schwarzschild (4.5) as an approximation to that of the caged black hole, we find that its entropy is roughly

$$S_{BH} \sim \mu^{3/2} \tag{4.10}$$

Consequently, the uniform black string is favored at small radii, corresponding to large μ, while for large radii it becomes entropically favorable for the string to "clump" on the circle, forming a caged black hole. Assuming that these are the only solutions that ever maximize the entropy, this signals the existence of a transition in the microcanonical ensemble at a critical value $\mu = \mu_c$ separating regions where the uniform black string and caged black hole dominate the thermodynamics. Determining the location of the critical

point precisely is quite difficult, though, since near $\mu = \mu_c \sim 1$ the approximation of the caged black hole horizon as that of five-dimensional Schwarzschild isn't expected to work very well. Instead, a numerical constricution of the caged black hole metric is required and this is not a trivial task.

So is it impossible to learn anything precise about the phase diagram without appealing to complicated numerics? The answer to this is essentially yes with one notable exception. One might expect the uniform black string to develop a tachyonic mode at a particular value $\mu = \mu_{GL}$ and, since we have the uniform black string metric in hand, there is no obvious obstacle to determining μ_{GL}. If the transition is of second or higher order, this will accomplish a lot as μ_{GL} will coincide with the critical point. The possibility remains, though, that the transition is of first order in which case μ_{GL}, if such a point even exists, will not give any information about μ_c.

4.1.3 The Gregory-Laflamme Instability

The question of whether black strings develop perturbative instabilities is one that was considered long ago by Gregory and Laflamme [57, 58], whose work served to stimulate the subsequent research into the phase structure of higher dimensional gravity. They found that infinitely long black strings, corresponding to the $R \to \infty$ limit of our present considerations, are indeed perturbatively unstable. Moreover, this instability persists for sufficiently large but finite R. We now briefly review these results.

To study metric perturbations in the black string geometry we begin by writing the perturbation as

$$\delta g_{MN} = h_{MN} \qquad\qquad M, N = 0 \ldots 4 \tag{4.11}$$

Requiring the equations of motion to be satisfied at leading order is equivalent to

requiring that h_{MN} satisfy the Lichnerowicz equation

$$\tilde{\Delta}_L^{(5)} h_{MN} = \left(\delta_M^A \delta_N^B \nabla_C \nabla^C + 2R_M{}^A{}_N{}^B\right) h_{AB} = 0 \tag{4.12}$$

where $\tilde{\Delta}_L^{(5)}$ is the five-dimensional Lorentzian Lichnerowicz operator, for which we have given an explicit expression in the transverse-traceless de Donder gauge $h_M^M = 0 = h^M_{N;M}$. To look for instabilities, one searches for solutions to (4.12) that grow exponentially in time and are well-behaved both at infinity and at the future event horizon. The solutions must also be physical perturbations, rather than gauge artifacts. In the de Donder gauge, some residual gauge freedom remains and can be used to show that perturbations annihilated by $\tilde{\Delta}_L$ are unphysical.

It is straightforward to verify, following Gregory and Laflamme, that there are no unstable metric perturbations of the form $h_{\mu 5}$ or h_{55}, where $\mu = 0 \ldots 3$. As a result, we will focus our attention on perturbations of the form $h_{\mu\nu}$, namely tensor perturbations from the 4-dimensional point of view. Adding the assumption of three-dimensional rotational invariance, this leads to the s-wave ansatz of Gregory and Laflamme

$$h_{\mu\nu}(r, \phi, t) = e^{\Omega t} e^{ik\phi} H_{\mu\nu}(r) \tag{4.13}$$

where r, ϕ are as in (4.4), k denotes the inverse wavelength of the perturbation along the compact S^1, and $H_{\mu\nu}(r)$ is rotationally invariant. Plugging this in to the Lichnerowicz equation, we find the following

$$\left(\tilde{\Delta}_L^{(4)} + k^2\right) H_{\mu\nu}(r, 0, t) = 0 \tag{4.14}$$

where $\tilde{\Delta}_L^{(4)}$ is the four-dimensional Lorentzian Lichnerowicz operator. Our problem has thus been reduced to finding eigenfunctions of $\tilde{\Delta}_L^{(4)}$ that satisfy the appropriate

boundary conditions. Henceforth, we will refer to eigenfunctions with $\Omega < 0$ ($\Omega > 0$) as (un)stable solutions since the corresponding metric perturbation is (un)stable.

Had we been dealing with noncompact black strings, say in flat $4+1$-dimensional space, all values of k would be allowed and the question of stability would be equivalent to determining whether any unstable solutions to (4.14) exist. For the black string on S^1, though, the wave numbers k of perturbations along the length of the string are quantized in units of the inverse radius. Thus, the question of stability here is whether any unstable solutions exist that "fit" inside the S^1. In other words, the black string will become unstable only when there exists an unstable solution to (4.14) at $k = 2\pi n/R$ for some integer n. Carrying out this program directly, namely determining those values of k for which unstable eigenfunctions exist, is in general a difficult task but can be done [57, 58]. Instead of proceeding along these lines, though, we follow [59] to argue that the existence of instabilities is connected with a well-known fact about Schwarzschild black holes.

To start, we first note a few elementary facts. Since the black string is stable for small radii, solutions to (4.14) for sufficiently large k are necessarily stable. As the radius is increased, we expect an unstable mode to appear and, given our picture of the black string "clumping" along the circle, it is natural to assume that this instability will have maximal wavelength along the S^1. The two anti-nodes of this perturbation will then correspond to the regions of maximal and minimal clumping. Since increasing the radius is equivalent to decreasing the minimum wave number that can "fit" in the S^1, our picture suggests that (4.14) admits unstable solutions for k less than a critical value k_{GL} while all solutions with a larger value of k are necessarily stable. What is of interest, then, is determining the critical value k_{GL} separating the unstable and stable regimes. Precisely at the point k_{GL}, we expect to find what [59] terms a threshold unstable mode, namely a time-independent mode having $\Omega = 0$. If we can determine when this solution exists, we will obtain the

critical wave number k_{GL} that signals the onset of perturbative instability.

Looking for time-independent solutions to (4.14) is not a new problem, though. In particular, using the fact that $H_{\mu\nu}^{(\Omega=0)}$ is time-independent and rotationally invariant, we can easily Wick rotate the equation (4.14), obtaining

$$\Delta_L^{(4)} H_{\mu\nu}^{(\Omega=0)}(r) = -\lambda^2 H_{\mu\nu}^{(\Omega=0)}(r) \tag{4.15}$$

where $\Delta_L^{(4)}$ is the four-dimensional Euclidean Lichnerowicz operator. This equation is familiar, though, as it arises when studying the thermodynamics of 4-dimensional Schwarzschild black holes! To see this note that, in the Euclidean path integral approach to quantum gravity at finite temperature, expanding the Euclidean action I_E to quadratic order in perturbations $H_{\mu\nu}$ about a saddle point $g_{\mu\nu}$, such as 4-dimensional Schwarzschild, yields

$$I_E \to I_E + \int d^4x \sqrt{g} H^{\mu\nu} \Delta_L^{(4)} H_{\mu\nu} \tag{4.16}$$

The eigenvalues of $\Delta_L^{(4)}$ give the "masses" of various perturbations with negative eigenvalues corresponding to tachyonic modes that trigger thermodynamic instability. What we need for our threshold unstable mode, though, is precisely (the Wick rotation of) an eigenfunction with negative eigenvalue so we see that the question of classical instability of our black string is intimately related to the question of thermodynamic instability of the 4-dimensional Schwarzschild black hole. A relation of roughly this sort was first conjectured by Gubser and Mitra [60, 61] and we will have more to say about it later.

For now, we recall that the Schwarzschild black hole is well-known to be thermodynamically unstable. For instance, it is trivial to compute the specific heat and demonstrate that it is negative. This is already enough to permit the conclusion that a threshold unstable mode indeed exists and that the black string exhibits a classical instability at a critical

radius.

More interestingly, the Schwarzschild instability from the Euclidean gravity point of view has been studied previously by Gross, Perry, and Yaffe [62] who found that there exists exactly one negative mode of the Euclidean Lichnerowicz operator with eigenvalue

$$-k_{GPY}^2 \approx -\frac{0.19}{M^2} \tag{4.17}$$

in units where $G^{(4)} = 1$. This corresponds to a critical wavenumber

$$k_{GL} = \sqrt{k_{GPY}^2} \approx \frac{0.44}{M} \tag{4.18}$$

and agrees with the results obtained by Gregory and Laflamme [57, 58, 59]. From this, we see conclude that there exist unstable modes with wavelengths longer than k_{GL}^{-1}. Such modes can "fit" in the circle and trigger an instability provided

$$\mu \leq \mu_{GL} = \frac{M k_{GL}}{2\pi} \approx 0.07 \tag{4.19}$$

We thus conclude that, for $\mu \leq \mu_c$, the uniform black string wrapping S^1 becomes perturbatively unstable and is classically driven to a configuration of higher entropy.

The Gubser-Mitra Correlated Stability Conjecture

As noted above, the connection between existence of a classical Gregory-Laflamme instability and existence of a thermodynamic instability of the 4-dimensional Euclidean Schwarzschild black hole is not an accident. Rather, it is related to the following striking conjecture of Gubser and Mitra:

A noncompact black brane is classically stable if and only if

it is thermodynamically stable (4.20)

Our previous analysis essentially "proves" (4.20) for the case of noncompact black strings, which inherit the thermodynamic instability of 4-dimensional Schwarzshild and suffer from perturbatively unstable modes with $k < k_{GL}$. We have also seen the necessity of assuming noncompactness as the unstable modes persist for compact strings wrapping S^1 only if they "fit" in the circle. It is now useful to pause for a moment and recast our analysis in a slightly different language that makes the connection between classical and thermodynamic instsability even more transparent and easy to generalize [59]. Considering again a static perturbation of the GL form, $h_{mn} = H_{mn}(r)e^{ik\phi}$, and expanding the Lorentzian action to quadratic order we obtain

$$I \to I + \int d^5x \sqrt{g} H^{MN} \left(-\tilde{\Delta}_L^{(4)} - k^2 \right) H_{MN} \tag{4.21}$$

On the other hand, expanding the Euclidean action to quadratic order in the Wick rotated perturbation yields

$$I_E \to I_E + \int d^5x \sqrt{g} H^{MN} \left(\Delta_L^{(4)} + k^2 \right) H_{MN} \tag{4.22}$$

As we have seen, the key point is that the eigenvalues of $\Delta_L^{(4)}$ and $\tilde{\Delta}_L^{(4)}$ agree when acting on static H_{MN}. Consequently, the absence of tachyonic modes in (4.21) is equivalent to the absence of tachyonic modes in (4.22). On the other hand, if $\Delta_L^{(4)}$ has a negative eigenvalue, λ, then perturbations of the GL form are tachyonic modes of both the Lorentzian and Euclidean actions for $k^2 < \lambda$. Moreover, the perturbation with $k^2 = \lambda$ satisfies the equations of motion that follow from (4.21) and hence corresponds to the

classical threshold unstable mode. This analysis can be easily extended to more general examples, including branes of higher dimension and branes that carry charges [59, 63, 64].

Of course, what we have said is intended only to make the result (4.20) plausible and is far from rigorous. To actually prove that (4.20) holds for a given example, there are many issues that one must deal with. For instance, simply demonstrating that the existence of a Euclidean tachyonic mode implies thermodynamic stability requires the construction of a family of metrics near the brane solution along which one can locally vary. We refer the reader to [64] for a discussion of the general requirements of proof[1].

4.1.4 Horowitz-Maeda and the Nonuniform String

So far, we have argued that the uniform black string is stable at small radius, develops a perturbative instability at a finite radius, and has lower entropy than the caged black hole at large radius. It is then natural to conjecture, as Gregory and Laflamme did, that the flow induced by triggering the perturbative instsability of the black string ends with the caged black hole. This process is potentially interesting for a host of reasons, not the least of which being that it involves a change in topology of the horizon. Understanding the dynamics associated with "pinching" of the horizon and the potential violation of cosmic censorship that may occur are both interesting questions.

It was the study of precisely these questions by Horowitz and Maeda [70] that stimulated a rethinking of this picture, which had been generally accepted for a number of years. In particular, they proved on quite general grounds that any process during which a horizon "pinches" off cannot proceed in finite affine time. With this conclusion, they then argued that the caged black hole could not be the endpoint of the Gregory-Laflamme

[1]There is a vast literature that studies the application of (4.20) to various systems [60, 61, 59, 65, 66, 67, 64, 68]. It should also be noted that at least one counterexample to (4.20) has been constructed [69] but we will not review this here as the features apparently required to violate (4.20) do not appear in the examples of interest to us.

instability. This led them to conjecture an alternative possibility for the endpoint, namely a nonuniform black string!

4.1.5 Conjectured Phase Structure of 5-Dimensional Gravity on S^1

If we accept the existence of nonuniform black string solutions, how can they fit with what we already know to form a consistent picture of the phase structure? It turns out that we can actually say quite a bit given only a few simplifying assumptions. Our strategy in this subsection will be to build a consistent phase diagram from the limited information at hand by recalling that the various possible phases are associated with extrema of the entropy, a single function of (infinitely) many variables. Requiring then that extrema appear and disappear consistently will restrict the various possible phase structures [71]. The arguments that follow are a simplification of those of Kol [71].

Instead of studying the entropy function on the full space of physical metrics, let us assume for simplicity that one can construct an order parameter, λ, which distinguishes all possible phases [71]. An order parameter of this sort can be realized explicitly near the uniform black string solution, where it roughly parametrizes nonuniformity. We won't need any details of its construction or extension beyond this neighborhood other than the fact that one can take $\lambda \geq 0$ with $\lambda = 0$ corresponding to the uniform black string.

In general, the dynamics of λ can be determined from an effective Landau-Ginzburg potential $V(\mu, \lambda)$ which, in this case, arises roughly from thinking of $-S$ as a function of λ and μ. The various phases that exist at fixed μ correspond to extrema of V with respect to λ, with the global minimum determining the dominant phase.

For large μ, we have seen that the uniform black string is the only solution so the potential must have a single minimum at $\lambda = 0$ there. As we decrease μ, the form of V will change and new extrema will appear. We already know of one place this occurs,

namely the GL point μ_{GL} where the uniform black string becomes unstable and merges with the branch of nonuniform black string solutions. As μ decreases through μ_{GL}, consistency requires that such a merger must either consist of the annihilation of a previously existing unstable solution or the nucleation of a new stable solution. Both of these possibilities can be seen in figures 4.1 and 4.2.

We now make the minimal assumption that the only other relevant phase is the caged black hole, which we expect to be stable whenever it exists. A new minimum of V such as this, though, can only arise from "pair production", in which a maximum and minimum appear simultaneously, or by "rolling in from infinity", a possibility that we neglect as unlikely. If the nonuniform black string that emerges from the GL point is unstable, the simplest possibility then is that it merges with the caged black hole at a critical value $\mu_c > \mu_{GL}$. If the nonuniform black string is stable the simplest possibility is again a merger. However, the fact that two minima cannot annihilate without the existence of additional extrema requires that this merger actually take the form of a smooth crossover to the caged black bole.

By assuming that V is as simple as possible while remaining consistent with all previously known information, we have thus arrived at two possible phase diagrams. In the first, the caged black hole and nonuniform string solutions are stable and unstable, respectively, and emerge simultaneously at a critical point $\mu_c > \mu_{GL}$. Decreasing μ from μ_c, the nonuniform string merges with the uniform string at the Gregory-Laflamme point, μ_{GL}. Because the caged black hole has a higher entropy than the uniform black string, we see that the system undergoes a first order phase transition at μ_c before the Gregory-Laflamme point is even reached. It is not difficult to write an effective potential that realizes this qualitative structure

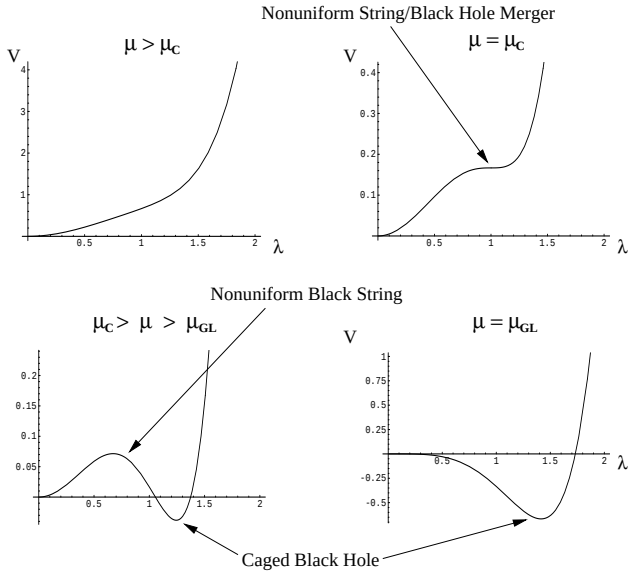

Figure 4.1: Qualitative behavior of an effective potential, V, exhibiting a first order black string/black hole phase transition

$$V(\mu, \lambda) = \frac{1}{2}(\mu - \mu_{GL})\lambda^2 - \frac{1}{2}\sqrt{\mu_c - \mu_{GL}}\lambda^4 + \lambda^6 \tag{4.23}$$

We depict the evolution of this potential for decreasing μ in figure 4.1. Note that the λ^6 term is necessary to avoid having runaway directions.

The second possibility is that the uniform black string remains the only solution for $\mu > \mu_{GL}$, with a stable nonuniform black string emerging there. As μ is decreased, this solution then "merges" smoothly into the stable caged black hole. One example of an effective potential that realizes this qualitative structure is

$$V(\mu, \lambda) = \frac{1}{2}(\mu - \mu_{GL})\lambda^2 + \lambda^4 \tag{4.24}$$

and its evolution for decreasing μ is depicted in figure 4.2.

While we have assumed that the entropy can be thought of as a function of a single variable, λ, the above argument captures the essential features of the more general one in

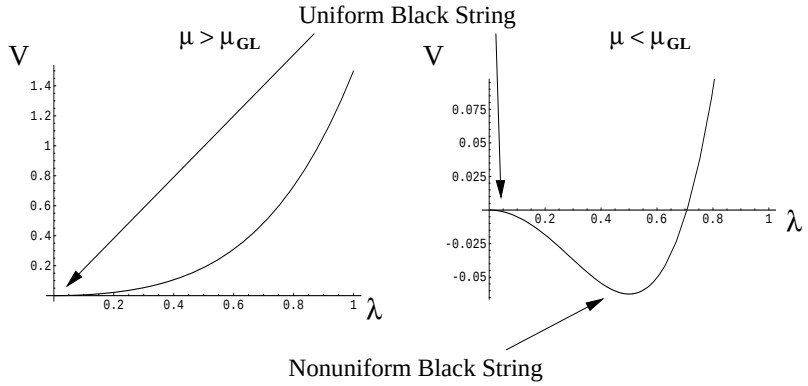

Figure 4.2: Qualitative behavior of an effective potential, V, exhibiting a second order uniform/nonuniform string phase transition. The nonuniform phase is expected to crossover smoothly to the caged black hole for sufficiently small μ.

[71], which arrives at precisely this picture. The key input was the trivial observation that, for functions of one variable, new maxima and minima only arise in maximum/minimum pairs. This can be easily generalized, using Morse theory, to restrict the appearance of new extrema in a multivariate function and leads essentially to the same conclusion.

Which of the two possible phase structures that we have suggested is more likely? A key difference between them is the mass at which the caged black hole becomes a viable solution. The existence of the caged black hole for $\mu > \mu_{GL}$ is consistent with the picture of a first order transition while failure of this existence is consistent with the picture of a second order one. Since μ is related to the Schwarzschild radius ρ_0 of five-dimensional Schwarzschild by

$$\mu = \left(\frac{\rho_0}{R}\right)^2 \tag{4.25}$$

the result (4.19) for μ_{GL} implies that, at the GL critical point

$$\rho_0 < R \tag{4.26}$$

This suggests that the black hole should be able to "fit" in the circle for a range of $\mu > \mu_{GL}$ and hence that the qualitative structure of figure 4.1 accurately captures the physics of the system in question. We thus arrive at the prediction that a uniform black string in 5-dimensions on S^1 undergoes a first order phase transition to the caged black hole at a critical value $\mu_c > \mu_{GL}$ [2].

It is amusing to note that the simplified picture we have used above, with the phase structure being determined by an effective potential for a single order parameter, is precisely that which arose when we studied the gauge theory dual of the Hawking-Page transition. Moreover, in the next chapter we will see that it arises again when studying the gauge theory dual of a black string/black hole transition.

4.1.6 Brief Summary of Numerical Evidence

How can one attempt to verify the above predictions for the phase structure? A natural place to begin is with the order of the phase transition, which can be studied in the neighborhood of the uniform black string solution. The key question here is whether the entropy increases or decreases as one moves along the nonuniform branch. This has been studied by Gubser [46] and Wiseman [47], who numerically constructed the nonuniform branch near the GL point and found evidence in support of a first order phase transition.

The predicted phase diagram contained even more information than this, though, including the instability of the entire nonuniform string branch as well as the existence of a critical point at which the nonuniform black string and black hole branches merge. A great deal of work has been invested in the construction of uniform black string [46, 47, 48] and caged black hole solutions [53, 54, 55, 56] and, in the case of six dimensions, Kudoh and

[2] This prediction also applies for black strings in D dimensions for sufficiently small D. One can show that μ_{GL} increases with dimension as $\sqrt{D}$ [72] so that eventually it is reached before the caged black hole exists. Approximating the horizon size by 5-dimensional Schwarzschild gives a critical dimension of $D = 12.5$ [72, 73] while numerical studies show the actual critical dimension to be $D = 13.5$ [74]

Wiseman have completed the full phase diagram [56], which is in excellent agreement with Kol's picture presented above [71]. In the case of five dimensions, the supporting evidence is also quite strong [56].

The techniques required to perform such detailed studies of the phase structure are quite intricate and we do not attempt to discuss them here. Instead, we refer the interested reader to the original papers and the review [39].

4.1.7 Summary

Let us now summarize, for clarity, what we have learned about the phase structure of 5-dimensional gravity on an S^1 of radius R. There are three sorts of black solution, namely the uniform black string, nonuniform black string, and caged black hole. At large mass $\mu \gg 1$, only the uniform black string solution exists. As the mass is decreased to $\mu = \mu_c$, the nonuniform black string and caged black hole solutions emerge. The uniform black string and caged black hole are both stable solutions here, but the caged black hole has higher entropy and the system undergoes a first order phase transition. As μ is decreased further to $\mu = \mu_{GL}$, the uniform black string develops a perturbative instability of wavelength R that connects to the nonuniform black string branch. While we haven't mentioned it explicitly, the uniform black string develops additional instabilities of higher wavelength, from which increasingly nonuniform string branches emerge, as μ is decreased further. None of these new solutions are relevant for the thermodynamics, though, so we can safely ignore them.

In what follows, we will be interested in higher dimensional examples, specifically ten-dimensional gravity with one compact direction since it is there that one can easily make connection with gauge theories. As the discussion of section 4.1.5 was quite general, we will assume the picture that emerged there carries over to these higher-dimensional systems as well. There have been studies of uncharged black strings which indicate that for $D \leq 13$

(12) dimensions the nonuniform string branch emerging at the GL point has lower entropy (higher free energy) than the uniform branch [74, 75]. As a result, the qualitative picture described above is expected to capture the essential physics of both the microcanonical and canonical ensembles. Beyond this, however, no numerical data is currently available for $D > 6$ so, while there is supporting evidence that the basic structure remains the same, for clarity we remind the reader that this is presently an assumption.

Finally, we conclude this brief review of GL physics with a puzzle. Where did the arguments of Horowitz and Maeda [70], which led them to conjecture a second order phase transition to a stable nonuniform string, go wrong? This question is not easily answered and in fact, to the best of my knowledge, remains currently unsolved.

4.2 Black String/Black Hole Phase Transitions in SUGRA

We now seek to determine whether GL structure persists in systems that readily admit gauge theory duals and, if so, how one might use the techniques of gauge theory to probe it. As mentioned above, we will move from five to ten dimensions since there a Yang-Mills description will be easy to obtain. In particular, we will find, perhaps surprisingly, that the physics of uncharged black strings in ten dimensions can be directly connected, via a short chain of boosts and dualities, with wrapped $D1$-branes, whose near-horizon physics is captured by the maximally supersymmetric Yang-Mills theory in two-dimensions [1, 76]. Our discussion of this roughly follows that of [77], which built on the earlier works [78, 79, 80]. More general studies that relate GL instabilities of p-branes to the phase structure of Yang-Mills theories in $1 + p$-dimensions can be found in [81, 64].

4.2.1 From Uncharged String to Wrapped $D1$-Brane

The ten-dimensional analog of the compact uniform five-dimensional black string is a simple generalization of (4.4)

$$ds^2 = -f(r)d\tau^2 + f^{-1}(r)\,dr^2 + r^2\,d\Omega_7^2 + dy^2 \tag{4.27}$$

where

$$f(r) = 1 - \frac{r_0^6}{r^6} \qquad\qquad y = y + \bar{L} \tag{4.28}$$

As before, the family of strings is conveniently parametrized by a dimensionless mass, μ

$$\mu = \frac{G^{(10)}M}{\bar{L}^7} \sim \frac{r_0^6}{\bar{L}^6} \tag{4.29}$$

As this parameter is varied, we expect to find a GL instability analagous to that discussed in the 5-dimensional case at a critical value of order unity

$$\mu_{GL} \sim \mathcal{O}(1) \tag{4.30}$$

corresponding to the Schwarzshild radius being of the same order as the circle size

$$(r_0)_{GL} \sim \bar{L} \tag{4.31}$$

We would now like to map the instability and corresponding nontrivial phase structure of (4.27) to one of the familiar p-brane type solutions of type II SUGRA since their near-horizon physics admit Yang-Mills descriptions. To do this, we must first address the fact that the p-branes carry charge, something our uniform string solution (4.27) lacks.

To proceed, we adopt a "charging up" technique for generating charged solutions from uncharged ones based on the equivalence of KK momentum in circle compactifications and dimensionally-reduced gauge field charge. We will make use of the most common example of this, namely the relation between momentum along the M-theory 11th circle and $D0$-brane charge.

The basic procedure now consists of three steps. First, we uplift the solution (4.27) to 11-dimensions, where it will describe an uncharged membrane solution of 11-dimensional SUGRA. We then boost this membrane along the 11th circle, generating KK momentum. Finally, we reduce back to 10-dimensions along the 11th circle, whereby the KK momentum descends to $D0$-brane charge. The uplift of (4.27) is trivial

$$ds_{11}^2 = -f(r)d\tau^2 + f^{-1}(r)\,dr^2 + r^2\,d\Omega_7^2 + dy^2 + dx^2 \tag{4.32}$$

where $x = x + L_{11}$. Performing the boost

$$\begin{pmatrix} \tau \\ x \end{pmatrix} \rightarrow \begin{pmatrix} \cosh\beta & \sinh\beta \\ \sinh\beta & \cosh\beta \end{pmatrix} \begin{pmatrix} \tau \\ y \end{pmatrix} \tag{4.33}$$

then yields the 11-dimensional solution

$$\begin{aligned} ds_{11,\text{boost}}^2 = &-\left(f(r)\cosh^2\beta - \sin^2\beta\right)\,d\tau^2 - 2\left(1-f(r)\right)\cosh\beta\sinh\beta\,d\tau\,dx \\ &+\left(-f(r)\sinh^2\beta + \cosh^2\beta\right)\,dx^2 + dy^2 + f^{-1}(r)\,dr^2 + r^2\,d\Omega_7^2 \end{aligned} \tag{4.34}$$

Finally, reducing back to 10 dimensions along the x circle and converting to string frame yields the metric

$$ds_{\text{smeared D0}}^2 = -H^{-1/2}(r,\beta)f(r)\,d\tau^2 + H^{1/2}(r,\beta)\left(f^{-1}(r)\,dr^2 + dy^2 + r^2\,d\Omega_7^2\right) \tag{4.35}$$

along with a nontrivial dilaton and 1-form gauge potential

$$e^{2\phi} = H^{3/2}(r,\beta) \qquad A_\tau = \coth\beta\left(H^{-1}(r,\beta) - 1\right) \tag{4.36}$$

where

$$H(r,\beta) = 1 + \frac{r_0^6 \sinh^2\beta}{r^6} \tag{4.37}$$

We immediately recognize this solution as that which describes the low energy physics of non-extremal $D0$-branes smeared uniformly along the y-circle in type IIA theory.

While we have succeeded in mapping the 10-dimensional uniform black string (4.27) to a familiar system, namely smeared $D0$-branes, what has happened to the nontrivial phase structure? In particular, does (4.35) suffer from a GL instability? To answer this, recall that onset of the instability is associated with the existence of a threshold unstable mode which, among other things, is time-independent. It is trivial to see that the boost has absolutely no effect on this mode and, consequently, the GL instability carries over to the smeared $D0$-brane system [77, 64]. The form of the instability will be affected, of course, as the boost will turn on components along the 11th circle which, upon reducing back to 10 dimensions, give rise to variations of the dilaton and 1-form as well as the metric. However, the point at which the instability sets in does not change so that μ_{GL} for the uniform string is identical to μ_{GL} for the smeared $D0$-brane system[3].

For the phase structures to agree, though, we need a little more. It is not enough that the GL points, at which the uniform and nonuniform branches merge, agree for both systems. We also need the relative ordering of free energies to remain the same as this fixes the order of the transition. While it is not immediately obvious that the uplift/boost

[3]Of course, throughout all of this we are assuming that the unstable modes remain normalizable. For finite boosts, this is obviously the case. In fact, this is true also for infinite boosts provided the limit is taken carefully [64].

procedure utilized here preserves the order, it is at least plausible that this is the case. After all, following the discussion of section 4.1.5, one expects that the two scenarios corresponding to first and second order transitions can be distinguished by determining when, relative to the GL point, the caged black hole can "fit" inside the S^1. It seems reasonable that the boost doesn't affect this size and consequently that the order of the phase transition is preserved. That this is the case can also be checked explicitly in six dimensions [77], where the nonuniform string and caged black hole branches have been constructed [47, 55, 56]. We will therefore assume that the smeared $D0$-brane solution (4.35) exhibits the same qualitative phase structure as the original uniform black string (4.27) from this point onward.

We now move to the final step in our chain of boosts and dualities, namely to notice that a collection of $D0$-branes uniformly smeared along a circle in type IIA theory is T-dual to a $D1$-brane wrapping the dual S^1 in type IIB theory. This relation is manifested in SUGRA by our ability to generate the nonextremal $D1$-solution from (4.35) using the Buscher rules [82, 83]. Applying these rules, we obtain the usual metric, dilaton, and two-form potential

$$ds^2_{D1} = -H^{-1/2}(r,\beta)\left[f(r)\,d\tau^2 + dy^2\right] + H^{1/2}(r,\beta)\left(f^{-1}(r)\,dr^2 + r^2\,d\Omega_7^2\right) \tag{4.38}$$

$$e^{2\phi} = H(r,\beta) \qquad\qquad A_{\tau y} = \coth\beta\left(H^{-1}(r,\beta) - 1\right) \tag{4.39}$$

$$y = y + L \tag{4.40}$$

To close this section, we remind the reader that, from the SUGRA point of view, the solutions (4.35) and (4.38) do not necessarily describe the same physics. Rather, they

represent two different approximations to the low energy dynamics of the same physical system provided we make the identifications

$$L\bar{L} = \alpha' \qquad \frac{g_s}{\bar{g}_s} = \sqrt{\frac{L}{\bar{L}}} \tag{4.41}$$

where g_s ($\bar{g}_s$) is the value of $e^{-\Phi}$ at infinity for the $D1$-brane (smeared $D0$-brane) solution. Note that the range of parameter space for which these approximations are valid is not identical as, for instance, the $D1$-brane description breaks down due to the appearance of string winding modes when L is small while the $D0$-brane description breaks down for similar reasons when $\bar{L}$ is small.

4.2.2 The Near Horizon Limit

So far, we have succeeded in mapping the GL instability of the 10-dimensional compact uniform black string to an instability of the SUGRA approximation to a collection of $D0$-branes smeared on an S^1. By T-duality, this is also an approximation to a collection of $D1$-branes wrapping the S^1, whose near horizon physics is completely captured by the gauge theory on their world volume, namely the maximally supersymmetric 1+1-dimensional Yang-Mills theory on S^1. Any instability that appears in the low energy SUGRA description should manifest itself in the gauge theory somehow provided, of course, that it survives the near-horizon limit. Since the GL unstable modes decay exponentially away from the horizon [57, 58], it is natural to expect that this is the case away from extremality [77]. One can explicitly verify this fact as well as demonstrate that the unstable modes of (4.35) become marginal at extremality [64].

Let's be a little more concrete about the near-horizon limit and resulting geometries. What we would like to do is decouple the world-volume gauge theory from gravity in the bulk while keeping the energy ϵ above extremality finite in order to preserve the non-

trivial GL physics. Explicitly, this is accomplished for the $D1$-brane solution (4.38)-(4.39) by taking

$$\alpha' \to 0 \qquad\qquad r \to \infty \tag{4.42}$$

keeping fixed proper distances as measured at infinity, the coupling constant of the gauge theory on the brane, and the energy above extremality

$$r/\alpha' \qquad g_{YM}^2 = (2\pi\alpha')^{-1} g_s \qquad \epsilon = \frac{\Omega_{8-p}}{16\pi G} r_0^6 \left[7 + 6\sinh\beta\left(\sinh\beta - \cosh\beta\right)\right] \tag{4.43}$$

Defining a dimensionless 't Hooft coupling constant λ' by

$$\lambda' = g_{YM}^2 N L^2 \tag{4.44}$$

it is straightforward to write the resulting metric in gauge theory variables [76]

$$ds^2 = \alpha' \left\{ \sqrt{\frac{u^6}{d_1\lambda'}} \left[-\left(1 - \frac{u_0^6}{u^6}\right) \frac{dt^2}{L^2} + \frac{d\theta^2}{(2\pi)^2} \right] + \sqrt{\frac{d_1\lambda'}{u^6}} \left(1 - \frac{u_0^6}{u^6}\right)^{-1} du^2 + u^{-1}\sqrt{d_1\lambda'}\, d\Omega_7^2 \right\} \tag{4.45}$$

Here, the coordinate u is related to the original r by

$$u = \frac{rL}{\alpha'} \qquad\qquad \theta = \theta + 1 \tag{4.46}$$

the variable θ is periodic

$$\theta = \theta + 1 \tag{4.47}$$

and the constants u_0, d_1 are given by

$$u_0 = 2^7 3\pi^5 \left(\frac{\lambda'}{N}\right)^2 \epsilon \qquad\qquad d_1 = 2^6\pi^3 \tag{4.48}$$

There is also a nonzero dilaton and 2-form field strength but we will not need either.

The precise duality statement that we shall utilize is the equivalence of string theory propagating in this background (4.45) and the maximally supersymmetric Yang-Mills theory on the world-volume. Since the branes are not extremal, the dual gauge theory has a nonzero vacuum energy and is most easily studied in the canonical ensemble at finite temperature. As we mentioned briefly at the end of subsection 4.1.7, one expects the qualitative phase structure of the canonical ensemble to resemble that of the microcanonical ensemble[4]. For this reason, it is natural to parametrize the solutions not by μ, but rather by a dimensionless temperature t

$$t = TL \tag{4.49}$$

For the near-horizon solution (4.45) it is not difficult to see that t is is determined according to

$$u_0^2 = \frac{16\pi^{5/2}}{3} t\sqrt{\lambda'} \tag{4.50}$$

From this, it is easy to determine the critical point t_{GL} at which the instability sets in. We simply need to recall that, for the uniform black string, it occurred for

[4]One might worry that the phase structure in the canonical ensemble may differ from that in the microcanonical ensemble. The discussion in section 4.1.5 was quite general, though, and can be applied to thermodynamics controlled by the free energy, F, and dimensionless temperature, t, just as easily as it was applied to thermodynamics controlled by the entropy, S, and dimensionless mass, μ. If we accept the two phase structures elucidated there as the only possibilities, the only worry then is that the canonical ensemble may exhibit second order behavior while the canonical ensemble exhibits first order behavior. While there is evidence that this may occur in 13 dimensions, for $D < 13$ numerical evidence suggests otherwise [74, 75].

$$r_0 \sim \bar{L} = \frac{\alpha'}{L} \leftrightarrow u_0 \sim 1 \tag{4.51}$$

Using (4.50), we see that this is equivalent to

$$t_{GL} \sim \frac{1}{\sqrt{\lambda'}} \tag{4.52}$$

The next question of importance is when SUGRA provides good approximation in this background. Near the horizon, the solution (4.45) has characteristic length scale

$$\ell = \left(\frac{d_1 \lambda' \alpha'^2}{u_0^2} \right)^{1/4} \tag{4.53}$$

To ensure that α' corrections are negligible, we must have $\ell \gg \sqrt{\alpha'}$, which is equivalent to

$$t \ll \sqrt{\lambda'} \tag{4.54}$$

This is not the only sort of stringy correction that we must worry about, though. For t sufficiently small, winding modes wrapping the S^1 can potentially become light. The mass of these modes is given roughly by

$$M_w \sim \left(\frac{u_0^3}{d_1 \alpha' \lambda'} \right)^{1/4} \tag{4.55}$$

Since there are negligible provided $M_w \ell \gg 1$, we see that winding modes can be neglected for t such that

$$t \gg \frac{1}{\sqrt{\lambda'}} \tag{4.56}$$

Note that in order to simultaneously satisfy (4.54) and (4.56) one must have $\lambda' \gg 1$ so that, as usual, the SUGRA regime corresponds to the limit of strong coupling in the dual gauge theory.

The potential importance of winding modes at $t \sim \lambda'^{-1/2}$ should not be very surprising since we have already seen that this is precisely when the GL instability sets in. In the T-dual $D0$-brane picture, the instability takes the form of momentum modes along the S^1. In the $D1$-brane picture, these are precisely the winding modes that are becoming light.

While SUGRA in the $D1$-brane background doesn't know how to deal with these winding modes, the $D0$-brane picture does so it is to this that we turn in order to obtain a gravity description for $t <\sim \lambda'^{-1/2}$. The quickest way to find the relevant geometry is a simple application of the Buscher rules [82, 83] to the solution (4.45). This leads to the metric

$$ds^2 = \alpha' \left\{ -\sqrt{\frac{u^6}{d_1\lambda'}} \left(1 - \frac{u_0^6}{u^6}\right) \frac{dt^2}{L^2} + \sqrt{\frac{d_1\lambda'}{u^6}} \left[\left(1 - \frac{u_0^6}{u^6}\right)^{-1} du^2 + (2\pi)^2 \, d\tilde{\theta}^2 \right] + u^{-1}\sqrt{d_1\lambda'}\, d\Omega_7^2 \right\} \tag{4.57}$$

along with a dilaton and RR field strength that we don't bother to write down. As before, the SUGRA approximation is valid when α' corrections and winding modes are negligible. The characteristic length scale near the horizon is again ℓ (4.53) so that α' corrections are negligible provided

$$t \ll \sqrt{\lambda'} \tag{4.58}$$

Now, however, winding mode masses are given roughly by

$$M_w \sim \left(\frac{d_1 \lambda'}{u^6 \alpha'^2}\right)^{1/4} \tag{4.59}$$

so that the condition that they are negligible becomes

$$t \ll 1 \tag{4.60}$$

In particular, we see that there is no problem describing the system near $t \sim \lambda'^{-1/2}$ using SUGRA in the $D0$-brane picture.

Summary of the $D1$-brane system

To summarize, we have demonstrated that the GL instability of uniform 10-dimensional compact black strings can be related to a similar instability of N nonextremal $D1$-branes wrapping an S^1 in otherwise flat space, for which the near horizon physics is captured by maximally supersymmetric Yang-Mills theory on the worldvolume at finite temperature. At high temperatures, corresponding to large circle size, the approximation of SUGRA in the near-extremal $D1$-brane background is valid at strong coupling $\lambda' \gg 1$. This background has no clumping instability since it is physically impossible for $D1$-brane charge to do so in SUGRA. One might naively think that a $D1$-brane wrapping a circle is always stable for this reason but at smaller temperatures, corresponding to smaller circle size, winding modes invalidate the SUGRA approximation. To proceed further, we T-dualize to a collection of $D0$-branes smeared on the dual circle. The winding modes, which SUGRA couldn't describe in terms of black 1-branes, have become momentum modes in the $D0$-brane picture. Moreover, these momentum modes destabilize the system at a critical temperature, t_{GL}, below which we expect the $D0$-brane charge to "clump" on the circle.

4.2.3 Implications for the dual gauge theory

What are the implications of GL physics for the gauge theory dual to our $D1$-brane system? More specifically, how does the gauge theory "know" about the distribution of $D0$-brane charge?

The answer to this last question is remarkably simple once we recall the relation between $D0$-branes and holonomies, W_C, in the world volume theory:

$$W_C = P \exp i \oint_C A \tag{4.61}$$

In particular, the expectation value of W_C is a unitary matrix whose eigenvalues take the form $e^{i\alpha}$. The α are circle-valued and, when C is the spatial circle, correspond to the locations of $D0$-branes on the dual circle. As with the $\mathcal{N} = 4$ theory, we expect to generate an effective potential for the holonomies, obtaining a unitary matrix model that can be solved by saddle point techniques. What we are seeing here is that the eigenvalue distributions which arise during the course of such a solution have a physical meaning in the case of the spatial holonomy – it is telling us the distribution of $D0$-brane charge! The three possibilities that we saw before, namely uniform, wavy, and clumped, correspond precisely to the three sorts of $D0$-brane charge distributions that we expect to find.

It is thus quite clear how we can proceed to probe GL physics from the dual gauge theory point of view. We need only determine the dominant spatial eigenvalue distributions throughout the parameter space. This should permit us to map out the phase struture, at least for the part of the parameter space where the gauge theory analysis can be carried out, and find one of the two possibilities enumerated by Kol.

The only question that remains is what relevance the gauge theory analysis may have for the phase structure of the 10-dimensional uniform black string. We saw that the

GL point in that setup is identical to that of the $D1$-brane setup which we directly probe via Yang-Mills theory. If the transition is of second order, this is where it will occur so the critical points of the uncharged uniform string and $D1$-brane system agree. If instead it is of first order, though, there is no reason to believe that the transition points are the same and the agreement is simply qualitative.

It isn't even obvious, though, that the order is preserved by the uplift/boost procedure. We have argued based on numerical analysis that the 10-dimensional uniform string undergoes first order transitions in both the microcanonical and canonical ensembles [74, 75]. However, the uplift/boost procedure could potentially disrupt the relative ordering of entropies and/or free energies of the various solutions, interchanging first and second order scenarios. Where numerical constructions are available, namely in six dimensions, one can argue that this doesn't occur and that the phase structure of the charged string obtained via uplifting/boosting is qualitatively identical to that of the uniform string. It seems reasonable that these arguments will hold also in the ten-dimensional case but we should be clear that this is an assumption. Later we will see, though, that this assumption fits nicely with the gauge theory results.

Of course, when discussing the relevance of our gauge theory analysis for uniform uncharged strings, it is also necessary to emphasize that, as usual, the gauge theory probes a region of the full phase diagram complementary to that accessible to SUGRA analysis. We can make simplifying assumptions concerning the manner in which the weak and strong coupling regimes are connected and gain satisfaction if this can be done simply. However, we simply cannot directly probe the SUGRA regime from perturbative gauge theory. Fortunately, the gauge theory analysis of the next chapter will fit in nicely with everything we've learned on the gravity side to form a consistent picture that is quite compelling.

Chapter 5

Yang-Mills Theories on Low Dimensional Tori

In this final chapter, we seek to study the phase structure of the maximally supersymmetric Yang-Mills theory (SYM) on S^1 at finite temperature, or Euclidean SYM on T^2. As argued in the previous chapter, the strong coupling regime of this theory captures the physics of Gregory-Laflamme (GL) black string/black hole phase transitions. As usual, the standard methods of gauge theory analysis are unable to directly probe this structure at strong coupling so we turn instead to the opposite limit. We shall see, however, that it is difficult to use such techniques even throughout most of the weak coupling regime since perturbative methods often break down there as well. Indeed, all of the interesting structure that exists at weak coupling is outside of the realm of perturbative control. Numerical analysis will help us considerably by allowing a direct study of this structure for some of the parameter space, including part of the phase transition line, but a systematic study of even the full weak coupling regime is presently out of reach.

As in our study of the $\mathcal{N} = 4$ theory on S^3, where only limited information was

available from weak and strong coupling, we will be forced to take what data we have and make reasonable conjectures regarding the remainder of the phase diagram. Instead of restricting only to the SYM theory in question, though, we will make up for our limited data by increasing the sample size, so to speak. In particular, we will consider deformations of the SYM theory as well as related bosonic models where more direct analysis can be done and a feel for the physics obtained. We shall also enlarge the class of models that we consider to include those of dimension less than 2. Strictly speaking this isn't much of an enlargement since the 0- and 1-dimensional theories describe the physics of the 2-dimensional theory when cycles are small. We will treat them in their own right, though, as they provide simple laboratories in which essential techniques can be developed.

We are thus led to undertake a systematic study of Yang-Mills theories on low dimensional tori. We will follow roughly the structure of [84], beginning with the simple models in low dimensions and working up from there. By the end, we will find a remarkably rich phase structure of which the GL transition is an important piece.

5.1 Preliminaries

Before proceeding with our study, we first comment on some general features of the analysis. As our eventual goal is to study theories with maximal supersymmetry, we shall restrict ourselves to models with adjoint matter fields having the usual quartic couplings. Occasionally we shall include masses as well in order to provide means of deformation to regions of parameter space where the models become easier to analyze.

As we have seen already in the $\mathcal{N} = 4$ theory, Wilson loops provide natural order parameters which can be used to distinguish the various phases of Yang-Mills at finite temperature. For the deconfinement transition studied in chapter 3, we argued on physical

grounds that the two phases could be distinguished by the value of the Polyakov loop. That this is the relevant object to study is also clear simply from a practical point of view, as it captures the dynamics of the only light degree of freedom in the problem.

Similarly, we will focus on the light degrees of freedom in our study of Yang-Mills theories on tori. These technically include not only constant modes of the gauge field, but also those of the scalars since there is no curvature to give make them massive as happened on S^3. The dynamics of the scalar field zero modes turns out to be quite boring, though, as their eigenvalue distributions are always clumped. Had this not been the case, one would have worried about convergence issues since the scalar eigenvalues can take arbitrary real values, as opposed to the gauge field eigenvalues which are circle-valued.

We thus focus our attention primarily on the dynamics of gauge field zero modes. Unlike what we saw on S^3, each component of the gauge field will have such modes here, the dynamics of which are captured by Wilson loops about nontrivial cycles of the torus. Since we limit our considerations to tori of dimension $d \leq 2$, we will have up to two such Wilson loops, U and V, and can use the corresponding eigenvalue distributions to distinguish among the various possible phases. We will be a bit sloppy in this discussion and enumerate the possibilities according to whether $\mathrm{tr}\,(U)$ and $\mathrm{tr}\,(V)$ vanish or not. What makes this a bit crude is that it does not make a distinction between the nonuniform and clumped distributions, for both of which the trace of the corresponding holonomy is nonzero. However, we shall see that if nonuniform phases exist in the theories under study, it is likely over only very small parameter ranges so this simplification is acceptable to describe the bulk of the phase diagram.

For Yang-Mills theories on S^1, there is a single holonomy $\mathrm{tr}\,(U)$ which, provided the fermions have appropriate boundary conditions, we can think of as the Polyakov loop associated to a 0+1-dimensional gauged quantum mechanics system at finite temperature.

The phases with $\mathrm{tr}\,(U)$ vanishing and nonvanishing are interpreted as the usual confined and deconfined phases of this system. Of course, we are being sloppy here since the quantity that takes values zero and nonzero at large N is actually $N^{-2}\mathrm{tr}\,(U)$. Throughout this chapter, we will not write the N^{-2} explicitly though its presence is implied.

For Yang-Mills theories on T^2, there are two holonomies and consequently four possible phases. We will always consider fermion boundary conditions that permit one of the cycles to be thought of as a thermal circle so the corresponding holonomy, V, has the interpretation of a Polyakov loop that distinguishes between confined and deconfined phases of 1+1-dimensional quantum mechanics on a circle. The interpretation of the spatial holonomy, U, is similar in the sense that, as happens with V, a nonzero expectation value of U spontaneously breaks a global symmetry. In the case of confinement transitions, the symmetry is a $\mathbb{Z}_N$ arising from gauge transformations that are not periodic around the thermal circle. Spontaneous breaking of this $\mathbb{Z}_N$ by a nonzero expectation value of the Polyakov loop $\mathrm{tr}\,(V)$ is a standard signal of deconfinement. While we cannot use the words confinement and deconfinement to describe the physics associated to the spatial holonomy, U, a nonzero expectation value of $\mathrm{tr}\,(U)$ indeed spontaneously breaks an analagous $\mathbb{Z}_N$ symmetry that arises from nonperiodic gauge transformations about the spatial circle.

For the maximally supersymmetric theories, the phases discussed above are connected with those of the gravity duals as we have discussed in detail already. When an S^1 is identified as a thermal circle, the eigenvalue distribution of the corresponding holonomy indicates the presence or absence of a horizon in analogy to the discussion in 2.4.1. On the other hand, when an S^1 is identified as a spatial circle the eigenvalue distribution of the corresponding holonomy is giving a snapshot of the distribution of $D0$-brane charge along the circle. It is this picture that permits us to connect the phase structure that we find here to the physics of black string/black hole transitions in chapter 4. Identifying V as the

holonomy of the time circle, the black string phase corresponds to $\mathrm{tr}\,(V) \neq 0$, $\mathrm{tr}\,(U) = 0$ while the black hole phase corresponds to $\mathrm{tr}\,(V) \neq 0$, $\mathrm{tr}\,(U) \neq 0$.

5.2 Bosonic Matrix Integrals

We now begin our systematic study of Yang-Mills theories on low-dimensional tori with the simplest possible example, namely 0-dimensional Yang-Mills coupled to p adjoint scalars with a quartic interaction. There are no Yang-Mills fields in 0-dimensions and the effect of gauging is trivial, introducing only an overall factor of the gauge group volume. As a result, the partition function that we wish to study takes the form of a simple matrix integral

$$\begin{aligned} Z &= \int D\Phi_i \, \exp\left\{ -\frac{N}{2\lambda_0} \mathrm{tr} \left(\sum_i m_i^2 \Phi_i^2 - \sum_{i<j} [\Phi_i, \Phi_j]^2 \right) \right\} \\ &= \int D\phi_i \, \exp\left\{ -\frac{N}{2} \mathrm{tr} \left(\sum_i \frac{\tilde{\Phi}_i^2}{2} - \sum_{i<j} \frac{\lambda_0}{m_i^2 m_j^2} [\tilde{\Phi}_i, \tilde{\Phi}_j]^2 \right) \right\} \end{aligned} \tag{5.1}$$

where we have rescaled the Φ_i in the second line to make clear that the effective couplings are $\lambda_0/m_i^2 m_j^2$.

We are interested in studying the eigenvalue distributions of the Φ_i as a function of λ_0. Doing so generally is quite difficult, but there are two limits in which an analytic treatment is possible. The first corresponds to the limit of weak coupling, $\lambda_0/m_i^2 m_j^2 \to 0$, in which the partition function reduces to that of N decoupled Gaussian matrix integrals. The dominant saddle point configuration of such integrals is well-known to be given by the Wigner semicircle

$$\rho(x) = \frac{2}{\pi} \sqrt{1 - x^2} \tag{5.2}$$

and consequently the eigenvalues of the $\tilde{\Phi}_i$ are clumped on an interval of size 1, corresponding to a clumping of the Φ_i eigenvalues on an interval of size $\sqrt{\lambda_0}/m_i$.

The other analytically tractable regime is the limit of very large coupling, $\lambda_0/m_i^2 m_j^2 \gg 1$. Here, the quadratic term is negligible and we are left with

$$Z = \int D\Phi_i \, \exp\left\{ \frac{N}{2\lambda_0} \sum_{i<j} [\Phi_i, \Phi_j]^2 \right\} \tag{5.3}$$

Because the squared commutator is negative definite, the configurations of least action are those for which all Φ_i are diagonal. Denoting the eigenvalues of the Φ_i by ϕ_i, we can expand about the diagonal configuration to quadratic order in the off-diagonal terms

$$S = \frac{N}{4\lambda_0} \sum_{i<j} \left[\left(\Delta\phi^I\right)_{ij}^2 |\Phi_{ij}^j|^2 - \left(\Delta\phi^I\right)_{ij} \left(\Delta\phi^J\right)_{ij} \Phi_{ij}^I \Phi_{ij}^{Jast} + \ldots \right] \tag{5.4}$$

where the $(\Delta\phi^I)_{ij}$ are the eigenvalue differences

$$\left(\Delta\phi^I\right)_{ij} = \phi_i^I - \phi_j^I \tag{5.5}$$

The cubic term that we have neglected will have coefficient linear in eigenvalue differences while the quartic term has no eigenvalue dependence at all. If the distance between eigenvalues is characterized by the scale a, then the effective coupling of the off-diagonal components is simply λ_0/a^4. When this is small, we can reliably integrate out the off-diagonal components at one-loop to obtain

$$Z \sim \det(M)^{-1} \qquad\qquad M^{IJ} = \delta^{IJ} \sum_K \left(\Delta\phi^K\right)_{ij}^2 - \left(\Delta\phi^I\right)_{ij} \left(\Delta\phi^J\right)_{ij} \tag{5.6}$$

which can be evaluated once we note that the eigenvalues of M are simply

$$\left[\sum_K \left(\Delta\phi^K\right)^2_{ij}\right] \text{ with degeneracy } p-1 \text{ and } 0 \text{ with degeneracy } 1 \tag{5.7}$$

The presence of a zero eigenvalue may seem troublesome at first, but its appearance is easily understood. In particular, we have run into this potential divergence because we neglected the existence of flat directions in the space of off-diagonal components which arise due to the $SU(N)$ gauge symmetry of (5.1). In other words, we could use gauge invariance to exactly diagonalize one of the matrices so we had no business integrating over the corresponding set of off-diagonal modes.

To proceed, we go back to (5.3) and fix this $SU(N)$ symmetry by using it to diagonalize Φ^1. In doing this, we pick up a Fadeev-Popov determinant factor that is nothing other than the usual Vandermonde that one typically encounters when moving to eigenvalue variables

$$\Delta_{FP} = \det\left(\left[\Phi^1, *\right]\right) \sim \prod_{i<j} \left(\Delta\phi^1\right)^2_{ij} \tag{5.8}$$

Once Φ^1 is diagonalized, its off-diagonal components no longer contribute to the 1-loop computation above. This has the effect of removing the first row and column of the matrix M (5.6), leaving a $(p-1)\times(p-1)$ matrix with eigenvalues

$$\left[\sum_K \left(\Delta\phi^K\right)^2_{ij}\right] \text{ with degeneracy } p-2 \text{ and } \left(\Delta\phi^1\right)^2_{ij} \text{ with degeneracy } 1 \tag{5.9}$$

The contribution of $(\Delta\phi^1)^2_{ij}$ to the determinant cancels against Δ_{FP}, leaving the following result for (5.3)

$$Z \sim \int d\phi^I_j \prod_{i<j} \left(\sum_K \left(\phi^K_i - \phi^K_j\right)^2\right)^{-(p-2)} \tag{5.10}$$

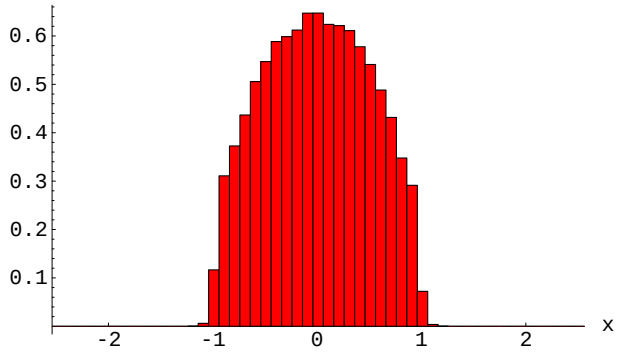

Figure 5.1: Sample eigenvalue distribution from a Monte Carlo analysis of (5.1) with $\lambda_0 = 1$, $p = 10$, $N = 20$. Reprinted from [77].

We see that the effective potential for the eigenvalues generated by integrating out the off-diagonal components at 1-loop is attractive, leading to a clumped distribution. From (5.10), one might naively conclude that, in fact, this distribution is a δ-function with all eigenvalues on top of one another. Of course, we do not expect this to be the case as the approximation that the off-diagonal modes are weakly coupled breaks down when the eigenvalues are within a distance of order $\lambda_0^{1/4}$ from one another. At this point, off-diagonal modes become strongly coupled and, presumably, the distribution stabilizes at the scale $a \sim \lambda_0^{1/4}$ suggested by 't Hooft scaling.

That this is actually the case can be checked using Monte Carlo techniques to compute the integeral (5.3) numerically and determine not only the $\lambda_0^{1/4}$ scaling but also the numerical prefactor that sets the precise length of the clumping interval. We include a sample plot of the eigenvalue distributions that may be obtained from such a computation in figure 5.1.

Summary

Because the essential features of the bosonic matrix integral (5.1) studied here will arise again in the more complicate examples considered throughout the remainder of this chapter, we close this section with a brief summary of what we have found. In the limit of infinite masses, the integral can be solved exactly at large N and seen to be dominated by a clumped eigenvalue distribution of characteristic size $\sqrt{\lambda_0}/M$. In the opposite limit, $m_i \to 0$, the problem is perturbatively tractable provided the eigenvalues are sufficiently far apart, in which case the effective eigenvalue interactions are attractive. Rather than maximally clumping, though, the distribution is expected to stabilize at a scale $\lambda_0^{1/4}$. This lies outside of the weak coupling regime where perturbation theory can be trusted, though, so to see this stabilization we must turn to numerics.

We will see this pattern continue, with the massless theories becoming effectively strongly coupled when interesting physics is expected to set in. Deforming the theory by turning on large masses is one way to get a qualitative handle on things but ultimately numerical techniques become necessary to probe the full structure when fields are light.

5.3 Bosonic Yang-Mills on S^1

We now move up in dimension to consider bosonic Yang-Mills on an S^1. The particular model that we consider is

$$S = \frac{N}{2\lambda_1} \int dt \, \mathrm{tr} \left(\sum_{i=1}^{p} D_0 \Phi_i D_0 \Phi_i + \sum_{i=1}^{p} M^2 \Phi_i^2 - \sum_{i<j}^{p} [\Phi_i, \Phi_j]^2 \right) \tag{5.11}$$

From λ_1, M, and the size R of the S^1, which we will think of as an inverse temperature, we can construct two dimensionless parameters

$$\tilde{t} = \left(R\lambda_1^{1/3}\right)^{-1} \qquad m = M\lambda_1^{-1/3} \tag{5.12}$$

5.3.1 High temperatures – $\tilde{t} \gg 1$

There are two regimes for which the theory is easily analyzed. The first is the limit of large temperature, $\tilde{t} \gg 1$, in which case the model (5.11) reduces to the zero-dimensional matrix integral (5.1) studied in section 5.2. There, we saw that the dominant eigenvalue distributions of all fields were clumped. Note in particular that this includes the dimensional reduction of the gauge field, A_0, which is indistinguishible from the scalars in this limit[1].

5.3.2 Large masses – $m \gg 1$

The second regime that one can study corresponds to the limit of large mass $m \gg 1$ and displays a much more interesting and nontrivial structure. Here, the theory is effectively weakly coupled and, since all modes except the zero component of the gauge field, A_0, are massive, they can be integrated out in perturbation theory. The result of this procedure will be an effective action for A_0 which, by analogy to the discussion in section 3.3.1, is constrained by gauge invariance to be a function of a unitary matrix U

$$Z = \int DU \, \exp\left[-N^2 S_{\text{eff}}(U)\right] \qquad U = e^{i \oint dt \, A_0} \tag{5.13}$$

The computation of $S_{\text{eff}}(U)$ now proceeds exactly as in the $\mathcal{N} = 4$ theory with the identification

$$x = e^{-MR} = e^{-m/\tilde{t}} \tag{5.14}$$

[1]One might worry about the fact that A_0 is circle valued, which didn't appear in the 0-dimensional problem. More specifically, though, $A_0 = A_0 + 2\pi n/R$ so the circle on which A_0 takes values has size $1/R$ and decompactifies in the limit $R \to \infty$.

Indeed, it is the same calculation as that of sections 3.2 and 3.3 with the result again depending on letter partition functions that one can associate with state counting (3.3). Here, the letter partition function is rather trivial as there is only one bosonic state at energy 1 for each scalar field

$$z(x) = x \tag{5.15}$$

This leads to a simple effective action for U

$$S_{\text{eff}}(U) = p\sum_{n=1}^{\infty}\frac{x^n}{n}\text{tr}\,(U^n)\text{tr}\,(U^{-n}) \tag{5.16}$$

where the factor of p arises because S_{eff} receives contributions from p scalar fields. Writing this in terms of moments ρ_n of the corresponding eigenvalue distribution as in section 3.4, this becomes

$$S_{\text{eff}}(\rho_n) = \sum_{n=1}^{\infty}\frac{1}{n}m_n^2|\rho_n|^2 \tag{5.17}$$

$$m_n^2 = 1 - px^n \tag{5.18}$$

where the 1 in (5.18) arises from the Vandermonde measure as usual. We have thus arrived at an effective action for eigenvalue moments that precisely resembles that which arose in our study of the $\mathcal{N} = 4$ theory. Since we studied it in detail in section 3.4 and appendix (B), we simply repeat a few facts here. For small temperatures, the ρ_n are all massive and the saddle point distribution is uniform. For sufficiently high temperatures, on the other hand, ρ_1 will become tachyonic and condense, leading to the GWW clumped distribution (B.8). This phase transition is weakly first order and occurs at a critical temperature that is easily read from (5.18)

$$\tilde{t}_c = m\,(\ln p)^{-1} \tag{5.19}$$

Away from the strict $m \to \infty$ limit, (5.17) will receive corrections that can potentially alter the order of the transition. In particular, as we have seen many times it is the sign of the quartic term in the effective potential for ρ_1 that is the difference between first and second order. This can be determined by computing higher-loop perturbative corrections to (5.17) and integrating out the modes ρ_i with $i > 1$ that remain massive at the transition point. The result is an effective potential for ρ_1

$$S(\rho_1) = m_1^2(x, m^{-3})|\rho_1|^2 + \frac{1}{m^6} b(x, m^{-3})|\rho_1|^4 + \dots \tag{5.20}$$

The calculation of m_1 and b to the requisite orders is straightforward but tedious, yielding [84]

$$\begin{aligned} m_1^2 &= (1 - px) - \frac{1}{4m^6}(p^2 - p)(x^2 + 2x)\ln x \\ b &= -\frac{1}{32}\frac{(p-1)\ln p}{p^3}\left(\ln(p)(9p^2 + 2p) + 4p^3 + 7p^2 - 4p - 4\right) m^{-6} + \dots \end{aligned} \tag{5.21}$$

Since $b < 0$ for all $p > 1$, we see that the phase transition is indeed of first order as one moves away from $m = \infty$. From the correction to m_1^2 in (5.21), we can also compute the leading order shift in the phase transition temperature, obtaining [84]

$$\tilde{t}_c = m\,(\ln p)^{-1} + \frac{1}{4m^2}\frac{(p-1)(2p+1)}{p\ln p} + \dots \tag{5.22}$$

This result will fit in nicely the picture of the $m = 0$ theory that we now describe.

5.3.3 Massless theory – $m = 0$

Now that we have treated the two regimes of the $m - \tilde{t}$ plane that admit analytic treatments, we move now to the case of massless fields. The phase structure here will effectively describe a region of the supersymmetric theory on T^2 relevant for GL physics so we try to understand it as best we can.

From our analysis above, we already know that the eigenvalues of U are clumped at high temperatures. What we don't know is whether the system undergoes a phase transition analagous to what we saw at large m. It seems plausible that it does since a naive extrapolation of the critical temperature (5.22) to small masses indicates that the critical line meets the positive $\tilde{t}$ axis at $m = 0$. However, we would like to have more convincing evidence than this.

To study the theory directly, we can attempt to use perturbation theory. Provided the KK modes are weakly coupled, we can integrate them out at 1-loop, obtaining an effective matrix model for the zero modes that can be treated by analogy to (5.1). As in that case, the eigenvalue potential is purely attractive when the eigenvalue separations are sufficiently large [84]

$$S_{\text{eff}} = (p-1) \sum_{m \in \mathbb{Z}} \sum_{i<j} \ln \left[\left((\Delta A_0)_{ij} - \frac{2\pi m}{R} \right)^2 + \sum_I \left(\Delta \phi^I \right)_{ij}^2 \right] \tag{5.23}$$

where $(\Delta A_0)_{ij}$ denote A_0 eigenvalue separations analagous to $(\Delta \phi^I)_{ij}$ (5.5). When eigenvalue separations become small, off-diagonal components again become strongly coupled and we expect stabilization to occur on a scale set by $\lambda_1^{1/4}$.

What we have seen using these perturbative methods is not too surprising and, unfortuantely, doesn't go very far beyond what we already knew. The effective coupling of the KK modes is $\tilde{t}^{-3}$ so at infinite $\tilde{t}$, they completely decouple. This is just another

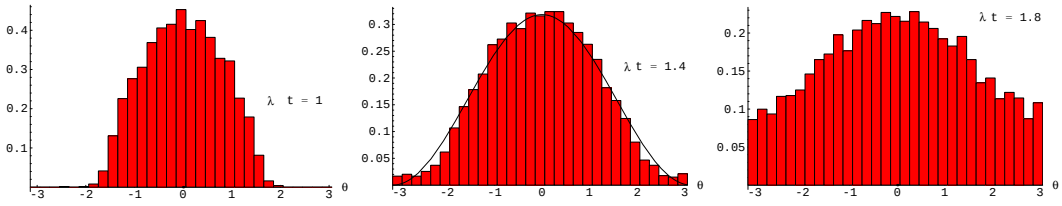

Figure 5.2: Sample eigenvalue distributions in massless bosonic Yang-Mills on S^1 (5.11) for $p = 9$ and various values of $\lambda t = \tilde{t}^{-3}$. The middle distribution is near the numerically estimated critical point. Reprinted from [77]

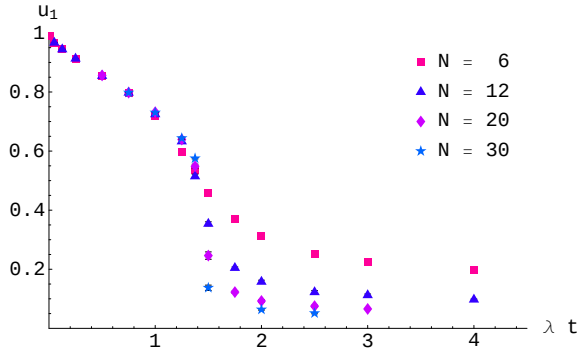

Figure 5.3: $|\rho_1|$ as a function of $\lambda = \tilde{t}^{-3}$ in massless bosonic Yang-Mills on S^1 (5.11) for various values of N. Reprinted from [77, 84]

statement of the dimensional reduction that we used above to study the theory with $\tilde{t} \gg 0$ generally. What we have shown is that if the KK modes are weakly coupled, perturbative corrections do not change the conclusion that eigenvalues continue to clump.

If the phase transition at $m \to \infty$ truly does persist in the $m = 0$ theory, it apparently lies in the strong coupling regime where perturbation theory is of no use to us. That this is the case isn't too surprising since the absence of any scale other than the torus volume suggests a critical point at $\tilde{t} \sim 1$. Unfortunately, it seems that no analytic techniques are available to help us verify this conjecture.

However, one-dimensional matrix quantum mechanics isn't too terribly complicated and can be simulated on a lattice using Monte-Carlo methods. This was done in [77]

with the result that the massless theory indeed exhibits a phase transition at

$$\tilde{t} = \tilde{t}_c^{(p)} \sim \mathcal{O}(1) \tag{5.24}$$

When $p = 9$, for instance, $\tilde{t}^{(9)} \approx 0.89$. This can be seen either by eyeballing the eigenvalue distributions, a few of which we plot in figure 5.2, or from plots of the moment $|\rho_1|$, which we present in figure 5.3.

While the presence of a phase transition is clear from the data, what is not so clear is the order. Of course, naively we might expect that the order remains first throughout the downward flow from infinite m. The data seems consistent with this, as the jump in figure 5.3 at $\tilde{t}_c$ looks as though it is sharpening as N is increased. Without the ability to study arbitrarily large N, though, it is difficult to rule out the possibility of two successive second order transitions. To make progress in this direction, we note that in all of our studies thus far, we have encountered the same standard Landau-Ginzburg potential for first and second order transitions[2]

$$V_{LG}(U) = a|\mathrm{tr}(U)|^2 + b|\mathrm{tr}(U)|^4/N^2 \tag{5.25}$$

As we have seen, the sign of b determines the order of the phase transition. Thus, an alternative means of studying the order is to ask for what sign of b does the potential (5.25) most accurately fit the Monte Carlo data? One can try simulate both the original model (5.11) as well as that constructed from (5.25) and attempt to compare the results for various values of a and b. It turns out that the LG model (5.25) works very well for b very small. In fact, the agreement is quite good even at $b = 0$, for which data from both models is plotted in figure 5.4.

[2]We write it as a matrix potential rather than as a potential for moments of the eigenvalue density but the structure is clearly the same

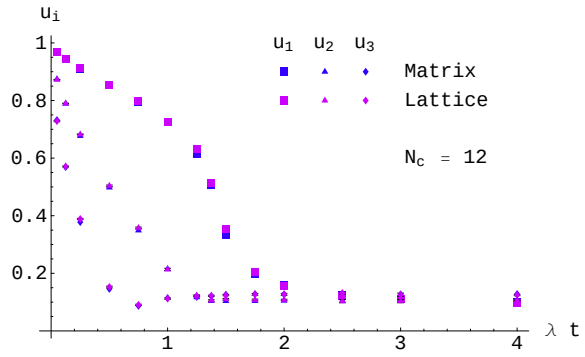

Figure 5.4: Comparison of Monte-Carlo simulations of massless bosonic Yang-Mills on S^1 (5.11) with results from the LG model (5.25) at $b = 0$ for $N = 12$. Reprinted from [77].

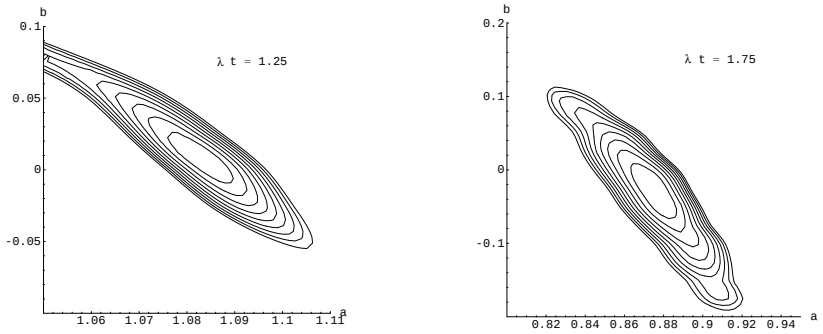

Figure 5.5: Level contours of the least-squares-fit function $L(a, b)$ (5.26) just below and above the phase transition in massless bosonic Yang-Mills on S^1 (5.11), which occurs at $\lambda t = \tilde{t}^{-1/3} \approx 1.44$. Reprinted from [77]

One can attempt to go further and determine how small the parameter b is. This was done in [77] by performing a least squares fit to the first two moments, $|\rho_1|$ and $|\rho_2|$, of the eigenvalue distribution over a range of N. To get a feel for the size of b, one can plot level contours on the ab plane of the function L that is minimized in this approach

$$L(a,b) = \sum_{i=1,2} \sum_{N=6,12,20} \Big(|\rho_i|^{MM(a,b)}(N) - |\rho_i|(N) \Big)^2 \tag{5.26}$$

We reproduce such plots just above and below the transition point in figure 5.5. We see explicitly that b is small near the transition. From the numerics, it seems most likely that b is negative, indicating a first order transition, so from this point onward we will simply assume this to be the case. Let us be clear, however, that positive b, indicating a second order transition, is certainly not ruled out. In fact, $b = 0$, in which case the transition might be of even higher order, is not ruled out either. One might expect the smallness of b to have a simple physical explanation but so far none exists so this remains an oustanding puzzle.

Summary

We can now summarize the phase structure that we have found for (5.11). At high temperatures, the eigenvalues of the holonomy are always clumped on the circle. At large mass, we found a clumping/declumping transition line that asymptotes to $\tilde{t} \sim m/\ln p$. We conjectured that this transition persists even in the massless theory at a finite critical temperature $\tilde{t}_c$ and used Monte Carlo techniques to demonstrate this explicitly. It seems likely that the transition is of first order but a sequence of closely spaced second order transitions cannot be ruled out. All of this data leads to the phase diagram of figure 5.6.

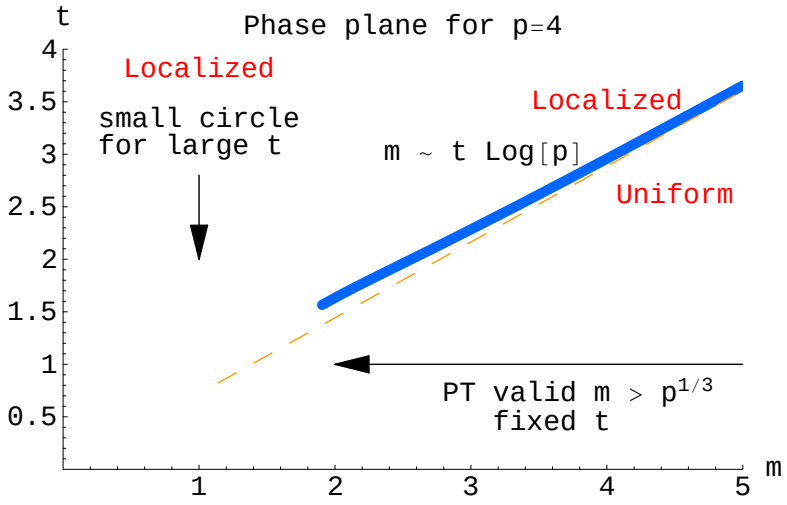

Figure 5.6: Phase diagraom of bosonic Yang-Mills on S^1 coupled to p interacting adjoint scalars (5.11).

5.4 Supersymmetric Yang-Mills on S^1

In this section we move on to the maximally supersymmetric Yang-Mills theory on S^1 with action

$$S = \frac{N}{\lambda_1}\int dt\,\mathrm{tr}\left(\frac{1}{2}\left(D_0\Phi_i\right)^2 + \frac{i}{2}\Psi^\dagger D_0\Psi - \frac{1}{4}\left[\Phi_i,\Phi_j\right]^2 + \frac{1}{2}\Psi^\dagger\gamma^i\left[\Phi_i,\Psi\right]\right) \tag{5.27}$$

which we study as a function of the dimensionless parameter $\tilde{t}$ defined as in (5.12).

With the introduction of fermions comes a choice of the boundary conditions that we impose on them. If we choose periodic boundary conditions then the corresponding partition function computes the Witten index of the associated 1+0-dimensional quantum mechanics system. To see this, we interpret the S^1 as a thermal circle so that one naively expects the partition function to be the usual thermal one $\mathrm{tr}\,(e^{-\beta H})$. However, the connection between the thermal partition function and Euclidean path integral requires the fermions to have antiperiodic boundary conditions around the thermal circle. The object

that is computed by the Euclidean path integral with periodic fermion boundary conditions has an extra insertion of $(-1)^F$

$$\int_{\text{periodic fermions}} e^{-S_E} = \text{tr}\left((-1)^F e^{-\beta H}\right) \tag{5.28}$$

This is precisely the Witten index [85], which counts the number of supersymmetric vacua. The result is, under relatively mild assumptions, independent of β and has no interesting phase structure.

For this reason, we focus instead on the case of antiperiodic fermion boundary conditions. A key feature of this case is that there are no fermi zero modes on the circle. This implies that for very large temperatures, $\tilde{t} \gg 1$, all fermi modes become massive and can be effectively neglected so that there is effectively no difference between the bosonic (5.11) and supersymmetric (5.27) theories in this limit. The holonomy eigenvalues are clumped in both cases and $\text{tr}\,(U) \neq 0$.

We now look at the opposite limit, $\tilde{t} \ll 1$, which is equivalent to large 't Hooft coupling λ_1. For this, we can use the fact that this theory (5.27) has a string theory dual for which we expect the SUGRA approximation to be valid. Indeed, the dual geometry is simply the near-horizon limit of a collection of non-extremal $D0$-branes [76]

$$ds^2 = \alpha' \left[-\sqrt{\frac{u^7 \tilde{t}^3}{d_0}} \left[1 - \left(\frac{u_0}{u}\right)^7\right] d\tau^2 + \sqrt{\frac{d_0}{u^7 \tilde{t}^3}} \left(\left[1 - \left(\frac{u_0}{u}\right)^7\right]^{-1} du^2 + u^2\, d\Omega_8^2 \right) \right] \tag{5.29}$$

where β is the size the S^1, $d_0 = 240\pi^5$ and

$$u_0 \sim \tilde{t}^{21/5} \tag{5.30}$$

Using this last result, it is now easy to verify directly that SUGRA is a good approximation for $\tilde{t} \ll 1$. The key point here is that the solution (5.29) has a horizon and

consequently $\mathrm{tr}\,(U)$ is nonzero in this regime as well. While this is not enough to distinguish between nonuniform and clumped eigenvalue distributions, the simplest assumption is that the the eigenvalues remain clumped and the model (5.27) undergoes no phase transition at all. This will have implications for the two-dimensional theories that we study next and fits with the other data there. We thus find this conjecture quite compelling though it would be nice to understand it further.

5.5 Bosonic Yang-Mills on a Rectangular T^2

We now consider the first of our two-dimensional models, namely bosonic Yang-Mills on a rectangular two-torus with radii R_1, R_2. Unlike the lower-dimensional models that we have studied so far, this system will not have any direct relevance to the maximally supersymmetric theory whose analysis is our primary goal in this chapter. However, the phase structure is similar in some respects and, moreover, the bosonic theory at large scalar masses is an example where one can probe almost all nontrivial aspects of the phase structure, including a tricritical point, analytically. For this reason we find it an interesting playground in which to learn about these theories in general and worth the brief digression.

The specific model that we consider has action

$$S = \frac{N}{2\lambda_2}\int d^2x\,\mathrm{tr}\left(F_{12}^2 + \sum_{i=1}^{p}\left[\left(D_\mu\Phi^I\right)^2 + M^2\Phi_I^2\right] - \sum_{I<J}\left[\Phi^I,\Phi^J\right]^2\right) \tag{5.31}$$

and can be parametrized by the two dimensionless radii

$$r_1 = R_1\sqrt{\lambda_2} \qquad\qquad r_2 = R_2\sqrt{\lambda_2} \tag{5.32}$$

and the dimensionless mass

$$m = \lambda_2^{-1/2} M \tag{5.33}$$

Throughout the ensuing discussion, we will refer to the holonomy about the r_1 (r_2) circle as V (U).

5.5.1 Infinite masses $m = \infty$

We begin our study of (5.31) by considering the strict limit $m = \infty$. The reason we do this is to recall some elementary facts about the exact solution of pure Yang-Mills on a two-torus that will be useful when we study large but noninfinite masses.

The exact result for the two-dimensional Yang-Mills partition function was first obtained by Migdal [86] using a lattice regularization of the theory. We consider putting unitary matrices U_L on the links of the lattice and consider the partition function

$$Z = \int \prod_L DU_L \prod_P Z_P(U_P) \tag{5.34}$$

where the product is over plaquettes P of the lattice and Z_P is a plaquette action chosen so that the continuum theory coincides with Yang-Mills. One example of a plaquette action is the usual Wilson one

$$Z_P = \exp\left\{ \frac{N}{\lambda_2} \mathrm{tr}\, \left(U_P + U_P^{-1} \right) \right\} \tag{5.35}$$

One can imagine integrating out some of the links to generate an effective action for the larger plaquettes that remain. Under this RG flow, the action (5.35) is not invariant, instead flowing to the plaquette action [86]

$$Z_P(U_P) = \sum_R d_R \chi_R(U_P) \exp\left\{ -\frac{\lambda_2 A}{2N} C_2(R) \right\} \tag{5.36}$$

where the representation R has dimension d_R and quadratic Casimir $C_2(R)$ and A is the area of the new plaquettes in units of the fundamental ones. It is easy to verify that (5.36) satisfies the additivity property

$$\int DU\, Z_P(V_1 U, A_1) Z_{P'}(U^\dagger V_2, A_2) = Z_{P+P'}(V_1 V_2, A_1 + A_2) \tag{5.37}$$

and consequently is an RG fixed point. To compute the partition function of 2-dimensional Yang-Mills, we are equally justified in using (5.35) or (5.36). The former is easier to work with as the property (5.37) can be used to integrate out all of the links except those wrapping nontrivial cycles. Restricting to the torus for simplicity, we arrive at the following expression for the partition function

$$Z = \int DU\, DV \sum_R d_R e^{-\frac{r_1 r_2}{2N} C_2(R)} \chi_R(UVU^{-1}V^{-1}) \tag{5.38}$$

where we have used the definitions (5.32) of r_1, r_2. The links which remain are precisely the holonomies that we wish to study. The remaining integrals (5.38) are now sufficiently simple that we can perform them exactly to obtain

$$Z = \sum_R e^{-\frac{r_1 r_2}{2N} C_2(R)} \tag{5.39}$$

This partition function is very well-behaved and exhibits no nontrivial phase structure. As an exercise, let us obtain this conclusion in a manner more in line with the sort of analysis that we have used to study other theories above. In particular, let us consider integrating out only one holonomy, say V, from (5.38). We obtain

$$Z = \int DU \sum_R e^{-\frac{r_1 r_2}{2N} C_2(R)} \chi_R(U) \chi_R(U^\dagger) \tag{5.40}$$

Using the generalized Frobenius relations of [87, 88, 89] it is possible to write the integrand in terms of an effective action for U [84]

$$Z = \int DU \, \exp\left\{ \sum_n \frac{1}{n} \left(-e^{-r_1 r_2 n} + 2e^{-r_1 r_2 n/2} \right) \mathrm{tr}\,(U^n) \mathrm{tr}\,(U^{-n}) \right\} \tag{5.41}$$

Introducing an eigenvalue density ρ as usual, we can obtain an effective action for the moments of ρ

$$S_{eff}(\rho_n) = \sum_n \frac{1}{n} \left(1 - e^{-r_1 r_2 n/2} \right)^2 |\rho_n|^2 \tag{5.42}$$

We see that for all values of the coupling $\lambda_2 A = r_1 r_2$ the effective masses of the ρ_n are positive. In the limit $r_1 r_2 \to \infty$ they become arbitrarily light but the never become tachyonic. The eigenvalue distributions are thus always uniform and there is no phase transition.

5.5.2 Large masses $m \gg 1$

While we saw that the infinitely massive theory had no nontrivial phase structure, this shouldn't come as too much of a surprise since analagous conclusions could be drawn in the 1-dimensional case of section 5.3 as well. We now move to the regime of large but finite masses so that the scalars are present but heavy and can be reliably integrated out at one-loop. As we saw above, the eigenvalue moments become arbitrarily light at high temperatures so even a small attractive force from the scalars can induce a phase transition. Indeed, we will find several transition lines and can say more about the structure of this regime than any other two-dimensional example we shall study.

Large radius $r_1 \gg r_2, m$

We begin our analysis of the massive model (5.31) with the limit in which one of the circle sizes, say r_1, approaches infinity. In this limit, the theory becomes effectively decompactified so that it approaches that which describes the thermodynamics of the associated 1+1-dimensional theory in flat space. Because the r_1 circle grows to infinity, the circle on which the V eigenvalues take values shrinks to zero size so their distribution is uniform. The dynamics of U is a bit more interesting, though, as it corresponds to the Polyakov loop of the flat space theory, which one expects to exhibit a deconfinement transition. This can be studied as usual by integrating out all massive degrees of freedom to obtain an effective action for U [90]

$$S = \int dx \left\{ \frac{N}{2\lambda_2 R_2} \mathrm{tr} \left(|\partial_x U|^2 \right) - p\sqrt{\frac{M}{2\pi R_2}} e^{-MR_2} \mathrm{tr}\,(U(x)) \mathrm{tr}\,(U^\dagger(x)) \right\} \tag{5.43}$$

Note that since the spatial direction is flat the corresponding spectrum of U modes is ungapped. It is for this reason that U is a function of x above and cannot be reduced to a zero mode as we have done in the compact cases.

The effective action (5.43) is a bit more complicated than what we are used to, but it can be analyzed using techniques of collective field theory [90]. One finds that U undergoes a clumping/declumping transition at critical temperature

$$r_{2,c}^{-1} = \frac{2}{m} \ln(m) + \ldots \tag{5.44}$$

that is of first order. In particular, $\mathrm{tr}\,(U) = 0$ for $r_2 > r_{2,c}$ while $\mathrm{tr}\,(U) \neq 0$ and the eigenvalues are clumped for $r_2 < r_{2,c}$. There is of course an analagous transition at $r_{1,c}^{-1} = 2 \ln m/m$ in the limit of infinite r_2 at which V undergoes a clumping/declumping transition.

Small radius $r_1 \ll r_2, m^{-1}$

We now turn to the opposite limit, namely that for which one of the circle sizes r_1 approaches zero. Provided the KK masses are larger than all other scales in the problem, the theory reduces to that of the 1-dimensional model (5.11) considered in section 5.3 with an extra massless scalar arising from the gauge field component A_1 along r_1. The precise conditions for the validity of this reduction are those indicated above, $r_1 \ll r_2, m^{-1}$, and correspond to KK masses being larger than all scalar masses as well as the temperature. The parameters of the reduced 1-dimensional model are related to r_1, r_2, m by

$$\tilde{t} = \frac{r_1^{1/3}}{r_2} \qquad\qquad m^{(d=1)} = m r_1^{1/3} \tag{5.45}$$

For $r_1 \ll m^{-3}$ the dimensionally reduced theory is effectively massless and we expect a phase transition separating regions with $\mathrm{tr}\,(U)$ vanishing and nonvanishing at the critical temperature

$$\tilde{t} = \tilde{t}_c^{(p+1)} \tag{5.46}$$

where $\tilde{t}_c^{(p+1)}$ is the critical point of (5.24). For $r_1 \gg m^{-3}$, the dimensionally reduced theory has all scalars massive except that arising from A_1, which is massless. This isn't quite the large mass scenario that we studied in section 5.3 since all scalars are not heavy. It turns out, though, that the case of one additional massless scalar remains tractable because a mass for that field is generated by the heavy scalars at 1-loop [84]. One can then integrate out everything except for the holonomy U at 1-loop level, finding a transition line along

$$\tilde{t} = \frac{2m^{(d=1)}}{3 \ln m^{(d=1)}} + \ldots \tag{5.47}$$

Translating these results back to the parameters r_1, r_2, m of the two-dimensional theory in question, we find explicit expressions for the transition line in two regimes

$$r_1 = r_{1,c}(r_2) = \begin{cases} \left(r_2 \tilde{t}_c^{(p+1)}\right)^3 & r_1 \ll m^{-3} \\ m^{-3} e^{2mr_2} & m^{-3} \ll r_1 \ll m^{-1} \end{cases} \tag{5.48}$$

For $r_1 > r_1, c$, $\mathrm{tr}\,(U) \neq 0$ and its eigenvalues are clumped. For $r_1 < r_{1,c}$, on the other hand, $\mathrm{tr}\,(U) = 0$ and its eigenvalues are uniform. On the other hand, A_1 becomes a typical scalar field in the reduction so $\mathrm{tr}\,(V) \neq 0$ and its eigenvalues are clumped. As with the large radius case, there is an analagous transition at small r_2 along which the holonomy V undergoes a declumping transition.

Intermediate radii

So far, we have probed only a few corners of the phase diagram, corresponding to cycle sizes very large or small. A summary of what we have found is illustrated in figure 5.7, which also depicts the three simplest conjectures for the interior region about which we have said nothing so far. Our goal in this subsection is to utilize the simplicity of pure two-dimensional Yang-Mills theory reviewed in section 5.5.1 to probe this region as precisely as possible. In particular, the effect of the massive scalars is to slightly perturb an otherwise exactly solvable theory. Treating this carefully will permit us to probe a large interior region of the phase diagram 5.7 that will distinguish among the three possibilities indicated.

Our general strategy will be to integrate out the scalars at 1-loop and obtain a deformation of the matrix model (5.38) that solves the pure Yang-Mills theory without scalars. This a bit trickier than it might seem at first since the determinant one obtains in this manner will be a complicated function of the gauge fields that doesn't obviously reduce to the zero modes to which U and V correspond. It is thus possible in some regimes

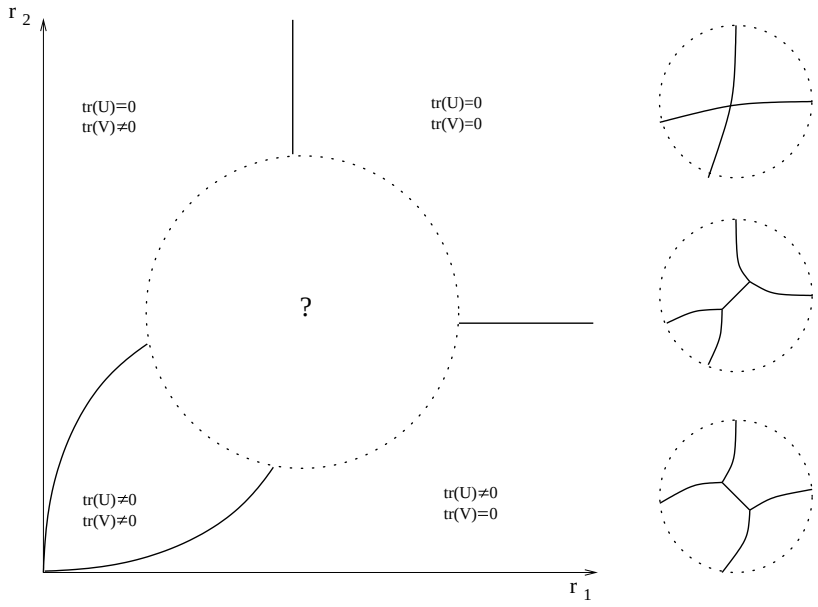

Figure 5.7: Partial phase structure of massive bosonic Yang-Mills on T^2 (5.31). The qualitative structure of this phase diagram also captures what we know about the massless theory.

that the deformation has a much more drastic effect on the Yang-Mills theory than simply modifying (5.38) in a simple way.

All is not lost, though, as we can see from the following situation. Let us return to the result (5.43) for the effective action of the spatially varying holonomy U about the r_2 circle in the limit $r_1 \to \infty$. Rather than taking r_1 strictly infinite, let us consider instead taking r_1 large and continue to utilize this action. Mode expanding the holonomy $U(x) = \sum_n U_n e^{inx}$ and integrating over the r_1 direction, x, we obtain

$$S \sim \sum_n \left(\frac{n^2}{2r_1 r_2} - p r_1 \sqrt{\frac{m}{2\pi r_2}} e^{-m r_2} \right) |U_n|^2 \tag{5.49}$$

From this we see that nonconstant modes of U are very massive and should be negligible over a large region

$$r_1^2 \ll \frac{1}{\sqrt{mr_2}} e^{mr_2} \tag{5.50}$$

Moreover, we see that a very specific potential is generated for the constant mode

$$V_{eff}(U) = f(U) = -\frac{p}{\sqrt{2\pi}} \frac{r_1}{r_2} \sqrt{mr_2} e^{-mr_2} \mathrm{tr}\,(U) \mathrm{tr}\,(U^{-1}) \tag{5.51}$$

We could perform a similar exercise for the analagous regime

$$r_2^2 \ll \frac{1}{\sqrt{mr_1}} e^{mr_1} \tag{5.52}$$

and find there an effective potential for V

$$V_{eff}(V) = g(V) = -\frac{p}{\sqrt{2\pi}} \frac{r_2}{r_1} \sqrt{mr_1} e^{-mr_1} \mathrm{tr}\,(V) \mathrm{tr}\,(V^{-1}) \tag{5.53}$$

The simplest possible conjecture for how to modify (5.38) in the presence of massive scalars is then to simply include both of the effective potentials, (5.51) and (5.53). While this seems overly simplistic, it turns out to be completely valid for a surprisingly large range of parameters!

To justify this, we turn to a direct computation of the one-loop determinant arising from the scalar fields

$$S_{eff} = \frac{p}{2} \ln \det \left(-D_\mu^2 + M^2\right) \tag{5.54}$$

As mentioned before, the result can be quite complicated but we will make the simplifying assumption that nonzero modes of U and V can be neglected. In fact, we have already argued that this is the case when (5.50) and (5.52) are satisfied so we restrict ourselves to this regime. Evaluating the determinant is then straightforward and yields the result

$$
\begin{aligned}
S_{eff} &= -p \sum_{(k,n)\neq(0,0)} \mathrm{tr}\,(U^n V^k)\mathrm{tr}\,(U^{-n}V^{-k}) m r_1 r_2 \frac{K_1\left(m\sqrt{r_1^2k^2+r_2^2n^2}\right)}{2\pi\sqrt{r_1^2k^2+r_2^2n^2}} + \ldots \\
&\to -p \sum_{(k,n)\neq(0,0)} \mathrm{tr}\,(U^n V^k)\mathrm{tr}\,(U^{-n}V^{-k}) \sqrt{m} r_1 r_2 \frac{\exp\left(-m\sqrt{r_1^2k^2+r_2^2n^2}\right)}{2\sqrt{2\pi}\left(r_1^2k^2+r_2^2n^2\right)} + \ldots
\end{aligned}
\tag{5.55}
$$

where we have used the asymptotic form of the Bessel function K_1 and the omitted terms $\ldots$ denote additional contributions in which the ordering of U's and V's inside the traces is permuted. The key point here is that terms with increasing powers of U and V are exponentially damped so that for $mr_1 \gg 1$ and $mr_2 \gg 1$ only the leading terms contribute. These are precisely the potentials $f(U)$ and $g(V)$ that we found above

$$
S_{eff} = f(U) + g(V) + \ldots \tag{5.56}
$$

so for a large range of parameters the naive approximation that we suggested there is completely justified.

We have thus managed to reduce the theory (5.31) to the matrix integral

$$
Z = \int DU\, DV \sum_R d_R e^{-\frac{r_1 r_2}{2N} C_2(R)} \chi_R(UVU^{-1}V^{-1} e^{-f(U)} e^{-g(V)} \tag{5.57}
$$

in the parameter range

$$
r_1^2 \ll \frac{1}{\sqrt{mr_2}} e^{mr_2} \qquad r_2^2 \ll \frac{1}{\sqrt{mr_1}} e^{mr_1} \qquad m \gg r_1^{-1}, r_2^{-1} \tag{5.58}
$$

The effect of the new potentials $f(U)$ and $g(V)$ is easily seen by first considering the limit $r_1 \gg r_2$, in which case $g(V)$ is negligible compared to $f(U)$. Performing the V integration exactly as we did to derive (5.40) we obtain

$$
Z = \int DU\, e^{-f(U)} \sum_R e^{-\frac{r_1 r_2}{2N} C_2(R)} \chi_R(U)\chi_R(U^{-1}) \tag{5.59}
$$

Using the result (5.41) and introducing the eigenvalue density ρ, we then find an effective action for the moments ρ_n

$$S_{\text{eff}}(\rho_n) = \left[\left(1 - e^{-r_1 r_2/2}\right)^2 - \frac{p}{\sqrt{2\pi}}\frac{r_1}{r_2}\sqrt{m r_2}e^{-m r_2}\right]|\rho_1|^2 + \sum_{n>1}\frac{1}{n}\left(1 - e^{-r_1 r_2 n/2}\right)|\rho_n|^2 \tag{5.60}$$

We see that the deformation gives a small tachyonic contribution to the mass of ρ_1. Because ρ_1 was becoming massless in the pure Yang-Mills matrix integral (5.40) as $r_1, r_2 \to \infty$, this small tachyonic kick is all that we need to generate a phase transition at a location determined by the point at which ρ_1 becomes tachyonic

$$\left(1 - e^{-r_1 r_2/2}\right)^2 = \frac{p}{\sqrt{2\pi}}\frac{r_1}{r_2}\sqrt{m r_2}e^{-m r_2} \tag{5.61}$$

This curve intersects the parameter range (5.58) in the region $r_1 r_2 \ll 1$ so we can replace the conditions there with

$$m^{-1} \ll r_2 \ll r_1 \ll r_2^{-1} \ll m \tag{5.62}$$

where the curve (5.61) takes the simpler form

$$r_{1,c}(r_2) = \frac{4p}{\sqrt{2\pi}}\frac{\sqrt{m}}{r_2^{5/2}}e^{-m r_2} \tag{5.63}$$

For $r_1 < r_{1,c}(r_2)$ the moment ρ_1 is massive, the eigenvalue distribution of U is uniform, and $\text{tr}\,(U) = 0$. For $r_1 > r_{1,c}(r_2)$ the moment ρ_1 is tachyonic, the eigenvalue distribution of U is clumped, and $\text{tr}\,(U) \neq 0$. Meanwhile, there was no potential for V in this limit so its eigenvalues remain uniformly distributed and $\text{tr}\,(V) = 0$ throughout.

Note that at $r_1 r_2 \sim 1$, the curve (5.63) roughly approaches the point

$$(r_1, r_2) \sim \left(\frac{m}{2\ln m}, \frac{2\ln m}{m} \right) \tag{5.64}$$

so that the naive $r_1 \to \infty$ limit of (5.63) reproduces the earlier result (5.44). What we have thus found is an extension of the previously obtained transition lines (5.63) into the interior.

We would like to do better, though, and study the regime where these transition lines meet. For this, we must consider the full matrix integral (5.57). As written it is quite complicated, but we can make some progress by changing variables according to $U \to WUW^{-1}$ for unitary W and integrating over this quantity, which is roughly a relative "angle" between U and V. The result of this manipulation is that Z can be written as

$$\begin{aligned} Z = \int DU\, DV \sum_R e^{-\frac{r_1 r_2}{2N} C_2(R)} \frac{d_R^2}{d_R^2 - 1} e^{-f(U)} e^{-g(V)} \\ \times \left\{ -1 + \chi_R(V)\chi_R(V^{-1}) + \chi_R(U)\chi_R(U^{-1}) - \frac{1}{d_R^2}\chi_R(U)\chi_R(U^{-1})\chi_R(V)\chi_R(V^{-1}) \right\} \end{aligned} \tag{5.65}$$

where we can replace $d_R^2/(d_R^2 - 1)$ by 1 at large N. This isn't quite of the form of an effective action, though the first three terms can be individually written that way. The fourth term, on the other hand, is much more problematic but we now argue that it can be neglected for the purpose of computing expectation values of $\mathrm{tr}\,(U), \mathrm{tr}\,(V)$ for a range of parameters and consequently doesn't impact the phase structure. To be specific, suppose we wish to compute a correlator involving only one of the two matrices, say U. The contribution from the last two terms in (5.65) is given by

$$\int DU\, DV \sum_R e^{-\frac{r_1 r_2}{2N} C_2(R)} \left\{ \left[e^{-g(V)} \left(1 - \frac{1}{d_R^2}\chi_R(V)\chi_R(V^{-1}) \right) \right] \left[e^{-f(U)} \mathcal{O}(U) \chi_R(U)\chi_R(U^{-1}) \right] \right\} \tag{5.66}$$

where $\mathcal{O}(U)$ denotes the operator insertion in question. Let us suppose now that we can pass the V integration through the sum over representations[3]. Doing so, the V-dependent terms can be written as

$$\int DV\, e^{-g(V)} \left(1 - \frac{1}{d_R^2}\chi_R(V)\chi_R(V^{-1})\right) = \langle 1\rangle_g - \frac{1}{d_R^2}\langle \chi_R(V)\chi_R(V^{-1})\rangle_g \tag{5.67}$$

where we have introduced the notation $\langle\,\rangle_g$ for the expectation value in a model with action g. Provided the coefficient of $\mathrm{tr}\,(V)\mathrm{tr}\,(V^{-1})$ in g (5.53) is small

$$r_2 \ll \frac{1}{p}\sqrt{\frac{r_1}{m}}e^{mr_1} \tag{5.68}$$

the eigenvalue repulsion factor will dominate in this model and the corresponding matrix integral will be in a confined phase. This always holds in the regime (5.62) and hence

$$\frac{1}{d_R^2}\langle \chi_R(V)\chi_R(V^{-1})\rangle_g = 0 \tag{5.69}$$

at large N and the corresponding term can be neglected. Similarly, this term can be neglected when computing expectation values involving only the matrix V provided

$$r_1 \ll \frac{1}{p}\sqrt{\frac{r_2}{m}}e^{mr_2} \tag{5.70}$$

Again, this is always true in the regime (5.62). Our problem is now greatly simplified as the partition function can be written as a sum of effective decoupled models

$$Z = -\langle 1\rangle_{M=\infty}\langle 1\rangle_g\langle 1\rangle_f + \langle 1\rangle_f\langle 1\rangle_{S_\infty(V)+g} + \langle 1\rangle_g\langle 1\rangle_{S_\infty(U)+f} \tag{5.71}$$

[3]This sort of operation can actually be quite troublesome when analyzing the matrix integral in question but in the present situation we will demonstrate that the result of the V integral doesn't scale with representation size so such a manipulation can be trusted here.

where $\langle 1 \rangle_{M=\infty}$ is the partition function (5.38) of pure Yang-Mills and $S_\infty(U)$ ($S_\infty(V)$) is the effective action (5.41) obtained from (5.38) by integrating over V (U).

The models with actions g and f are confined when (5.68) and (5.70) are satisfied, as we discussed above, so the corresponding partition functions are of order 1 at large N. We have seen, though, that the model with action $S_\infty(V)+g(V)$ ($S_\infty(U)+f(U)$) exhibits a clumping/declumping phase transition separating regions where $\mathrm{tr}\,(V)$ ($\mathrm{tr}\,(U)$) is vanishing or nonvanishing. When $\mathrm{tr}\,(V)$ ($\mathrm{tr}\,(U)$) is nonzero, the free energy scales as N^2 and hence the partition function diverges at large N in that phase. From (5.71) we see that the full partition function exhibits this behavior precisely when one of $Z_{S_\infty(V)+g}$ or $Z_{S_\infty(U)+f}$ does. So, if we start in the regime of large r_1, r_2 where all eigenvalues are uniform and start to move toward the interior, the full model will not undergo a phase transition until one of the one-matrix models does. Consequently, the transition lines that we found above, (5.63) and its $r_1 \leftrightarrow r_2$ counterpart, extend all the way into the interior until they meet at

$$r_1 = r_2 = \frac{4}{m} \ln m + \dots \tag{5.72}$$

Let's push this even further and attempt to go beyond this first transition line. For definiteness, we consider $r_2 < r_1$ so that the transition line separates regions with $\mathrm{tr}\,(U) = 0$ and $\mathrm{tr}\,(U) \neq 0$. In the "deconfined" phase with $\mathrm{tr}\,(V) \neq 0$ we can compute the expectation value of $\mathrm{tr}\,(U)^4$ as

$$\left\langle \frac{1}{N^2} |\mathrm{tr}\,(U)|^2 \right\rangle = \frac{-Z_{M=\infty} Z_g Z_f \langle |\rho_1|^2 \rangle_f + Z_f Z_{S_\infty(V)+g} \langle |\rho_1|^2 \rangle_f + Z_g Z_{S_\infty(U)+f} \langle |\rho_1|^2 \rangle_{S_\infty(U)+f}}{-Z_{M=\infty} Z_g Z_f + Z_f Z_{S_\infty(V)+g} + Z_g Z_{S_\infty(U)+f}} \tag{5.73}$$

where ρ_1 is the first moment of the U eigenvalue distribution. The quantities $Z_{M=\infty}$, Z_f, and Z_g are all of order one so the first terms in the numerator and denomina-

[4] As usual, what we mean by $\mathrm{tr}\,(U)$ is the suitably normalized object $N^{-2}\mathrm{tr}\,(U)$.

tor may be neglected. Before the transition point of the model $Z_{S_\infty(U)+f}$, it can also be neglected and we are left with

$$\left\langle \frac{1}{N^2}|\mathrm{tr}\,(U)|^2 \right\rangle = \langle|\rho_1|^2\rangle_f = 0 \tag{5.74}$$

so there is no further phase transition in this region. One might expect, however, that U undergoes a clumping transition at the critical point of the model $Z_{S_\infty(U)+f}$ so that the phase transition line (5.63) continues right through the meeting point (5.72). This isn't the case, though, as beyond this point the expectation value above becomes

$$\begin{aligned}\left\langle \frac{1}{N^2}|\mathrm{tr}\,(U)|^2 \right\rangle &= \frac{Z_f Z_{S_\infty(V)+g}\langle|\rho_1|^2\rangle_f + Z_g Z_{S_\infty(U)+f}\langle|\rho_1|^2\rangle_{S_\infty(U)+f}}{Z_f Z_{S_\infty(V)+g} + Z_g Z_{S_\infty(U)+f}} \\ &\to \langle|\rho_1^2|\rangle \\ &= 0\end{aligned} \tag{5.75}$$

The reason for this is that the model with action $S_\infty(V)+g$ has smaller free energy than that with action $S_\infty(U)+f$ and consequently terms involving the former dominate.

What we conclude from all of this is that beyond the transition line formed from (5.63) and its $r_1 \leftrightarrow r_2$ counterpart only one of the two matrices is clumped. The regions in which $\mathrm{tr}\,(U) \neq 0$ and $\mathrm{tr}\,(V) \neq 0$ are thus separated by a new phase transition line that extends toward the origin along $r_1 = r_2$. Of course, given what we know about the small r_1, r_2 regimes this cannot continue all the way to $r_1 = r_2 = 0$. Indeed, our assumption that higher order terms in the determinant (5.55) are negligible breaks down for r_1 or r_2 of the order m^{-1} so presumably the structure changes in that regime. The most natural conjecture to complete the phase diagram is that the $r_1 = r_2$ line splits into two lines which join those that we found in the limit of small r_1 and r_2.

Throughout this analysis we have seen that, while the model (5.31) at large m

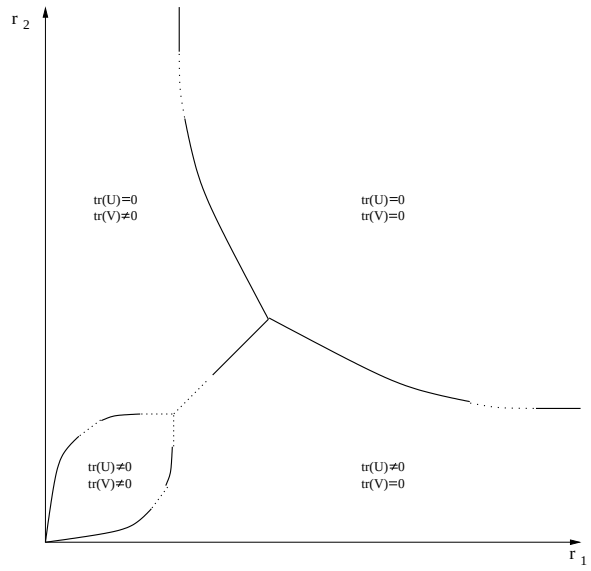

Figure 5.8: Phase diagram of the bosonic Yang-Mills theory (5.31) for large scalar masses. The solid lines denote those for which we have analytic expressions (see figure 5.9). Dashed lines denote the conjectures that provide the most simple completion of the phase diagram.

isn't exactly solvable, we can use the exact solution of pure Yang-Mills to say quite a lot about the phase structure. Our results are summarized in the phase diagram of figure 5.8 where we explicitly show the transition lines for which analytic expressions can be found. Half of these analytic expressions are tabulated in figure 5.9, with the other half given by flipping $r_1 \leftrightarrow r_2$ and $U \leftrightarrow V$.

5.5.3 Massless theory $-$ $m = 0$

How much of the structure that we found above persists in the massless theory? We begin with the limit $r_1 \ll r_2$ where, as in the massive case, the theory reduces to a one-dimensional model (5.11). Since the scalars are massless here, an analytic treatment is not available. Nonetheless, the numeric studies of subsection (5.3.3) suggest a clumping transition associated to the matrix U at a value of the 1-dimensional temperature $\tilde{t}$ that is of order unity. As with the massive theory this translates to a critical line

Critical Line $r_{1,c}(r_2)$	Regime of Validity	Phase for $r_1 > r_{1,c}$	Phase for $r_1 < r_{1,c}$
$\left(r_2\tilde{t}_c^{(p+1)}\right)^3$	$r_1 \ll m^{-3}$	$\mathrm{tr}\,(U) = 0$ $\mathrm{tr}\,(V) \neq 0$	$\mathrm{tr}\,(U) \neq 0$ $\mathrm{tr}\,(V) \neq 0$
e^{2mr_2}/m^3	$m^{-3} \ll r_1 \ll m^{-1}, r_2$	$\mathrm{tr}\,(U) = 0$ $\mathrm{tr}\,(V) \neq 0$	$\mathrm{tr}\,(U) \neq 0$ $\mathrm{tr}\,(V) \neq 0$
r_2	$m^{-1} \ll r_1 < 4\frac{\ln m}{m}$	$\mathrm{tr}\,(U) = 0$ $\mathrm{tr}\,(V) \neq 0$	$\mathrm{tr}\,(U) \neq 0$ $\mathrm{tr}\,(V) = 0$
$4p\sqrt{m}e^{-mr_2}/\sqrt{2\pi r_2^5}$	$m^{-1} \ll r_2 < r_1$ $\ll r_2^{-1} \ll m$	$\mathrm{tr}\,(U) = 0$ $\mathrm{tr}\,(V) = 0$	$\mathrm{tr}\,(U) \neq 0$ $\mathrm{tr}\,(V) = 0$
$m/2\ln m$	$r_2 \gg m^{-1}, r_1$	$\mathrm{tr}\,(U) = 0$ $\mathrm{tr}\,(V) = 0$	$\mathrm{tr}\,(U) = 0$ $\mathrm{tr}\,(V) \neq 0$

Figure 5.9: Summary of analytic results for transition lines in the bosonic Yang-Mills theory (5.31) and their regimes of validity ($m \gg 1$ throughout).

$$r_1 = r_{1,c}(r_2) = \left(r_2\tilde{t}_c^{(p+1)}\right)^3 \tag{5.76}$$

The dimensional reduction is valid provided $r_1 \ll r_2$ so that this critical line extends throughout the region $r_1, r_2 \ll 1$. There is of course the usual $r_1 \leftrightarrow r_2$ partner of this line. In between these two lines we can, as usual, study the system perturbatively by integrating out KK modes at 1-loop. This produces an attractive potential for the eigenvalues of the form (5.23) and is thus consistent with our expectation that $\mathrm{tr}\,(U) \neq 0, \mathrm{tr}\,(V) \neq 0$ there.

At large radius an effective action of the form (5.43) is unavailable so analytic results are also difficult to come by here as well. Again the $r_1 \to \infty$ theory describes the thermodynamics of a $1+0$-dimensional Yang-Mills theory that is expected to deconfine at a critical value of the effective temperature r_2^{-1} [5]. In general, we expect this to occur at the scale set by the coupling and consequently for r_2 of order unity. The numerical coefficient is, unfortunately, out of our reach.

[5]For the case of one scalar, this has been demonstrated explicitly in [91].

What we have thus argued for here is a phase diagram of the qualitative form depicted in figure 5.7. That the structure in asymptotic regimes is similar to that of the massive theory is not completely unexpected and it is natural to conjecture a completion in the interior of the form (5.8). Unfortunately, we do not know of any controlled manner in which to probe this regime in the massless theory. Even the numerics is more demanding there since a full 2-dimensional calculation is needed.

5.6 Supersymmetric Yang-Mills on a Rectangular T^2

We finally arrive at the example of most relevance to our study of black string/black hole phase transitions, namely the maximally supersymmetric Yang-Mills theory on a torus

$$S = \frac{N}{2\lambda_2} \int d^2x \, \mathrm{tr} \left(F_{12}^2 + \sum_{I=1}^{8} \left(D_\mu \Phi^I \right)^2 - \sum_{I<J} \left[\Phi^I, \Phi^J \right]^2 + \text{fermions} \right) \tag{5.77}$$

For simplicity we shall consider rectangular tori throughout most of the discussion that follows though we will make a few comments about more general tori later. As with the one-dimensional supersymmetric theory (5.27), we are presented with a choice regarding boundary conditions to impose on the fermions. In all, there are four choices since the fermions can be periodic or antiperiodic about each of the two nontrivial cycles. If we take the fermion boundary conditions to be periodic about both cycles, the resulting partition function will amount to an index computation of a one-dimensional theory analagous to (5.28) and consequently exhibit no nontrivial phase structure. We will thus always take antiperiodic boundary conditions about at least the r_2 cycle, which we think of as a thermal circle. This leaves two possible choices for the boundary conditions along r_1 that we now consider in turn.

5.6.1 Antiperiodic r_1 Boundary Conditions

The first case that we consider corresponds to antiperiodic boundary conditions about both cycles. Because of this choice the $r_1 \leftrightarrow r_2$, $U \leftrightarrow V$ symmetry of the phase diagram that we have grown used to will persist.

Small radius $r_1 \ll r_2$

Let us focus first on the limit in which one of the cycles becomes small $r_1 \ll r_2$. As we have become accustomed to, KK modes about the r_1 cycle are negligible in this limit and the theory reduces to a one-dimensional model. Since the fermion boundary conditions are antiperiodic, though, there are no fermi zero modes in the problem so, in particular, the dimensional reduction eliminates all of them and we are left with a purely bosonic theory! In particular, the small radius limit of the supersymmetric theory (5.77) is equivalent to that of the bosonic theory (5.31) at $m = 0$. Consequently, there is a clumping/declumping phase transition associated with the matrix U along

$$r_1 = \left(r_2 \tilde{t}_c^{(9)}\right)^3 \tag{5.78}$$

where $\tilde{t}_c^{(9)}$ is the critical point (5.24) of the one-dimensional model (5.11) at $m = 0$ with $p = 9$ scalar fields. As noted below (5.24) the value of $\tilde{t}_c^{(9)}$ has been determined from Monte Carlo methods to be

$$\tilde{t}_c^{(9)} \approx 0.89 \tag{5.79}$$

Large volume $r_1 r_2 \gg 1$

By analogy with our study of the bosonic theory (5.31) we look next at large radii. In the bosonic case, we relied on the fact that the problem reduced to the thermodynamics

of a $1+1$-dimensional model in flat space that is expected to exhibit deconfinement. We could estimate the location of the transition line by noting that the deconfinement scale is set roughly by the coupling λ_2. This was as far as we could take the analysis in the massless theory, though, as further analytic treatments were unavailable.

Here we can do a bit better since the large radius regime, which corresponds to strong coupling, admits a dual description in supergravity via AdS/CFT. In fact, we have already seen that the model in question arises as a description of SUGRA in the near-horizon region of N $D1$-branes wrapping an S^1. The relevant Euclidean solution is given by the analytic continuation of (4.45)

$$ds^2 = \alpha' \left\{ \sqrt{\frac{u^6}{d_1 \lambda'}} \left[\left(1 - \frac{u_0^6}{u^6} \right) \frac{dt_E^2}{L^2} + \frac{d\theta^2}{(2\pi)^2} \right] + \sqrt{\frac{d_1 \lambda'}{u^6}} \left(1 - \frac{u_0^6}{u^6} \right)^{-1} du^2 + u^{-1} \sqrt{d_1 \lambda'}\, d\Omega_7^2 \right\} \tag{5.80}$$

where we recall that

$$\lambda' = \lambda_2 L \qquad t = TL \qquad u_0^2 = \frac{16\pi^{5/2}}{3} t \sqrt{\lambda'} \tag{5.81}$$

and the angle θ and Euclidean time t_E are identified according to

$$\theta = \theta + 2\pi \qquad t_E = t_E + \frac{1}{T} \tag{5.82}$$

At this point, one might ask whether the t_E circle should be identified with the r_1 or r_2 cycles in the Yang-Mills theory (5.77). Of course the answer to this is that both possibilities should in principle be considered. Said more explicitly, the gauge theory partition function is computed, in the SUGRA regime, by a saddle point approximation to the Euclidean path integral which includes a sum over all geometries with the appropriate asymptotics [2, 5]

$$Z_{YM} = \sum_{\text{relevant geometries}} \exp(-S) \tag{5.83}$$

To compute the partition function of (5.77), we thus need to sum over all matchings of the torus at infinity of (5.80) with the torus of our Yang-Mills theory (5.77). We must take care, of course, to include only matchings that are consistent with fermion boundary conditions since one cannot have fermions that are periodic at infinity about a cycle that contracts in the interior.

In the case at hand, we have a rectangular torus with antiperiodic fermion boundary conditions about both cycles so there are two terms in the sum (5.83) distinguished by which of the two cycles of our torus contracts in the interior. In general, we expect one of these two geometries to give a dominant contribution to the partition function (5.83) with the possibility of a phase transition between the two as parameters are varied.

To determine which contribution dominates, we need only evaluate the Euclidean actions of the two and compare. This computation is slightly subtle since the Euclidean action for an individual solution diverges. The difference is finite, though, and can be evaluated without too much difficulty. Comparing solutions X_1, in which the r_1 circle is contractible, and X_2, in which the r_2 circle is contractible, yields [84]

$$S(X_1) - S(X_2) \sim N^2 \left(\frac{r_2^{3/2} - r_1^{3/2}}{(r_2 r_1)^{3/2}} \right) \tag{5.84}$$

Consequently, we see that the dominant geometry is that for which the smaller of the two cycles is contractible in the bulk.

The implications of this result for the Yang-Mills theory are now quite clear. When the r_1 (r_2) cycle contracts in the interior, the corresponding Wilson loop, $\mathrm{tr}\,(V)$ ($\mathrm{tr}\,(U)$) is nonzero while $\mathrm{tr}\,(U)$ ($\mathrm{tr}\,(V)$) vanishes. The two phases are separated by a phase boundary at $r_1 = r_2$ along which a first order transition takes place.

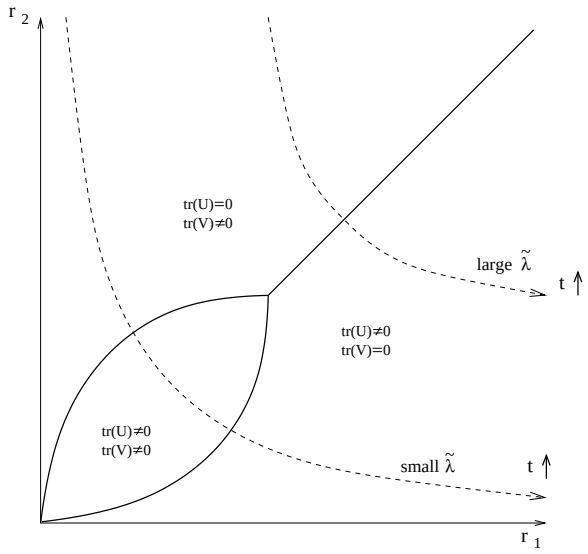

Figure 5.10: Phase diagram of maximally supersymmetric Yang-Mills theory on a rectangular T^2 (5.77) with antiperiodic boundary conditions along both cycles. We have directly probed the weak coupling ($r_1, r_2 \ll 1$) and strong coupling ($r_1, r_2 \gg 1$) regimes indicated. The interior region is our conjectured completion.

We can now combine this result with what we saw at small r_1, r_2 to make a conjecture for the full phase diagram of the theory (5.77) in the case of antiperiodic fermion boundary conditions about both cycles in figure 5.10. Note that the only regions that we have been able to probe are those corresponding to weak coupling ($r_1 r_2 \ll 1$) and strong coupling ($r_1 r_2 \gg 1$) so in particular we have not probed the region near the tricritical point.

What happened to the GL transition?

One might be a little puzzled at this point since, according to the phase diagram of figure 5.10, the phase with $\mathrm{tr}\,(U)$ and $\mathrm{tr}\,(V)$ both nonzero, which we would naturally identify as the localized black hole, apparently doesn't extend into the gravity regime. We saw ample evidence for this phase transition in the previous chapter, though, so what is going on?

To address this question, let us consider focus our attention on the geometry of the

form (5.80) with r_2 identified with the time circle t_E. In the previous chapter, we argued that SUGRA in this background was valid provided $\lambda'^{,-1/2} \ll t \ll \lambda'^{1/2}$ where t, λ' are as in (4.49) and (4.44). Translating this to the variables r_1 and r_2, this condition amounts to

$$1 \ll r_2 \ll r_1^2 \tag{5.85}$$

At the point $r_2 \sim r_1^2$, winding modes become light and drive the GL instability to the recently emerged localized black hole solution. Notice, however, that before this point is even reached the system undergoes the phase transition at $r_1 = r_2$ beyond which the dominant phase is that for which r_1 is identified with the time circle. In this background, SUGRA is valid in the regime

$$1 \ll r_1 \ll r_2^2 \tag{5.86}$$

and consequently we expect the new solution to completely mask the GL physics, which becomes relevant only for subdominant contributions to the partition function. That this occurs for the theory in question is not too surprising since our choice of boundary conditions implied a symmetry of the phase diagram under $r_1 \leftrightarrow r_2$. For GL physics, the time and space circles are distinguished by the fact that the holonomy of the former is always nonvanishing and consequently the corresponding phase diagram does not exhibit this symmetry.

To probe GL physics we are thus led to a slightly different situation, namely the case of periodic fermion boundary conditions about one of the cycles. In that case, only one of the cycles will be allowed to contract in the interior, eliminating the second saddle point which masked the GL phase transition.

5.6.2 Periodic r_1 Boundary Conditions

We finally turn to the model whose phase structure will include the GL transition, the maximally supersymmetric Yang-Mills theory on T^2 with periodic fermion boundary conditions along the "spatial" r_1 circle and antiperiodic fermion boundary conditions along the "thermal" r_2 circle. Because of the different boundary conditions, the $r_1 \leftrightarrow r_2$ symmetry of the phase diagram to which we have grown accustomed will no longer persist.

Small radius $r_1 \ll r_2$

As usual, we start with the limit $r_1 \ll r_2$ where a dimensionally reduced model describes the physics. Because of the periodic boundary conditions along the r_1 circle, though, there are fermi zero modes which survive in this limit and consequently the effective 1-dimensional theory is the supersymmetric model (5.27) considered in section 5.4. We saw there that a phase transition in this model was unlikely and, if such existed, would separate two phases with $\mathrm{tr}\,(U) \neq 0$. Consequently, the small radius transition line $r_1 \sim r_2^3$ that we have seen many times is absent here.

Small radius $r_2 \ll r_1$

In the limit $r_2 \ll r_1$, things are a bit different since there are no fermi zero modes about the r_2 circle. As a result, the effective 1-dimensional model that describes the physics is the bosonic one (5.11) considered in section 5.3 at $m = 0$. As discussed there, we expect a transition line along

$$r_2 = r_{2,c}(r_1) = \left(\tilde{t}_c^{(9)} r_1\right)^3 \tag{5.87}$$

where as we have mentioned before below (5.24), Monte Carlo studies yield the result $\tilde{t}_c^{(9)} \approx 0.89$. For $r_2 < r_{2,c}$ $\mathrm{tr}\,(U) \neq 0$ and $\mathrm{tr}\,(V) = 0$ while for $r_2 > r_{2,c}$ $\mathrm{tr}\,(U) \neq 0$ and

$\mathrm{tr}\,(V) \neq 0$.

Large radii $r_1, r_2 \gg 1$

At large radii, corresponding to strong coupling, we again turn to the SUGRA approximation provided by AdS/CFT where the relevant solution continues to be the Euclideanized near-horizon geometry of N $D1$-branes wrapping an S^1 (5.80). The situation is slightly different from that of section 5.6.1, though, since the periodic fermion boundary conditions around the r_1 circle prevent it from being identified with a circle at the boundary of (5.80) that degenerates in the bulk. This implies that the sum (5.83) has only one contribution in this case, namely that for which the r_1 circle is identified with θ and the r_2 circle with t_E. As discussed in section 5.6.1, the SUGRA approximation in this geometry is valid only for $1 \ll r_2 \ll r_1^2$. At the upper end of this regime, winding modes become light and trigger the GL instability. Consequently, we expect the GL phase transition to occur along

$$r_2 \sim r_1^2 \tag{5.88}$$

and to separate regimes in which $\mathrm{tr}\,(V)$ is zero and nonzero. The most natural conjecture for the remaining parts of the phase diagram is for the lines (5.87) and (5.88) to connect in the interior, producing the result depicted in figure 5.11.

Discussion

We have now seen the appearance of GL physics in the strong coupling regime of a gauge theory and have a natural conjecture for its continuation to weak coupling. Remarkably, the transition can be studied in a region that admits a lower dimensional description so that, in particular, the GL black string/black hole phase transition continues

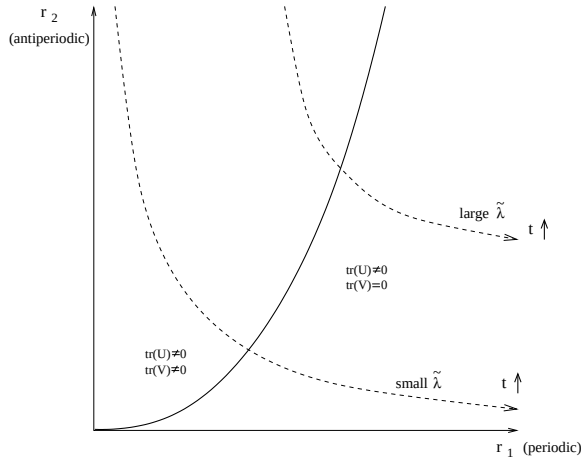

Figure 5.11: Phase diagram of maximally supersymmetric Yang-Mills theory on T^2 (5.77) with periodic (antiperiodic) fermion boundary conditions along r_1 (r_2). The phase transition line in the weak coupling region, $r_1, r_2 \ll 1$ can be studied numerically. In the strong coupling region, $r_1, r_2 \gg 1$, it is the GL transition discussed in chapter 4. The interior represents our conjectured completion of the phase diagram.

smoothly to the confinement/deconfinement transition of a 1+0-dimensional *bosonic* gauged matrix quantum mechanics model at finite temperature.

It is now clear why the extensive numeric effort in section 5.3.3 was expended and, in fact, why we found a determination of the order there important. It is natural to conjecture that the order of the transition doesn't change as one continues along the phase transition line in figure 5.11 so had the numerics there been able to yield a sharp answer then we would have had evidence from gauge theory in support of Kol's picture for black string/black hole phase transitions.

What we have seen instead is that two scenarios remain possible, though we find one more likely than the other. The most probable situation is that the phase transition is of first order at weak coupling. As mentioned in section 5.3.3, though, it remains possible that there are two second order transitions whose separation in $\tilde{t}$ is (unnaturally) small.

It is somewhat satisfying that the structures which emerge from the gauge theory

analysis correspond naturally to those anticipated in the previous chapter. In particular, the data is fit well by an effective potential (5.25) of precisely the form that we had hoped could capture the physics of GL transitions. Moreover, we have seen that the eigenvalue distributions corresponding to ρ_1 sitting at the origin and the boundary (roughly at 1/2) give snapshots of uniformly distributed and clumped $D0$-brane charge, respectively. It is natural to expect that the saddle points of ρ at the relative extremum in between, which is a maximum or minimum depending on the sign of b, corresponds to nonuniformly distributed $D0$-brane charge though we have not shown this explicitly. What we have in the end is a very concrete realization of the situations described in figures 4.1 and 4.2.

Of course, all of the intuition that one might gain from such analysis is limited by our inability to determine the parameters a and b in (5.25) analytically. Perhaps it is to be expected that a problem in gravity that is sufficiently complicated that analytical treatment is difficult will repel such treatment in the gauge theory regime as well. However, one might hope to obtain at least a qualitative understanding for the puzzle mentioned in section 5.3.3 related to the unnaturally small size of the parameter b. It seems as though something interesting, perhaps (weakly broken) symmetry, is at work here.

5.6.3 More general tori

Finally, we consider the supersymmetric theory on more general tori than the simple rectangular ones to which we have restricted our attention thus far. Among other things, this will allow us to continuously connect the two choices of boundary conditions that we have made above. To see how this works, consider taking both of the fundamental cycles of the torus to have antiperiodic boundary conditions for fermions. The torus with modular parameter $\tau = \tau_1 + i\tau_2$ such that $\tau_1 = 0$ is rectangular with the boundary conditions considered in section 5.6.1 and for which the conjectured phase diagram is that of figure

5.10. The torus with $\tau_1 = 1$, on the other hand, is equivalent to a rectangular torus with periodic boundary conditions for fermions along one of the cycles. This is precisely the situation considered in 5.6.2 for which the phase diagram is given in figure 5.11. Varying τ_1 from 0 to one should yield a continuous deformation connecting the two phase diagrams.

We can be surprisingly precise in describing this deformation. To elaborate on this, it is convenient to move from the parameters r_1 and r_2 to the modular parameter $\tau = ir_1/r_2$ and a dimensionless coupling $\tilde{\lambda} = \lambda A$ with A denoting the area of the torus[6]. With these variables, we can include the possibility of nonrectangular tori by simply permitting τ to take arbitrary complex values. Such a torus will have two fundamental cycles. Using the standard realization of the T^2 moduli space as $\mathbb{C}$ modulo a lattice generated by the vectors $z = 1$ and $z = \tau$, we denote the cycle associated to $z = 1$ by $(1, 0)$ and that associated $z = \tau$ by $(0, 1)$. By analogy with our notation in the rectangular case, we will then refer to the holonomies associated to these cycles by V and U, respectively.

The phase structure in the τ plane at fixed $\tilde{\lambda}$ is completely determined by modular invariance from that of the fundamental domain. Because of the fermion boundary conditions, though, the torus is not invariant under the usual modular group $SL(2, \mathbb{Z})$ but rather the subgroup Γ generated by $\tau \to -1/\tau$ and $\tau \to \tau + 2$. As a result, the relevant fundamental domain, which corresponds to regions I, II, and IV in figure 5.12, is a bit larger than than the usual one, which corresponds to region I only. We now proceed to study the phase structure of this fundamental domain at weak and strong coupling.

Weak coupling

As usual at weak coupling, or small volumes, we look for regimes in which the theory can be described by a dimensionally reduced model. To see when this is possible we

[6]For the rectangular torus, A is given by $A = r_1 r_2$. For more general tori, though, it will be given by $A = r_2^2 \tau_2$

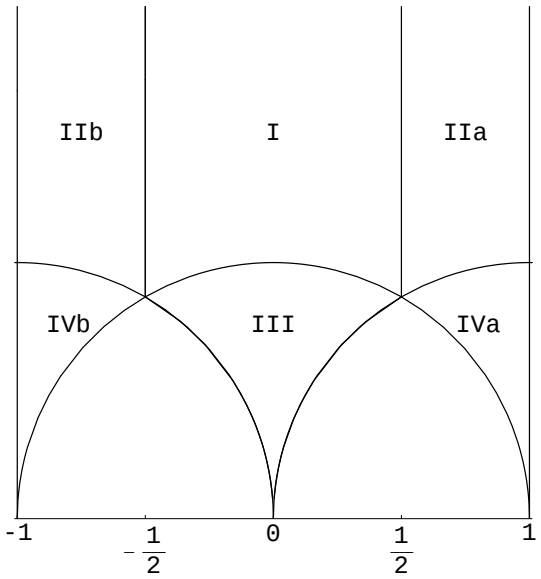

Figure 5.12: Depiction of the τ plane. The fundamental domain associated to the torus with antiperiodic boundary conditions corresponds to regions I, II, and IV.

will need the KK mass spectrum, which takes the form

$$m_{np}^2 = \frac{4\pi^2}{\tau_2}\left[(n\tau_1 - p)^2 + n^2\tau_2^2\right] \tag{5.89}$$

in units of inverse torus area with n and p corresponding to momentum quantum numbers about the fundamental cycles $(1,0)$ and $(0,1)$, respectively. Due to the boundary conditions, n and p take integer values for bosonic fields and half-integer values for fermionic ones.

The analog of the limit $r_1 \gg r_2$ that we studied for rectangular tori is the limit $\tau_2 \gg 1$, which introduces a scale separation between modes with $n = 0$ and those with $n \neq 0$. In particular, those with $n \neq 0$ become massive and decouple from the theory in this limit, leaving behind the familiar 1-dimensional bosonic theory (5.11) with effective temperature $\tilde{t}$ given by

$$\tilde{t} = \left(\tilde{\lambda}\tau_2^2\right)^{-1/3} \tag{5.90}$$

This amounts to a reduction to modes propagating on the $(0,1)$ cycle of the torus as it is becoming parametrically larger than the $(1,0)$ cycle as we take τ_2 to infinity. The phase transition that we found in the model (5.11) implies the existence of a similar transition in the present system along the curve

$$\tilde{\lambda}\tau_2^2 = \left(\tilde{t}_c^{(9)}\right)^{-1/3} \sim \mathcal{O}(1) \tag{5.91}$$

For $\tilde{\lambda}\tau_2^2$ larger than this, we expect the holonomies to satisfy $\mathrm{tr}\,(U) = 0$ and $\mathrm{tr}\,(V) \neq 0$ while for the opposite regime both holonomies have clumped eigenvalues $\mathrm{tr}\,(U) \neq 0$,$\mathrm{tr}\,(V) \neq 0$.

One can check this last fact perturbatively and, in fact, extend it beyond the regime $\tau_2 \gg 1$ by noting that, in regions I and II, the KK modes become weakly coupled and can be integrated out when

$$\tilde{\lambda}\tau_2^2 \ll 1 \tag{5.92}$$

As we have seen before, this results in an attractive potential for the holonomy eigenvalues of the form (5.10) that ensures clumped distributions.

We turn now to region IV, for which the analysis is a bit different. Specializing to IVa for simplicity, we consider the limit

$$\tau_1 \to 1 \qquad \tau_2 \to 0 \qquad \frac{\tau_1 - 1}{\tau_2}\text{fixed} \tag{5.93}$$

which is analagous to $r_1 \ll r_2$ and introduces a scale separation between modes with $n = p$ and those with $n \neq p$. The latter become massive and decouple, leaving us

with a one-dimensional supersymmetric theory that is nothing other than our old friend (5.27). We have argued previously that this model exhibits no nontrivial phase structure, though, as eigenvalues are clumped throughout. It is easy to check that this conclusion remains valid in the perturbative regime when the KK modes are weakly coupled and can be reliably integrated out at 1-loop

$$\frac{\tilde{\lambda}\tau_2^2}{\left[(1-\tau_1)^2+\tau_2^2\right]^2} \ll 1 \tag{5.94}$$

What we have seen then is that there is a single phase transition line in the fundamental region of figure 5.12 along

$$\tilde{\lambda}\tau_2^2 \sim \mathcal{O}(1) \tag{5.95}$$

above which $\mathrm{tr}\,(U) = 0$ and below which $\mathrm{tr}\,(U) \neq 0$. The holonomy $\mathrm{tr}\,(V)$, on the other hand, is nonzero throughout.

It is now straightforward to obtain the full phase diagram at weak coupling on the τ-plane using modular invariance. In particular, there will be infinitely many phase transition lines corresponding to the infinitely many images of the line (5.95). We exhibit some of these in figure 5.13.

From these results, we can see how figures 5.10 and 5.11 are related through variation of τ_1 in the weak coupling regime. To get a feel for the intricate structure involved, let us consider fixed r_2 so that the transition lines there reduce to points. These points correspond, in figure 5.13, to intersections of the transition lines with the slices $\tau_1 = 0$ for figure 5.10 and $\tau_1 = 1$ for figure 5.11. As expected, the former contains two points while the latter contains only one. We see now that as τ_1 is increased from 0 to 1, the number of transition lines changes many times with new phases appearing and annihilating one

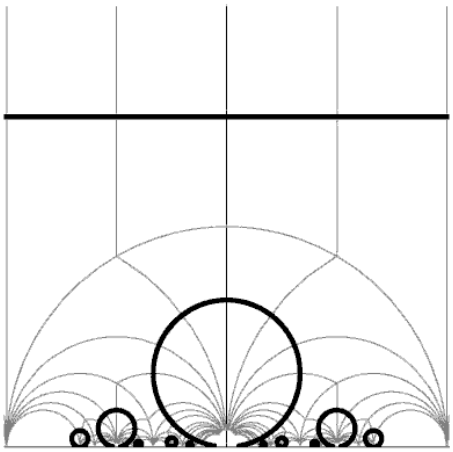

Figure 5.13: Phase transition line at $\tilde{\lambda}\tau_2^2 \sim \mathcal{O}(1)$ at weak coupling and some of its images under modular transformations.

another. In particular, the transition present in figure 5.10 that is absent in figure 5.11 annihilates against a transition that emerges from $\tau_2 = 0$ at infinitesimal τ_1. To be sure, the structure is quite a bit more intricate than one might have naively thought.

Strong coupling

In the strong coupling limit, we proceed as in our study of the supersymmetric theory on rectangular tori and use the SUGRA approximation (5.83). The relevant geometry continues to be of the form (5.80) but we must be particularly careful when matching the torus at infinity with that of the Yang-Mills theory (5.77). In particular, we must naively include not only SUGRA solutions with a torus of modular parameter τ equivalent to that of the gauge theory, but also all solutions with tori related to this one by an $SL(2,\mathbb{Z})$ transformation since these differ from the Yang-Mills torus only by what cycles we think of as being the fundamental ones.

To enumerate all of the terms that contribute, it suffices to consider all possible cycles of the Yang-Mills torus that can be identified with the Euclidean time circle of the

SUGRA solution. The only constraint is that the corresponding cycle must have antiperiodic fermion boundary conditions to be consistent with the fact that the thermal circle contracts in the bulk. The boundary conditions of a cycle (p, q) of the Yang-Mills torus are completely determined by our choice of antiperiodic fermion boundary conditions for the $(1, 0)$ and $(0, 1)$ cycles, though, so this condition amounts to the requirement that $p + q$ is odd. Combining this with the further requirement that p and q are coprime, which avoids overcounting of identical cycles, we have thus enumerated all geometries of the form (5.80) that contribute to the sum (5.83).

From this discussion, we see that the partition function of the Yang-Mills theory at strong coupling gets contributions from infinitely many terms [7], each of which we expect to contribute with action proportional to N^2. Consequently, we expect the sum to be dominated by a single term with the possibility of phase transitions as parameters are varied. We can determine which term dominates for a given choice of parameters by comparing the Euclidean actions of the various geometries that contribute. In particular, consider two terms in the sum corresponding SUGRA solutions with modular parameters τ and τ' when thinking of the Euclidean time circle as the $(1, 0)$ cycle[8]. The difference between the Euclidean actions of these solutions is straightforward to evaluate, up to the divergence issues discussed in sections 5.6.1 and 5.6.2 [84]

$$S(\tau) - S(\tau') \sim \left(\tau_2'^{3/2} - \tau_2^{3/2}\right) \tag{5.96}$$

From this, we see that the geometry with the largest value of τ_2 dominates the sum. To get a feel for what this means, note that the geometry with $\tau_{SUGRA} = \tau_{YM}$, corresponding to the $(1, 0)$ cycle of the Yang-Mills torus contracting in the bulk, dominates

[7] Note that, as mentioned there, we omitted a number of terms in the analagous discussions of sections 5.6.1 and 5.6.2. The analysis that follows justifies this assumption.

[8] The parameters τ and τ' here are of course necessarily related to the modular parameter of the Yang-Mills torus by an $SL(2, \mathbb{Z})$ transformation.

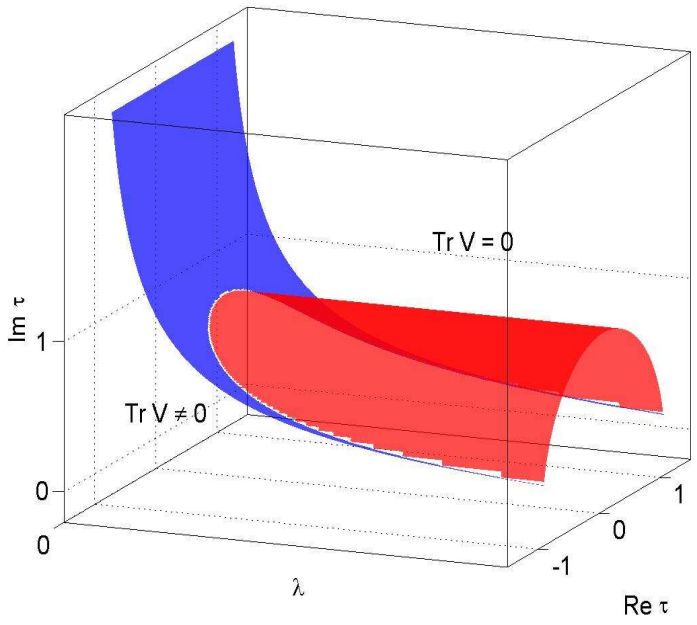

Figure 5.14: Conjectured phase boundary separating regions with $\mathrm{tr}\,(V)$ vanishing and nonvanishing within the fundamental domain.

throughout region I of figure 5.12. Since $\tau_1^2 + \tau_2^2 > 1$ there, the contracting cycle is the shorter of the two fundamental cycles. This generalizes the result for rectangular tori that the smaller of the two cycles shrinks in the bulk.

We can now use modular invariance to extend this result to the full τ plane. In particular, we see that the dominant geometry in any image of the fundamental domain is that for which the image of the $(1, 0)$ cycle contracts in the interior. As a result, the boundaries of fundamental domains correspond precisely with the phase transition lines! This generalizes the transition line $r_1 = r_2$ that we found at strong coupling in section 5.6.1 for the theory (5.77) on a rectangular torus with antiperiodic fermion boundary conditions along both cycles.

Of course, as discussed in section 5.6.2, we must be careful about where on the τ

plane the SUGRA approximation is valid. Indeed, we know that it must break down for a part of the $\tau_1 = 1$ line where, as we saw, the physics is captured by the T-dual $D0$-brane solution that exhibits a GL instability. Finding an explicit expression for the extension of this phase transition line away from $\tau_1 = 1$ is a difficult problem but its qualitative form is reasonably clear. We attempt to depict this situation in figure 5.14, which illustrates the phase transition surface associated to the matrix V in the fundamental domain. That part of the surface along the boundary of the fundamental domain corresponds to the transition at which $\mathrm{tr}\,(V)$ becomes nonzero and $\mathrm{tr}\,(U)$ vanishes. That part of the surface within the fundamental domain itself corresponds to an extension of the GL transition line along which only $\mathrm{tr}\,(V)$ becomes nonzero while $\mathrm{tr}\,(U)$ remains unchanged.

5.7 Summary

In this chapter, we have seen that Yang-Mills theories on tori admit a very rich phase structure of which the region relevant for GL physics is but a small part. Unfortunately, a constant theme throughout most of our analysis has been the inability to analytically probe the most interesting regions of the phase diagram directly. However, the numerics of section 5.3.3 combined with our enlargement of the parameter space via scalar masses to include more analytically tractable regions has led to the development of an intricate picture that is fully self-consistent. In the end, we have identified a series of transitions that can be interpreted for at least some values of parameters deconfinement in a dimensionally reduced theory. The GL transition itself, for instance, corresponds to the confinement/deconfinement transition of bosonic 0+1-dimensional gauged matrix quantum mechanics.

Appendix A

Counting states in $U(N)$ gauge theories

In this appendix we derive the precise formula (3.9) for the counting of gauge-invariant states in a large N theory with adjoint fields, and we discuss the single-particle partition functions for theories on a sphere with various field contents.

A.1 Counting gauge-invariant states precisely

In order to count the number of independent operators corresponding to traces of products of fields in the large N limit, we wish to count the number of different arrangements of objects subject to an identification of arrangements related by a cyclic permutation. This can be done using Polya's theorem [34, 92]

Consider a set of m types of objects, and associate a weight x_i with each of these objects. The weight associated with a collection of these objects is simply the product of the weights associated with each of the individual objects. Polya solved the general problem of summing over weights for all sets of k of these objects, two sets being treated as identical

if they are related to each other under the action of a specified subgroup of the permutation group. The subgroup relevant to us is simply the cyclic subgroup of order k; we will state Polya's result for this case. Define the polynomial

$$p_k(y_1, y_2, \ldots, y_k) = \frac{1}{k} \sum_{\pi} y_1^{n(\pi)_1} y_2^{n(\pi)_2} \ldots y_k^{n(\pi)_k} \tag{A.1}$$

where the summation in (A.1) runs over all elements π of the cyclic subgroup, and $n(\pi)_i$ is the number of cycles of length i in the permutation π. The answer to the question addressed earlier in this paragraph is simply

$$p_k(\sum_{i=1}^{m} x_i, \sum_{i=1}^{m} x_i^2, \ldots, \sum_{i=1}^{m} x_i^k) \tag{A.2}$$

Applying this result to our problem, we find that the large N partition function of single-trace states with k oscillators is precisely given by

$$Z_k = p_k(z(x), z(x^2), z(x^3), \cdots, z(x^k)) \tag{A.3}$$

where, as in section 3.2, $z(x)$ is the single-particle partition function. This implies that

$$\begin{aligned} Z_{ST} &= \sum_{k=1}^{\infty} p_k(z(x), z(x^2), z(x^3), \cdots, z(x^k)) \\ &= \sum_{k=1}^{\infty} \frac{1}{k} \sum_{l=1}^{k} z(x)^{n(k,l)_1} z(x^2)^{n(k,l)_2} \cdots z(x^k)^{n(k,l)_k} \end{aligned} \tag{A.4}$$

where $n(k,l)_q$ refers to the number of cycles of length q in the cyclic permutation by l shifts of k objects.

It is easy to convince oneself that for specific values of k and l, $n(k,l)_q$ is non-zero for only one value of q. At that value of q it is given by $G(l,k)$, the greatest common divisor

of l and k. It then follows that the q for which $n(k,l)_q$ is non-zero is given by $q = k/G(l,k)$. Consequently, (A.3) may be rewritten as

$$Z_{ST} = \sum_{k=1}^{\infty} \frac{1}{k} \sum_{l=1}^{k} z(x^{k/G(l,k)})^{G(l,k)} \tag{A.5}$$

We now group together all terms with the same (fixed) $q = k/G(l,k)$, so that $k = G(l,k)q$. Denoting $j = G(l,k)$, we change the sum over l and k to a sum over j and q, where each term appears once for every $l \leq jq$ such that $G(l,jq) = j$. The number of such l's is precisely $\varphi(q)$, the number of positive integers which are not larger than q and are relatively prime to q. Thus, we obtain

$$Z_{ST} = \sum_{j=1}^{\infty} \sum_{q=1}^{\infty} \frac{\varphi(q)}{jq} z(x^q)^j = -\sum_{q=1}^{\infty} \frac{\varphi(q)}{q} \ln(1 - z(x^q)) \tag{A.6}$$

as in (3.9).

A.2 Evaluating single-particle partition functions on spheres

Next, we turn to a different topic which is the evaluation of the single-particle partition functions for d-dimensional field theories compactified on $S^{d-1} \times \mathbb{R}$, with unit radius for S^{d-1}. This may be carried out directly by noting that the Laplacian on the sphere (or the spatial parts of the other wave operators corresponding to particles with spin) may be written directly in terms of angular momentum generators, which may be diagonalized in the usual way.

Alternatively, since free field theories are conformally invariant, and we are interested in conformally coupled fields (though it is easy to generalize our results also to other cases), we can use the conformal transformation that relates $S^{d-1} \times \mathbb{R}$ to $\mathbb{R}^d$. This transformation takes states of the field theory on $S^{d-1} \times \mathbb{R}$ to local operators on $\mathbb{R}^d$, with

the energy of the state becoming the scaling dimension of the operator. Thus, an equivalent way to define the partition function in such a case is by $z(x) = \sum_{\text{local operators}} x^{\Delta}$, where Δ is the scaling dimension of the operator.

We begin by considering a free scalar field ϕ. The local operators in the theory are ϕ, $\partial_i\phi$, $\partial_i\partial_j\phi$, and so on, modulo the equation of motion. Ignoring the equation of motion for a moment, these operators are all generated by repeated application of the d different derivative operators $\partial_1, \partial_2 \ldots \partial_d$, each of which is of unit dimension and so has the partition function $\frac{1}{1-x}$, on the free field ϕ of dimension $(d/2-1)$. Multiplying the various partition functions we find

$$z'_S(x) = \frac{x^{\frac{d}{2}-1}}{(1-x)^d} \tag{A.7}$$

In order to obtain $z_S(x)$ we must subtract from this the partition function for operators that vanish by the equation of motion $\partial^2\phi = 0$. Such operators are generated by acting with an arbitrary number of derivatives on $\partial^2\phi$, so their partition function is $x^2 z'_S(x)$. Thus, we find

$$z_S(x) = (1-x^2)z'_S(x) = \frac{x^{\frac{d}{2}} + x^{\frac{d}{2}-1}}{(1-x)^{d-1}} \tag{A.8}$$

As a check, we note that in $d = 4$ the operators that we get by acting with k derivatives are in the k^{th} traceless symmetric representation of $SO(4)$ which has $j_1 = j_2 = \frac{k}{2}$, and they have dimension $\Delta = k+1$. These are simply the scalar spherical harmonics on S^3. This implies that the number of operators of dimension Δ is $n_S(\Delta) = (2j_1+1)(2j_2+1) = \Delta^2$, consistent with the Taylor expansion of (A.8) for $d = 4$.

Next, we turn to the free vector field. The number of gauge-invariant operators is independent of the gauge, so we can fix an arbitrary gauge for the counting. We will use the gauge $A_0 = 0$ on $S^{d-1} \times \mathbb{R}$, which becomes the gauge $x^\mu A_\mu = 0$ after the conformal

transformation to $\mathbb{R}^d$ (recall that, according to the state-operator map, all operators are to be evaluated at $x = 0$). Differentiating the gauge condition at the point $x = 0$ we find the relations

$$A_\mu = 0 \qquad \partial_\mu A_\nu + \partial_\nu A_\mu = 0 \qquad \dots \qquad \partial_{\{i_1}\partial_{i_2}\dots\partial_{i_n}A_{i_{n+1}\}} = 0 \qquad \dots \tag{A.9}$$

where the brackets $\{\}$ denote symmetrization. To start with we ignore both (A.9) and the equation of motion – this leads to a single-particle partition function $z'_V(x) = x^{2-\frac{d}{2}}dz'_S(x)$ (since the gauge field must have scaling dimension one in any space-time dimension). Operators of dimension Δ that are set to zero by (A.9) are given by symmetric tensors of rank Δ; based on the previous paragraph the corresponding partition function is $x^{1-\frac{d}{2}}z'_S(x) - 1$, where the last subtraction comes because there are no tensors of rank zero in (A.9). With the condition (A.9), the Maxwell equation (at $x = 0$) simply reduces to $\partial^2 A_\mu = 0$. The number of independent operators set to zero by the equation of motion is, therefore, counted by $dx^{4-\frac{d}{2}}z'_S(x)$. Finally, the number of operators set to zero by both the constraint (A.9) and the equation of motion is encoded in the partition function $x^{5-\frac{d}{2}}z'_S(x)$. Putting it all together, using (A.7), we find

$$\begin{aligned} z_V(x) &= \frac{dx}{(1-x)^d} - \frac{1}{(1-x)^d} - \frac{dx^3}{(1-x)^d} + \frac{x^4}{(1-x)^d} + 1 \\ &= 1 - \frac{(1+x)(1+x^2-dx)}{(1-x)^{d-1}} \end{aligned} \tag{A.10}$$

As a check, we note that in four dimensions, the set of operators formed by acting with k derivatives on A_μ, obeying (A.9) and the equation of motion, transform in the $SO(4)$ representation $(j_1, j_2) = (\frac{k+1}{2}, \frac{k-1}{2}) \oplus (\frac{k-1}{2}, \frac{k+1}{2})$. These are the vector spherical harmonics on S^3. It follows that the number of operators at dimension Δ is $n_V(\Delta) = 2(\Delta^2 - 1)$, consistent with (A.10).

Finally, we turn to free fermions. For concreteness we work in even dimensions with complex spinors of no chirality restrictions. Such a spinor has $2^{\frac{d}{2}+1}$ real components. Ignoring the equation of motion, the partition function for spinors is $z'_F(x) = 2^{\frac{d}{2}+1}\sqrt{x}z'_S(x)$. The partition function that counts the operators which are set to zero by the Dirac equation, is $2^{\frac{d}{2}+1}x^{\frac{3}{2}}z'_S(x)$. Subtracting the second from the first we find

$$z_F(x) = \frac{2^{\frac{d}{2}+1}x^{\frac{d}{2}-\frac{1}{2}}}{(1-x)^{d-1}} \tag{A.11}$$

Of course, (A.11) should be divided by two for chiral spinors or real spinors, and by four for spinors that are both chiral and real. As a check on (A.11), note that, in $d = 4$, the operators made from a complex chiral fermion field, at dimension $k + \frac{1}{2}$, transform in the $SO(4)$ representation with $(j_1, j_2) = (\frac{k}{2}, \frac{k-1}{2})$; there are $2k(k+1)$ such operators (the factor of 2 is because the spinors are complex), in agreement with (A.11).

Note that each of (A.8), (A.10), and (A.11) tends as $x \to 1$ (the high temperature limit) to

$$z(x) \to \frac{2\mathcal{N}^{\rm dof}}{(1-x)^{d-1}} \tag{A.12}$$

where $\mathcal{N}^{\rm dof}$ is the number of physical real degrees of freedom in the corresponding field.

The formulas in this section, used for $d = 4$, imply the formula (3.4) of section (3.2).

Appendix B

Detailed Study of some Unitary Matrix Models

In this appendix, we study some of the unitary matrix models that arise in the study of Yang-Mills theories on S^3.

B.1 The Free Yang-Mills Matrix Model

We begin with the matrix model (3.25) describing the thermal partition function of a free Yang-Mills theory with matter content encoded in the letter partition function $z(x)$ (3.3), which we take to contain only bosonic fields for simplicity. We begin with the expression (3.54) for the partition function as an integral over eigenvalues

$$Z = \int \prod_k d\alpha_k \prod_{i<j} \sin^2\left(\frac{\alpha_i - \alpha_j}{2}\right) \exp\left\{\sum_n \sum_{i,j} \frac{1}{n} z(x^n) e^{in(\alpha_i - \alpha_j)}\right\} \tag{B.1}$$

We seek to study this system near the critical point x_H. Because the first moment ρ_1 becomes tachyonic there while the others remain massive, it is reasonable to expect that

the physics in this regime is well described by a truncated model in which we drop all terms in the sum over n with $n > 1$. We will later justify this approximation by demonstrating that for x sufficiently close to x_H, the expectation values of these terms are all negligible.

With this assumption, we are led to consider the reduced model

$$Z = \int \prod_i d\alpha_i \exp\left\{ \sum_{i \neq j} \ln \left| \sin\left(\frac{\alpha_i - \alpha_j}{2} \right) \right| + z(x) \sum_{i,j} e^{i(\alpha_i - \alpha_j)} \right\} \tag{B.2}$$

The saddle point equations of this model are easily determined to be

$$\sum_j \cot\left(\frac{\alpha_i - \alpha_j}{2} \right) = 2N \tilde{\rho}_1 z \sin \alpha_i \tag{B.3}$$

where we have defined $\tilde{\rho}_1$ as

$$\tilde{\rho}_1 = \frac{1}{N} \sum_j e^{i\alpha_j} \tag{B.4}$$

and implicitly assumed that it is real. In actuality, this isn't much of an assumption since if $\tilde{\rho}_1$ is not real to begin with, we can make it real with a $U(1)$ transformation of the form described in section 3.3.1. Introducing an eigenvalue density $\rho(\alpha)$ as usual, we can write the saddle point condition as a series of two equations

$$\begin{aligned} 2\tilde{\rho}_1 z \sin \alpha_i &= \int dx\, \rho(x) \cot\left(\frac{\alpha_i - x}{2} \right) \\ \tilde{\rho}_1 &= \int dx\, \rho(x) \cos x \end{aligned} \tag{B.5}$$

Expressing the problem in this manner greatly simplifies our life because the first of the equations (B.5) is the saddle point condition for a unitary matrix model of the Wilson type

$$\int dU \, \exp\left\{ \frac{N}{\lambda} \mathrm{tr} \left(U + U^\dagger \right) \right\} \tag{B.6}$$

which has been solved before by Gross and Witten [93] and Wadia [94, 95]. The solution for $\rho(x)$ takes the form

$$\rho(x) = \tfrac{1}{2\pi}\left(1 + \tfrac{2}{\lambda}\cos x\right) \qquad \lambda \geq 2 \tag{B.7}$$

$$= \tfrac{2}{\pi\lambda}\cos\left(\tfrac{x}{2}\right)\sqrt{\tfrac{\lambda}{2} - \sin^2\tfrac{x}{2}} \qquad \lambda \leq 2 \tag{B.8}$$

where

$$\lambda = \frac{1}{\tilde{\rho}_1 z} \tag{B.9}$$

We can now determine when the solutions (B.8) and (B.7) are saddle points for our reduced model (B.2) by studying when they also solve the second equation in (B.5).

Before doing this, though, let us comment for a moment about the form of the solutions (B.8) and (B.7). The first (B.7), valid for $\lambda \geq 2$, is a nonuniform distribution corresponding to turning on the moment ρ_1 only. It vanishes only at isolated points on the circle. On the other hand, the second solution (B.8), valid for $\lambda \leq 2$, corresponds to turning on infinitely many of the moments ρ_n. The distribution is clumped in the sense that it vanishes over a finite range on the circle. As λ approaches 2, the clump widens until eventually the gap over which the density vanishes closes to zero size.

It is easy to verify that, for $\lambda \leq 2$ the GWW solution (B.8) is a saddle point of our reduced model (B.2) provided

$$\lambda = 2\left(1 - \sqrt{1 - \frac{1}{z(x)}}\right) \tag{B.10}$$

We thus see that for $z(x) \geq 1$, the clumped distribution is a saddle point for our model. Evaluating the partition function on this saddle yields

$$\ln Z = N^2 \left(\frac{1}{\lambda} + \frac{1}{2} \ln \left(\frac{\lambda}{2} \right) - \frac{1}{2} \right) \tag{B.11}$$

We see from this that the free energy vanishes at $z(x) = 1$ while becoming negative and scaling as $\mathcal{O}(N^2)$ for $z(x) > 1$.

On the other hand, for $\lambda \geq 2$ the second condition (B.5) leads to the requirement

$$z(x) = 1 \tag{B.12}$$

Consequently, we have no consistent GWW saddle points for $z(x) < 1$. This isn't surprising, though, as we expect the system there to be dominated a saddle point configuration that we have neglected to include in our analysis above: the uniform distribution. The free energy in this regime scales as $\mathcal{O}(N^0)$ at large N as usual.

What we have seen here is that our reduced model exhibits precisely the behavior we expected of the full system. For temperatures sufficiently small that $z(x) < 1$, the uniform distribution dominates and the model is confined. For temperatures sufficiently large that $z(x) > 1$, the free energy is proportional to N^2 as the model is deconfined. In this simplified model, though, we have an explicit expression for the eigenvalue distribution in the high temperature phase. It is simply the GWW clumped distribution.

While we don't expect this distribution to describe the high temperature phase of the full model, it gives a reasonable approximation to the true distribution near the critical point since, by taking $z(x)$ arbitrarily close to 1 we can make the expectation values of the higher moments ρ_n as small as we like. Indeed, the nonuniform solution at $z(x)$ precisely equal to 1 is an exact saddle point of both the reduced and the full models.

It is actually possible to do better than this. As discussed in [6], the saddle point conditions for the full matrix integral (3.25) can be related to those of a model that generalizes (B.6)

$$\int dU \, \exp\left\{-N \sum_{n=1}^{\infty} \frac{a_n \rho_n}{n} \mathrm{tr} \left(U^n + U^{\dagger\, n}\right)\right\} \tag{B.13}$$

which has also been solved exactly [96]. The consistency equations that relate the couplings a_n to properties of $z(x)$ are quite complicated in this case, but it is possible to find a systematic expansion for the dominant eigenvalue distribution above the critical temperature T_H in powers of $T - T_H$. For details, the interested reader is referred to [6]

B.2 The Effective Model at Weak Coupling

The second model that we study in this appendix is the Landau-Ginzburg model (3.62) that we wrote in section 3.5 to describe the physics near the critical point for small nonzero coupling. Expressed as a unitary matrix integral, it takes the form

$$Z = \int dU \, \exp\left\{-\left(|\mathrm{tr}\,(U)|^2 \left(m_1^2 - 1\right) + \frac{b}{N^2} |\mathrm{tr}\,(U)|^4\right)\right\} \tag{B.14}$$

We now seek to study the phase structure of (B.14) as a function of m_1 and b. Of course, in the Yang-Mills theory these will themselves be potentially complicated functions of x and λ.

To study this model, we can proceed exactly as in the analysis of the truncated model. In particular, we rewrite Z as an integral over eigenvalues, obtain saddle point equations, and write them in terms of the quantity $\tilde{\rho}_1$ defined as in (B.4). The key point here is that the action is a polynomial in $\mathrm{tr}\,(U)$ and $\mathrm{tr}\,(U^{-1})$ only, the resulting saddle point equation is identical to the first equation of (B.5) with λ this time being given in terms of the parameters of the model as

$$\lambda^{-1} = \tilde{\rho}_1 \left(1 - m_1^2 - 2b\tilde{\rho}_1^2\right) \tag{B.15}$$

Note that at $b = 0$, this reduces to (B.9) as it should.

We thus see that the candidate eigenvalue densities are again the uniform distribution and GWW solutions (B.8) (B.7) with λ determined from m_1 and b by (B.15). As before, these distributions are actual saddles of the model in question (B.14) provided they satisfy the self-consistency condition

$$\tilde{\rho}_1 = \int d\theta \, \rho(\theta) \cos\theta \tag{B.16}$$

We now study each of the three possible phases in turn. The first possibility is the uniform distribution, on which the free energy vanishes at order N^2. We expect this distribution to describe a local minimum when the mass m_1^2 of the mode ρ_1 is positive.

We next turn the solution (B.7), which we refer to as the nonuniform distribution. The conditions (B.15) and (B.16) combine to imply that this is a true saddle point only when

$$\tilde{\rho}_1^2 = -\frac{m_1^2}{2b} \tag{B.17}$$

and

$$\lambda^{-2} = \left| \frac{m_1^2}{2b} \right| \tag{B.18}$$

Using these equations and the fact that $\lambda \geq 2$ for the nonuniform distribution, we see that it is a viable saddle point precisely when

$$b > 0 \qquad \text{and} \qquad -\frac{b}{2} \leq m_1^2 \leq 0 \tag{B.19}$$

or

$$b < 0 \qquad \text{and} \qquad 0 \leq m_1^2 \leq -\frac{b}{2} \tag{B.20}$$

The free energy evaluated on the nonuniform distribution is given by

$$F(T) = -\frac{N^2 T m_1^4}{4b} \tag{B.21}$$

so that it is positive for $b < 0$ and negative for $b > 0$. Comparing with the vanishing free energy of the uniform distribution , we see that the nonuniform phase is subdominant when it exists for $b < 0$ and dominant when it exists for $b > 0$. There is a phase transition when it takes over for the uniform phase at $m_1^2 = 0$ that, because m_1^2 is quadratic in $(T - T_H)$ near the critical point, is of second order.

We now move on to the solution (B.8), which we refer to as the clumped distribution. The analog of (B.18) in this case is

$$\tilde{\rho}_1 = 1 - \left[4\left(\tilde{\rho}_1(1 - m_1^2) - 2\tilde{\rho}_1^3 b\right)\right]^{-1} \tag{B.22}$$

Once $\tilde{\rho}_1$ is known, the free energy evaluated on this saddle is then determined to be

$$F(T) = N^2 T \left[\left(m_1^2 - 1\right)\tilde{\rho}_1^2 + b\tilde{\rho}_1^4 + \frac{1}{4} - \frac{1}{2}\ln\left(2(1 - \tilde{\rho}_1)\right)\right] \tag{B.23}$$

Using (B.22), it is straightforward to check that the clumped distribution is a viable saddle point whenever

$$m_1^2 < -\frac{b}{2} \tag{B.24}$$

Moreover, when $m_1^2 = -\frac{b}{2}$, the value of $\tilde{\rho}_1$ is $\frac{1}{2}$. This is interesting because it is the same value for $\tilde{\rho}_1$ that we find from (B.18) in the nonuniform phase. In fact, the

two distributions completely agree at this point. For $b < 0$, neither phase exists for $m_1^2 > |\frac{b}{2}|$ and both are subdominant to the uniform phase near their appearance at $m_1^2 = |\frac{b}{2}|$. We thus interpret $m_1^2 = |\frac{b}{2}|$ as the nucleation point of two subdominant saddles. Using the expressions (B.21) and (B.23), it is possible to demonstrate that the free energy of the clumped distribution decreases while that of the nonuniform distribution increases. Eventually, the former becomes negative and a first order phase transition is triggered.

For $b > 0$, the nonuniform phase exists and dominates for $m_1^2 > -\frac{b}{2}$ while the clumped phase exists and dominates for $m_1^2 < -\frac{b}{2}$. What is apparently happening here then is a transition between two dominant phases. To determine the order, one need only study the free energies (B.21) and (B.23) in the vicinity of this point. Expanding in powers of $y = -m_1^2 - \frac{b}{2}$, we find that the free energy of the clumped distribution takes the form [6]

$$F(T) = N^2 T \left[-\frac{m_1^4}{4b} + \frac{1}{6b^3} y^3 + \mathcal{O}(y^4) \right] \tag{B.25}$$

Comparing with (B.21) and using the fact that y is linear in temperature, we conclude that the transition that occurs at $m_1^2 = -\frac{b}{2}$ is of third order.

The picture that has emerged is precisely that of section 3.5 from the heuristic analysis of the effective potentials plotted in figures 3.2 and 3.4. For $b > 0$, we have seen that the new minimum emerging from the origin corresponds to the nonuniform GWW distribution (B.7). Moreover, we have demonstrated explicitly that this happens via a second order phase transition. We have also seen that when this minimum reaches the boundary, it undergoes a third order transition to a phase corresponding to the clumped GWW distribution (B.8).

For $b < 0$, we have seen explicitly that at a positive value of the ρ_1 mass m_1^2, a stable and unstable phase are nucleated corresponding to the new minimum and maximum that arise in the effective potential. The unstable phase at the maximum corresponds to the

nonuniform GWW distribution (B.7) while the stable one at the minimum corresponds to the clumped GWW distribution of (B.8). Eventually, the clumped distribution dominates the uniform one and a first order phase transition occurs.

Bibliography

[1] Juan M. Maldacena. The large n limit of superconformal field theories and supergravity. *Adv. Theor. Math. Phys.*, 2:231–252, 1998.

[2] Edward Witten. Anti-de sitter space and holography. *Adv. Theor. Math. Phys.*, 2:253–291, 1998.

[3] S. S. Gubser, Igor R. Klebanov, and Alexander M. Polyakov. Gauge theory correlators from non-critical string theory. *Phys. Lett.*, B428:105–114, 1998.

[4] S. W. Hawking and Don N. Page. Thermodynamics of black hole in anti-de sitter space. *Commun. Math. Phys.*, 87:577, 1983.

[5] Edward Witten. Anti-de sitter space, thermal phase transition, and confinement in gauge theories. *Adv. Theor. Math. Phys.*, 2:505–532, 1998.

[6] Ofer Aharony, Joseph Marsano, Shiraz Minwalla, Kyriakos Papadodimas, and Mark Van Raamsdonk. The hagedorn / deconfinement phase transition in weakly coupled large n gauge theories. *Adv. Theor. Math. Phys.*, 8:603–696, 2004.

[7] Ofer Aharony, Joseph Marsano, Shiraz Minwalla, Kyriakos Papadodimas, and Mark Van Raamsdonk. A first order deconfinement transition in large n yang- mills theory on a small s**3. *Phys. Rev.*, D71:125018, 2005.

[8] Ofer Aharony, Steven S. Gubser, Juan M. Maldacena, Hirosi Ooguri, and Yaron Oz. Large n field theories, string theory and gravity. *Phys. Rept.*, 323:183–386, 2000.

[9] Joseph Polchinski. Dirichlet-branes and ramond-ramond charges. *Phys. Rev. Lett.*, 75:4724–4727, 1995.

[10] Gary T. Horowitz and Andrew Strominger. Black strings and p-branes. *Nucl. Phys.*, B360:197–209, 1991.

[11] Gerard 't Hooft. A planar diagram theory for strong interactions. *Nucl. Phys.*, B72:461, 1974.

[12] J. L. F. Barbon and E. Rabinovici. Extensivity versus holography in anti-de sitter spaces. *Nucl. Phys.*, B545:371–384, 1999.

[13] J. L. F. Barbon, I. I. Kogan, and E. Rabinovici. On stringy thresholds in sym/ads thermodynamics. *Nucl. Phys.*, B544:104–144, 1999.

[14] S. A. Abel, J. L. F. Barbon, I. I. Kogan, and E. Rabinovici. String thermodynamics in d-brane backgrounds. *JHEP*, 04:015, 1999.

[15] S. A. Abel, J. L. F. Barbon, I. I. Kogan, and E. Rabinovici. Some thermodynamical aspects of string theory. 1999.

[16] David S. Berman and Maulik K. Parikh. Confinement and the ads/cft correspondence. *Phys. Lett.*, B483:271–276, 2000.

[17] J. L. F. Barbon and E. Rabinovici. Closed-string tachyons and the hagedorn transition in ads space. *JHEP*, 03:057, 2002.

[18] J. L. F. Barbon and E. Rabinovici. Remarks on black hole instabilities and closed string tachyons. *Found. Phys.*, 33:145–165, 2003.

[19] R. Hagedorn. Statistical thermodynamics of strong interactions at high- energies. *Nuovo Cim. Suppl.*, 3:147–186, 1965.

[20] Michael B. Green, J. H. Schwarz, and Edward Witten. Superstring theory. vol. 1: Introduction. Cambridge, Uk: Univ. Pr. (1987) 469 P. (Cambridge Monographs On Mathematical Physics).

[21] Joseph J. Atick and Edward Witten. The hagedorn transition and the number of degrees of freedom of string theory. *Nucl. Phys.*, B310:291–334, 1988.

[22] S. W. Hawking and W. Israel. General relativity. an einstein centenary survey. Cambridge, United Kingdom: Univ.Pr.(1979) 919p.

[23] (ed.) Gibbons, G. W. and (ed.) Hawking, S. W. Euclidean quantum gravity. Singapore, Singapore: World Scientific (1993) 586 p.

[24] Sean A. Hartnoll and S. Prem Kumar. Ads black holes and thermal yang-mills correlators. *JHEP*, 12:036, 2005.

[25] Juan M. Maldacena. Wilson loops in large n field theories. *Phys. Rev. Lett.*, 80:4859–4862, 1998.

[26] Ofer Aharony and Edward Witten. Anti-de sitter space and the center of the gauge group. *JHEP*, 11:018, 1998.

[27] Soo-Jong Rey and Jung-Tay Yee. Macroscopic strings as heavy quarks in large n gauge theory and anti-de sitter supergravity. *Eur. Phys. J.*, C22:379–394, 2001.

[28] Soo-Jong Rey, Stefan Theisen, and Jung-Tay Yee. Wilson-polyakov loop at finite temperature in large n gauge theory and anti-de sitter supergravity. *Nucl. Phys.*, B527:171–186, 1998.

[29] A. Brandhuber, N. Itzhaki, J. Sonnenschein, and S. Yankielowicz. Wilson loops in the large n limit at finite temperature. *Phys. Lett.*, B434:36–40, 1998.

[30] Andreas Brandhuber, Nissan Itzhaki, Jacob Sonnenschein, and Shimon Yankielowicz. Wilson loops, confinement, and phase transitions in large n gauge theories from supergravity. *JHEP*, 06:001, 1998.

[31] Alexander M. Polyakov. Thermal properties of gauge fields and quark liberation. *Phys. Lett.*, B72:477–480, 1978.

[32] Leonard Susskind. Lattice models of quark confinement at high temperature. *Phys. Rev.*, D20:2610–2618, 1979.

[33] David J. Gross, Robert D. Pisarski, and Laurence G. Yaffe. Qcd and instantons at finite temperature. *Rev. Mod. Phys.*, 53:43, 1981.

[34] Bo Sundborg. The hagedorn transition, deconfinement and n = 4 sym theory. *Nucl. Phys.*, B573:349–363, 2000.

[35] Joakim Hallin and David Persson. Thermal phase transition in weakly interacting, large n(c) QCD. *Phys. Lett.*, B429:232–238, 1998.

[36] M. B. Halpern. On the large n limit of conformal field theory. *Ann. Phys.*, 303:321–358, 2003.

[37] Yadin Y. Goldschmidt. $1/n$ expansion in two-dimensional lattice gauge theory. *J. Math. Phys.*, 21:1842, 1980.

[38] C. R. Gattringer, L. D. Paniak, and G. W. Semenoff. Deconfinement transition for quarks on a line. *Annals Phys.*, 256:74–113, 1997.

[39] Barak Kol. The phase transition between caged black holes and black strings: A review. *Phys. Rept.*, 422:119–165, 2006.

[40] Werner Israel. Event horizons in static vacuum space-times. *Phys. Rev.*, 164:1776–1779, 1967.

[41] Werner Israel. Event horizons in static electrovac space-times. *Commun. Math. Phys.*, 8:245–260, 1968.

[42] B. Carter. Axisymmetric black hole has only two degrees of freedom. *Phys. Rev. Lett.*, 26:331–333, 1971.

[43] D. C. Robinson. Classification of black holes with electromagnetic fields. *Phys. Rev. D*, 10:458–460, 1974.

[44] D. C. Robinson. Uniqueness of the kerr black hole. *Phys. Rev. Lett.*, 34:905–906, 1975.

[45] Roberto Emparan and Harvey S. Reall. A rotating black ring in five dimensions. *Phys. Rev. Lett.*, 88:101101, 2002.

[46] Steven S. Gubser. On non-uniform black branes. *Class. Quant. Grav.*, 19:4825–4844, 2002.

[47] Toby Wiseman. Static axisymmetric vacuum solutions and non-uniform black strings. *Class. Quant. Grav.*, 20:1137–1176, 2003.

[48] Toby Wiseman. From black strings to black holes. *Class. Quant. Grav.*, 20:1177–1186, 2003.

[49] Troels Harmark. Small black holes on cylinders. *Phys. Rev.*, D69:104015, 2004.

[50] Dan Gorbonos and Barak Kol. A dialogue of multipoles: Matched asymptotic expansion for caged black holes. *JHEP*, 06:053, 2004.

[51] D. Karasik, C. Sahabandu, P. Suranyi, and L. C. R. Wijewardhana. Analytic approximation to 5 dimensional black holes with one compact dimension. *Phys. Rev.*, D71:024024, 2005.

[52] Dan Gorbonos and Barak Kol. Matched asymptotic expansion for caged black holes: Regularization of the post-newtonian order. *Class. Quant. Grav.*, 22:3935–3960, 2005.

[53] Barak Kol, Evgeny Sorkin, and Tsvi Piran. Caged black holes: Black holes in compactified spacetimes. i: Theory. *Phys. Rev.*, D69:064031, 2004.

[54] Evgeny Sorkin, Barak Kol, and Tsvi Piran. Caged black holes: Black holes in compactified spacetimes. ii: 5d numerical implementation. *Phys. Rev.*, D69:064032, 2004.

[55] Hideaki Kudoh and Toby Wiseman. Properties of kaluza-klein black holes. *Prog. Theor. Phys.*, 111:475–507, 2004.

[56] Hideaki Kudoh and Toby Wiseman. Connecting black holes and black strings. *Phys. Rev. Lett.*, 94:161102, 2005.

[57] R. Gregory and R. Laflamme. Black strings and p-branes are unstable. *Phys. Rev. Lett.*, 70:2837–2840, 1993.

[58] Ruth Gregory and Raymond Laflamme. The instability of charged black strings and p-branes. *Nucl. Phys.*, B428:399–434, 1994.

[59] Harvey S. Reall. Classical and thermodynamic stability of black branes. *Phys. Rev.*, D64:044005, 2001.

[60] Steven S. Gubser and Indrajit Mitra. Instability of charged black holes in anti-de sitter space. 2000.

[61] Steven S. Gubser and Indrajit Mitra. The evolution of unstable black holes in anti-de sitter space. *JHEP*, 08:018, 2001.

[62] D. J. Gross, M. J. Perry, and L. G. Yaffe. Instability of flat space at finite temperature. *Phys. Rev.*, D25:330–355, 1982.

[63] Simon F. Ross and Toby Wiseman. Smeared d0 charge and the gubser-mitra conjecture. *Class. Quant. Grav.*, 22:2933–2946, 2005.

[64] Troels Harmark, Vasilis Niarchos, and Niels A. Obers. Instabilities of near-extremal smeared branes and the correlated stability conjecture. *JHEP*, 10:045, 2005.

[65] James P. Gregory and Simon F. Ross. Stability and the negative mode for schwarzschild in a finite cavity. *Phys. Rev.*, D64:124006, 2001.

[66] Veronika E. Hubeny and Mukund Rangamani. Unstable horizons. *JHEP*, 05:027, 2002.

[67] Sean A. Hartnoll. Casimir effect and thermodynamics of horizon instabilities. *Phys. Rev.*, D70:044015, 2004.

[68] Joshua J. Friess and Steven S. Gubser. Instabilities of d-brane bound states and their related theories. *JHEP*, 11:040, 2005.

[69] Joshua J. Friess, Steven S. Gubser, and Indrajit Mitra. Counter-examples to the correlated stability conjecture. *Phys. Rev.*, D72:104019, 2005.

[70] Gary T. Horowitz and Kengo Maeda. Fate of the black string instability. *Phys. Rev. Lett.*, 87:131301, 2001.

[71] Barak Kol. Topology change in general relativity and the black-hole black-string transition. *JHEP*, 10:049, 2005.

[72] Barak Kol and Evgeny Sorkin. On black-brane instability in an arbitrary dimension. *Class. Quant. Grav.*, 21:4793–4804, 2004.

[73] Barak Kol and Evgeny Sorkin. On black-brane instability in an arbitrary dimension. *Class. Quant. Grav.*, 21:4793–4804, 2004.

[74] Evgeny Sorkin. A critical dimension in the black-string phase transition. *Phys. Rev. Lett.*, 93:031601, 2004.

[75] Hideaki Kudoh and Umpei Miyamoto. On non-uniform smeared black branes. *Class. Quant. Grav.*, 22:3853–3874, 2005.

[76] Nissan Itzhaki, Juan M. Maldacena, Jacob Sonnenschein, and Shimon Yankielowicz. Supergravity and the large n limit of theories with sixteen supercharges. *Phys. Rev.*, D58:046004, 1998.

[77] Ofer Aharony, Joe Marsano, Shiraz Minwalla, and Toby Wiseman. Black hole - black string phase transitions in thermal 1+1 dimensional supersymmetric yang-mills theory on a circle. *Class. Quant. Grav.*, 21:5169–5192, 2004.

[78] Leonard Susskind. Matrix theory black holes and the gross witten transition. 1997.

[79] Miao Li, Emil J. Martinec, and Vatche Sahakian. Black holes and the sym phase diagram. *Phys. Rev.*, D59:044035, 1999.

[80] Emil J. Martinec and Vatche Sahakian. Black holes and the sym phase diagram. ii. *Phys. Rev.*, D59:124005, 1999.

[81] Troels Harmark and Niels A. Obers. New phases of near-extremal branes on a circle. *JHEP*, 09:022, 2004.

[82] T. H. Buscher. A symmetry of the string background field equations. *Phys. Lett.*, B194:59, 1987.

[83] T. H. Buscher. Path integral derivation of quantum duality in nonlinear sigma models. *Phys. Lett.*, B201:466, 1988.

[84] Ofer Aharony et al. The phase structure of low dimensional large n gauge theories on tori. *JHEP*, 01:140, 2006.

[85] Edward Witten. Constraints on supersymmetry breaking. *Nucl. Phys.*, B202:253, 1982.

[86] Alexander A. Migdal. Recursion equations in gauge field theories. *Sov. Phys. JETP*, 42:413, 1975.

[87] David J. Gross. Two-dimensional qcd as a string theory. *Nucl. Phys.*, B400:161–180, 1993.

[88] David J. Gross and IV Taylor, Washington. Two-dimensional qcd is a string theory. *Nucl. Phys.*, B400:181–210, 1993.

[89] David J. Gross and IV Taylor, Washington. Twists and wilson loops in the string theory of two- dimensional qcd. *Nucl. Phys.*, B403:395–452, 1993.

[90] G. W. Semenoff, O. Tirkkonen, and K. Zarembo. Exact solution of the one-dimensional non-abelian coulomb gas at large n. *Phys. Rev. Lett.*, 77:2174–2177, 1996.

[91] Kresimir Demeterfi, Igor R. Klebanov, and Gyan Bhanot. Glueball spectrum in a (1+1)-dimensional model for qcd. *Nucl. Phys.*, B418:15–29, 1994.

[92] Alexander M. Polyakov. Gauge fields and space-time. *Int. J. Mod. Phys.*, A17S1:119–136, 2002.

[93] D. J. Gross and Edward Witten. Possible third order phase transition in the large n lattice gauge theory. *Phys. Rev.*, D21:446–453, 1980.

[94] Spenta Wadia. A study of $u(n)$ lattice gauge theory in two-dimensions. EFI-79/44-CHICAGO.

[95] Spenta R. Wadia. $n = \infty$ phase transition in a class of exactly soluble model lattice gauge theories. *Phys. Lett.*, B93:403, 1980.

[96] J. Jurkiewicz and K. Zalewski. Vacuum structure of the $u(n \to \infty)$ gauge theory on a two-dimensional lattice for a broad class of variant actions. *Nucl. Phys.*, B220:167, 1983.